

University of Kentucky

UKnowledge

---

Theses and Dissertations--Chemistry

Chemistry

---

2014

## Salen Aluminum Compounds in the Dealkylation and Detection of Organophosphates

Rahul R. Butala

University of Kentucky, rrbu224@uky.edu

[Right click to open a feedback form in a new tab to let us know how this document benefits you.](#)

### Recommended Citation

Butala, Rahul R., "Salen Aluminum Compounds in the Dealkylation and Detection of Organophosphates" (2014). *Theses and Dissertations--Chemistry*. 47.  
[https://uknowledge.uky.edu/chemistry\\_etds/47](https://uknowledge.uky.edu/chemistry_etds/47)

This Doctoral Dissertation is brought to you for free and open access by the Chemistry at UKnowledge. It has been accepted for inclusion in Theses and Dissertations--Chemistry by an authorized administrator of UKnowledge. For more information, please contact [UKnowledge@lsv.uky.edu](mailto:UKnowledge@lsv.uky.edu).

## **STUDENT AGREEMENT:**

I represent that my thesis or dissertation and abstract are my original work. Proper attribution has been given to all outside sources. I understand that I am solely responsible for obtaining any needed copyright permissions. I have obtained needed written permission statement(s) from the owner(s) of each third-party copyrighted matter to be included in my work, allowing electronic distribution (if such use is not permitted by the fair use doctrine) which will be submitted to UKnowledge as Additional File.

I hereby grant to The University of Kentucky and its agents the irrevocable, non-exclusive, and royalty-free license to archive and make accessible my work in whole or in part in all forms of media, now or hereafter known. I agree that the document mentioned above may be made available immediately for worldwide access unless an embargo applies.

I retain all other ownership rights to the copyright of my work. I also retain the right to use in future works (such as articles or books) all or part of my work. I understand that I am free to register the copyright to my work.

## **REVIEW, APPROVAL AND ACCEPTANCE**

The document mentioned above has been reviewed and accepted by the student's advisor, on behalf of the advisory committee, and by the Director of Graduate Studies (DGS), on behalf of the program; we verify that this is the final, approved version of the student's thesis including all changes required by the advisory committee. The undersigned agree to abide by the statements above.

Rahul R. Butala, Student

Dr. David A. Atwood, Major Professor

Dr. Dong-Sheng Yang, Director of Graduate Studies

SALEN ALUMINUM COMPOUNDS IN THE DEALKYLATION AND DETECTION  
OF ORGANOPHOSPHATES

---

DISSERTATION

---

A dissertation submitted in partial fulfillment of the  
requirement for the degree of Doctor of Philosophy in the  
College of Arts and Sciences  
at the University of Kentucky

By

Rahul Butala

Director: Prof. David A. Atwood, Department of Chemistry  
Lexington, Kentucky

2014

Copyright © Rahul Butala 2014

## ABSTRACT OF DISSERTATION

### SALEN ALUMINUM COMPOUNDS IN THE DEALKYLATION AND DETECTION OF ORGANOPHOSPHATES

The focus of this dissertation is the use of aluminum Schiff base compounds, Salen(<sup>t</sup>Bu)AlBr (SAB), in the dealkylation and detection of organophosphates (OPs). Three SAB compounds, Salen(<sup>t</sup>Bu)AlBr (**1**), Salpen(<sup>t</sup>Bu)AlBr (**2**), and Salophen(<sup>t</sup>Bu)AlBr (**3**) were used to dealkylate a variety of trialkyl OPs. These reactions lead to unique organic-soluble aluminum phosphate compounds containing six-coordinate aluminum. Examples include [salen(<sup>t</sup>Bu)AlOP(O)(OCH<sub>3</sub>)<sub>2</sub>]<sub>n</sub> (**4**), [salen(<sup>t</sup>Bu)AlOP(O)(OCH<sub>2</sub>CH<sub>3</sub>)<sub>2</sub>]<sub>n</sub> (**5**), [salen(<sup>t</sup>Bu)AlOP(O)(OPh)<sub>2</sub>]<sub>n</sub> (**6**), [Salophen(<sup>t</sup>Bu)AlOP(O)(OCH<sub>3</sub>)<sub>2</sub>] (**7**), Salpen(<sup>t</sup>Bu)AlOOP(O)(O<sup>i</sup>Pr)<sub>2</sub> (**8**). These compounds are unique examples of polymeric (**4**, **5**, **6** and **7**) and dimeric compounds (**8**) with salenAl units connected by phosphate linkages. The compounds do not decompose in neutral water. This is an advantage in the use of SABs for the deactivation of phosphate esters such as nerve agents.

Water-soluble and stable group 13 salen complexes, Salen(SO<sub>3</sub>Na)MNO<sub>3</sub> (M = Al (**19**), Ga (**22**)), Salpen(SO<sub>3</sub>Na)MNO<sub>3</sub> (M = Al (**20**), Ga (**23**)), and Salophen(SO<sub>3</sub>Na)M(NO<sub>3</sub>) (M = Al (**21**), Ga (**24**)) were synthesized by using water-soluble Salen(SO<sub>3</sub>Na) ligand. All the compounds were characterized by various analytical techniques: <sup>1</sup>H, <sup>13</sup>C NMR, IR, and melting point.

One SAB was used to detect the nerve agents (NA). Salen(<sup>t</sup>Bu)Al(Ac), prepared *in situ* from Salen(<sup>t</sup>Bu)AlBr and NaAc, forms Lewis acid-base adducts with the NAs, GB (sarin) and GD (soman), and the VX hydrolysis product, EMPA, in aqueous solution. The [Salen(<sup>t</sup>Bu)Al(NA)]<sup>+</sup> compound is sufficiently stable to allow the identification of the NA with ESI-MS. Molecular ion peak was detected for every compound with little or no fragmentation. The distinctive MS signatures for [Salen(<sup>t</sup>Bu)Al(NA)]<sup>+</sup> compounds provide a new technique for identifying NAs in aqueous solution.

Keywords: Organophosphate dealkylation, water-soluble, salen, nerve agent, detection

Rahul Butala

---

12/16/201

---

SALEN ALUMINUM COMPOUNDS IN THE DEALKYLATION AND DETECTION  
OF ORGANOPHOSPHATES

By

Rahul Butala

Prof. David A. Atwood

Director of Dissertation

Prof. Dong-Sheng Yang

Director of Dissertation

12/16/2014

Date

Dedicated to my beloved parents

## ACKNOWLEDGEMENTS

Firstly, I would like to express my deepest gratitude to my mother (Alka Butala), father (Ramesh Butala) and brother (Rakesh Butala). After all, I would not be where I am today without their love, support, encouragement and patience. I am thankful to them for always wishing the best for me and being proud of my achievements,

It is a genuine pleasure to express my deep sense of thanks and gratitude to my advisor, Prof. David A. Atwood. I sincerely thank him for offering this opportunity to me. His constant motivation, criticism, and faith in me had been solely and mainly responsible to completing my work. I deeply appreciate his concern and support, not only inside the lab but also outside it. I am very grateful for the tremendous amount of independence that he allowed me in his laboratory, and I also must thank him for teaching me the art of publication writing. I thank my committee members, Professors John Selegue, Jason DeRouchey, and Alan Fryar for keeping me on the right track with their knowledge, experience, criticism, and very helpful ideas. I would like to thank Prof. Y. T. Wang for serving as the external examiner during my final defense.

I cannot express enough thanks to Dr. Sean Parkin for his help with X-ray crystallography. The support extended by John Layton from the NMR facility, and Jack Goodman from the MS facility, is greatly appreciated. I would like to thank William Creasy and Roderick Fry at the Aberdeen Proving Ground for wonderful collaboration. I am very thankful for another collaboration, involving computational work, with Dr. Michael McKee at the Department of Chemistry and Biochemistry, Auburn University. I wish to thank Justin Mobley for carrying out GPC analysis.

I would like to thank University of Kentucky, Department of Chemistry for giving me the opportunity. I also thank the wonderful staff in the Department of Chemistry for always being so

helpful and friendly. People here are genuinely nice and want to help you out and I'm glad to have interacted with many.

I thank the entire Atwood research group for their support and help in the lab, sharing their ideas and skills, and also for making the lab a very enjoyable workplace. I would like to extend sincere thanks to my forgiving, generous and loving friends (too many to list here but you know who you are!) without whom I could not have survived the process. Many thanks to Pallab Pahari for providing help during my early days in Lexington. I would like to thank Subrahmanyam Modekrutti and Aman Preet Dhillon for being supportive throughout my time here, and for helping me with presentations. To Anirban Chakraborty, Ishita Parikh, Mansi Sethi, Sampurna Arya, Mahendra Sreeramoju, and Shubhankar Dutta, thank you for your thoughtful support and generosity. Finally, I thank Almighty for His endless blessings and answered prayers.

## TABLE OF CONTENTS

TITLE.....	ii
ABSTRACT OF DISSERTATION.....	ii
ACKNOWLEDGEMENTS.....	iii
LIST OF TABLES.....	vii
LIST OF FIGURES.....	viii
LIST OF SCHEMES.....	ix
Chapter 1 Introduction.....	1
1.1. Organophosphates.....	1
1.1.1. Structure.....	1
1.1.2. Bonding.....	2
1.1.3. Reactivity Trends.....	4
1.1.4. Industrial Applications.....	7
1.1.5. Chemical Warfare Agents.....	13
Chapter 2 Salen-Supported Aluminum Phosphate Compounds.....	28
2.1. Introduction.....	28
2.2. Synthesis.....	29
2.3. Characterization.....	30
2.3.1. Spectroscopy.....	30
2.3.2. Structures.....	32
2.4. Stability.....	40
2.5. Total Dealkylation.....	41
2.6. Conclusion.....	44
2.7. Experimental.....	44

Chapter 3	Water-Soluble Salen Aluminum Compounds .....	50
3.1.	Introduction .....	50
3.2.	Dealkylation in Lewis Basic Solvents.....	51
3.3.	Water-Soluble Salen Compounds .....	56
3.3.1.	Synthesis.....	56
3.3.2.	Characterization .....	58
3.4.	Conclusion.....	61
3.5.	Experimental.....	61
Chapter 4	Detection of Nerve Agents in Water.....	68
4.1.	Introduction .....	68
4.2.	Research Background .....	69
4.3.	ESI-MS Analysis .....	72
4.4.	Result and Discussion .....	75
4.5.	Conclusion.....	84
4.6.	Experimental.....	84
Chapter 5	Conclusion and Future Work .....	87
Appendix	.....	90
References	.....	97
Vita	.....	101

## LIST OF TABLES

Table 1.1. Abbreviations and chemical names of nerve agents <sup>35</sup> .....	14
Table 1.2. Toxicity of the most important nerve agents <sup>37</sup> .....	15
Table 2.1. <sup>31</sup> P NMR shifts .....	31
Table 2.2. Selected bond distances (Å) and angles (°) for compounds 5-8 .....	37
Table 3.1. Selected bond distances (Å) and angles (°) for 15 .....	59
Table 4.1. Mass numbers for each compound formed in a sequence of reactions leading to formation of Lewis acid-base compounds between salen( <sup>t</sup> Bu)Al and the nerve agents .....	75
Table 4.2. Computational determination of ΔG values (kcal/mol) for the combination of SalenAl cations with Ac- (a), water (b) and (c), G-type nerve agents (d-g) and EMPA (h) .....	83

## LIST OF FIGURES

Figure 1.1. Organophosphorus compounds (a: phosphite ester, b: orthophosphate, c: organophosphate Esters, d: pentaoxyphosphoranes, e: hexaoxyphosphorides, f: phosphenites, g: phosphenates).....	1
Figure 1.2. Substituted phosphate.....	1
Figure 1.3. General structures of (a) Phosphate, (b) Phosphonate, and (c) Phosphinate .....	2
Figure 1.4. Alternative views for description of the P – O bond in phosphryl compound. ....	4
Figure 1.5. Structures of organophosphate flame retardants, triphenyl phosphate (a), (resorcinol-bis(diphenyl)phosphate) (b), (polysulfonyldiphenylene phenyl phosphonate) (c), (polysulfonyldiphenylene thiophenyl phosphonate) (d), [poly(2, 2-dimethylpropylene spirocyclic pentaerythritol bisphosphate)] (e), [poly(2-hydroxy propylene spirocyclic pentaerythritol bisphosphate) .....	9
Figure 1.6. General structure of organophosphate pesticides (X is leaving group) .....	11
Figure 1.7. Structures of nerve agents.....	14
Figure 1.8. Salben( <sup>t</sup> Bu)BBr <sub>2</sub> and salen( <sup>t</sup> Bu)AlBr .....	27
Figure 2.1. Crystal structure of 7 showing formation of polymer chain.....	32
Figure 2.2. Crystal structure of 5 .....	33
Figure 2.3. Crystal structure of 6 ( <sup>t</sup> Bu groups omitted for clarity).....	34
Figure 2.4. Crystal structure of 7 .....	34
Figure 2.5. Unit cell of 7 viewed down the c-axis showing staggered confirmation of <sup>t</sup> Bu groups .....	35
Figure 2.6. Crystal structure of 8 .....	36
Figure 2.7. A: MALDI mass spectra of 9; B: Isotope simulation for mol. wt 1648 .....	43
Figure 3.1. Dealkylation pathway of organophosphates with Salen( <sup>t</sup> Bu)AlBr compounds .....	53

Figure 3.2. $^{31}\text{P}$ NMR of dealkylation of VX with salen( $^t\text{Bu}$ )AlBr ; top: at t = 0 h; bottom: at t = 9 h .....	55
Figure 3.3. Crystal structure of 15 .....	59
Figure 3.4. Crystal structure of 19 .....	61
Figure 4.1. MALDI MS (+) of Lewis acid-base adduct of phosphine oxide with salen( $^t\text{Bu}$ )AlBr .....	71
Figure 4.2. Sketch of the apparatus for electrospray ionization .....	73
Figure 4.3. Schematic diagram of a quadrupole mass spectrometer .....	74
Figure 4.4. Schematic diagram of a triple quadrupole system .....	74
Figure 4.5. ESI-MS (+) of 1 in isopropanol.....	77
Figure 4.6. ESI-MS (-) of 1 in isopropanol .....	78
Figure 4.7. ESI-MS (+) of 26.....	79
Figure 4.8. ESI-MS (-) of 26.....	79
Figure 4.9. ESI-MS (+) of 27.....	80
Figure 4.10. ESI-MS (+) of 28.....	81
Figure 4.11. MS-MS of 28.....	81
Figure 4.12. ESI-MS (+) of 29.....	82
Figure 4.13. ESI-MS (-) of 29.....	82

## LIST OF SCHEMES

Scheme 1.1. Alkaline hydrolysis of trialkyl phosphate .....	5
Scheme 1.2. Hydrolysis of trialkyl phosphate in neutral or weak acidic medium .....	6
Scheme 1.3. Reaction of amine with phosphate ester .....	7
Scheme 1.4. Reaction of mercaptan with phosphate triester .....	7
Scheme 1.5. Inhibition of acetyl cholinesterase by organophosphate pesticide .....	12
Scheme 1.6. Mode of action of the enzyme acetylcholinesterase .....	17
Scheme 1.7. Inhibition and aging of AChE with organophosphate nerve agents .....	18
Scheme 1.8. Hydrolysis of soman and sarin .....	19
Scheme 1.9. Hydrolysis of VX.....	20
Scheme 1.10. Perhydrolysis of sarin .....	20
Scheme 1.11. Perhydrolysis of VX.....	21
Scheme 1.12. Reaction of VX with alkoxide anion.....	22
Scheme 1.13. Reaction of GB (a) and VX (b) with hypochlorite .....	23
Scheme 1.14. Autocatalytic hydrolysis mechanism of VX and R-VX.....	24
Scheme 1.15. Incineration process for sarin (a) and VX (b).....	25
Scheme 1.16. Dealkylation of VX by salen( <sup>t</sup> Bu)AlBr.....	27
Scheme 2.1. Synthesis of Salen( <sup>t</sup> Bu)AlBr .....	29
Scheme 2.2. Formation of Salen aluminum phosphate.....	30
Scheme 2.3. Total dealkylation of trimethyl phosphate.....	42
Scheme 3.1. Synthesis of Salen(SO <sub>3</sub> Na)H <sub>2</sub> .....	57
Scheme 3.2. Synthesis of Salen(SO <sub>3</sub> Na)MNO <sub>3</sub> .....	57

Scheme 4.1. Coordination of phosphine oxide to aluminum .....	70
Scheme 4.2. Sequence of reactions (a – c) leading to formation of Lewis acid-base compounds between salen( <sup>t</sup> Bu)AlBr (1) (which forms the ion pair, [salen( <sup>t</sup> Bu)Al( <sup>i</sup> PA)Br] (25) and the nerve agents GB (sarin, R = CHMe <sub>2</sub> , X = F (27)) GD (soman, R = CH(Me)CMe <sub>3</sub> , X = F (28)) and VX hydrolylate EMPA (ethylmethylphosphonate, R = Et, X = OH (29)). .....	76

## Chapter 1 Introduction

### 1.1. Organophosphates

#### 1.1.1. Structure

Phosphorus is a versatile element. It can form a variety of compounds including inorganic salts (sodium, ammonium, and calcium salts of phosphate, for example), transition metal complexes and organophosphorus compounds. Phosphorus has a high affinity for oxygen, and organophosphate compounds, which contain phosphorus-oxygen linkages, are probably the most important class of compounds in phosphorus chemistry. They may contain up to six oxygen atoms linked to a central phosphorus atom (Figure 1.1).

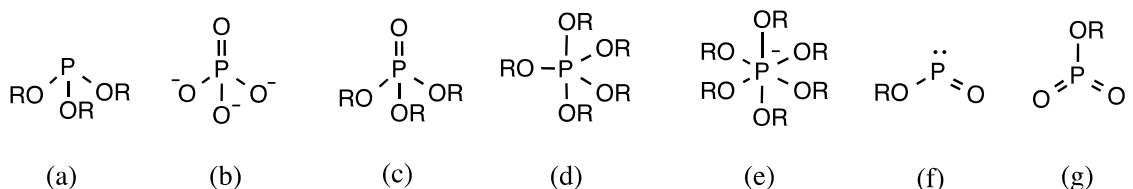


**Figure 1.1. Organophosphorus compounds (a: phosphite ester, b: orthophosphate, c: organophosphate Esters, d: pentaoxyphosphoranes, e: hexaoxyphosphorides, f: phosphenites, g: phosphenates)**

The term phosphate is used to refer to compounds in which the central phosphorus atom is linked to four oxygen atoms in a tetrahedral geometry (Figure 1.1 b and 1.1 c). If other atoms or groups replace some of the oxygen, the compounds are referred to as substituted phosphates (Figure 1.2).

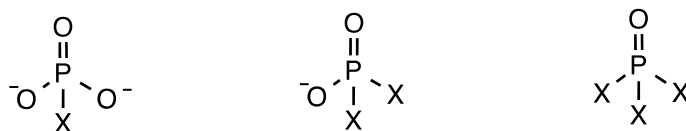


**Figure 1.2. Substituted phosphate**

Organophosphates (OP) are usually esters, amides or thiol derivatives of phosphoric ( $\text{H}_3\text{PO}_4$ ), phosphonic ( $\text{H}_3\text{PO}_3$ ) or phosphinic ( $\text{H}_3\text{PO}_2$ ) acids. Thus, phosphates are esters of phosphoric acid with four oxygen atoms surrounding a phosphorus atom. In phosphonates (esters of phosphonic acid), there are three O atoms and one P-C bond. Esters of phosphinic acid, i.e. phosphinates, have two O atoms and two P-C bonds. Phosphate esters contain one or more P-O-C linkages where the P-O ( $\sim 359 \text{ KJ mol}^{-1}$ ) and C-O ( $\sim 355 \text{ KJ mol}^{-1}$ ) bonds are of comparable energy.<sup>1</sup>

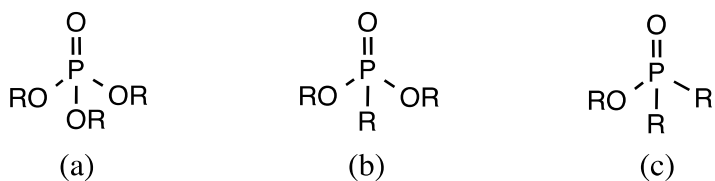


**Figure 1.3. General structures of (a) Phosphate, (b) Phosphonate, and (c) Phosphinate**

Phosphates play an important role in living systems. They appear in many biochemical reactions either as energy carriers, as coenzymes or as intermediates. DNA, RNA, and ATP are some of the examples of phosphate biomolecules. Phosphates, found in biological systems, are tetracoordinated with either tetrahedral or trigonal pyramidal geometry. OPs also play an important role in science and technology. A large number of OPs were used in the agriculture industry as pesticides and insecticides. Triaryl phosphates are used as additives for gasoline, plasticizers, lubricants, coolants, and flame-retardants.

### 1.1.2. Bonding

The nature of the bonding in the P-O bond in phosphoryl compounds ( $\text{R}_3\text{PO}$ ) has been the subject of great interest for many years. It has been reviewed extensively in the literature,<sup>2,3</sup> and experimental work and calculations both agree that the P-O bond is strong, polar, and short enough to be classified as a double bond.

A variety of resonance structures have been proposed including  $R_3P=O$ ,  $R_3P^+-O^-$ , partial double bonds, formal triple bonds, and various resonance mixtures of these structures. A purely donor bond,  $X_3P\rightarrow O$  is proposed on the basis that amine oxides have this kind of bond. In theory, bond angle data could be used to check the possibility of  $P\rightarrow O$  link. Phosphoryl compounds with a  $P\rightarrow O$  link should have bond angles approaching the tetrahedral angle of  $109.28^\circ$ . Observed  $XPX$  bond angles for  $X_3PO$  which are in the range of  $102.5^\circ$  for  $F_3PO$  to  $108^\circ$  for  $Br_3PO$ .<sup>4</sup> This bond angle data may consider as an evidence for the  $P\rightarrow O$  link. However, in adduct  $F_3P\rightarrow BH_3$  where there is definitely the formation of a donor  $\sigma$  bond,  $FPF$  bond angle is  $99.8^\circ$ . Hence, bond angle argument is inconclusive and steric factor dominate the geometry. Recently, an abinitio nuclear magnetic resonance calculation<sup>5</sup> and an atoms-in-molecule study<sup>6</sup> concluded that a P-O bond is a better described as being zwitterionic  $R_3P^+-O^-$ . It is also proposed that this bond cannot be represented as a conventional multiple bond.<sup>5</sup> However, other evidences (P-O bond length, bond energy, dipole moments) point towards the existence of a PO  $\pi$  bond. For example, the P-O bond in phosphoryl compounds is certainly stronger than a conventional PO single bond. The P-O bond dissociation energy in the compounds containing the phosphoryl group is in the  $500\text{-}600\text{ kJ mol}^{-1}$  range (e.g. P-O bond energy in  $(EtO)_3PO$  is  $630\text{ kJ mol}^{-1}$ )<sup>7</sup> while the P-O bond energy in compounds of the type  $(RO)_3P$  is around  $400\text{ kJ mol}^{-1}$ .<sup>8</sup> The phosphoryl link is also significantly shorter than other PO bonds. For example, the PO bond length in  $(MeO)_3PO$  is  $1.52\text{ \AA}$ , which is shorter than the MeO-P bond length,  $1.66\text{ \AA}$ .<sup>9</sup> The dipole moments of  $R_3PO$  (e.g.  $4.37\text{ D}$  for  $Me_3PO$ ) are smaller than the analogous nitrogen compounds  $R_3N-O$  ( $5.02\text{ D}$  for  $Me_3N-O$ ), and suggests the presence of a double bond character in the phosphoryl bond. In other words, there is expansion of octet on phosphorus and there is back bonding from oxygen to suitable orbitals on phosphorus. This results in the formation of  $\pi$  systems along with a donor  $\sigma$  bond.

Even though experimental and theoretical studies have proven the polar and multiple bond character of P-O bond, there is still strong debate over the exact electron distribution between P and O. Involvement of d orbitals in a  $\pi$  bond was proposed and this concept was well reviewed in 1970.<sup>10</sup> According to this approach, the  $\pi$  bond is formed by back donation of lone pairs from oxygen to empty 3d orbitals of P. Some theoretical chemists have questioned this concept<sup>2</sup>, and the role of d function is proposed as polarization functions rather than a primary valence orbital.<sup>11</sup> Currently, bonding in phosphoryl compounds is mostly discussed using 3 alternative views:<sup>12</sup> 1. One dative P-O  $\sigma$  bond and two  $\pi$  bonds formed by back bonding of two oxygen lone pairs to suitable  $R_3P$  antibonding orbitals. (Fig. 1.4a) 2. One dative P-O  $\sigma$  bond and the negative hyperconjugation of three  $n_0$  orbitals with  $R_3P$  antibonding orbitals. (Fig. 1.4b) 3. Three 'Banana / Bent multiple bonds. A PO bond, in this case, is viewed as a formal triple bond. Differences in the description of the PO bond arise in the interpretation of interaction between the  $R_3P$  group and the O atom based on different approaches. (Fig 1.4c)

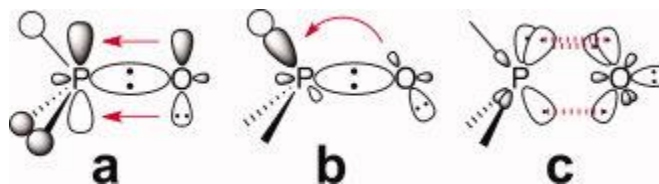


**Figure 1.4. Alternative views for description of the P – O bond in phosphoryl compound. (Adapted from J.Com.Chem. 2013,34,149 with permission from J. Wiley & Sons) (License number 3332610970405)**

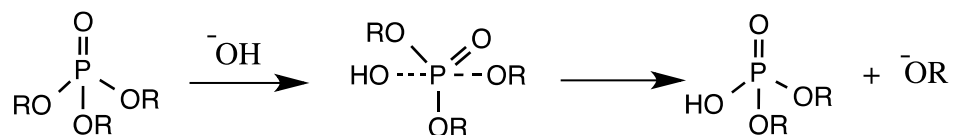
### 1.1.3. Reactivity Trends

The phosphate ester bond plays an important role in various systems ranging from biological molecules, such as DNA, RNA, ATP, and commercial products, like plasticizer, pesticides and nerve agents.<sup>13</sup> Reactions of phosphate esters, typically called phosphate-transfer reactions, play an important role in the chemical process of life. Reactions of trialkyl phosphates

are simple and follow the predictions of Pearson's theory of hard and soft reagents. Small nucleophiles such as hydroxide, alkoxide, enolates, thiolates, phenyllithiums, and Grignard reagents yield products arising from a nucleophilic attack on phosphorus, while bulky nucleophiles such as bromide, iodide and benzyl lithium yield products arising from nucleophilic attack on carbon.

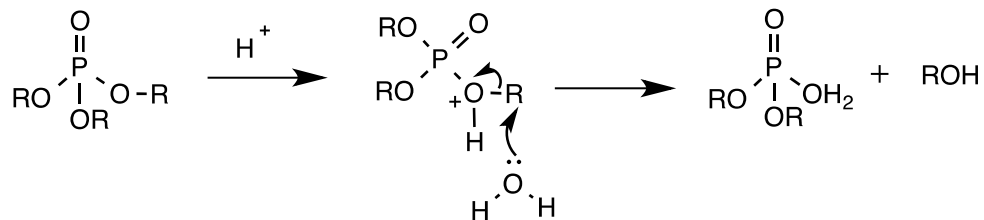
### 1.1.3.1. Hydrolysis, Alcoholysis

The hydrolysis of trialkyl phosphates in an alkaline medium is a first-order with respect to both hydroxyl ion and ester, and proceeds with the cleavage of P – O bond.<sup>14</sup> The attack of the hydroxyl group on the phosphoryl group is a one-step reaction and formulated as a concerted S<sub>N</sub>2 type reaction (Scheme 1.1). There is strong evidence for inversion of configuration in nucleophilic addition to the phosphoryl group.<sup>15</sup> Also, there is no observed exchange of oxygen between the phosphoryl group and water.<sup>16</sup>



**Scheme 1.1. Alkaline hydrolysis of trialkyl phosphate**

In a neutral or weak acidic aqueous media, hydrolysis of trialkyl phosphates proceeds via breakage of the C – O bond.<sup>16</sup> This reaction involves bimolecular attack. The protonation of the ester oxygen is followed by attack of a water molecule on the carbon atom (Scheme 1.2). However, in a strong acid, the direct attack of the hydroxyl ion on the phosphorus is observed.



**Scheme 1.2. Hydrolysis of trialkyl phosphate in neutral or weak acidic medium**

Hydrolysis of trialkyl phosphates follows the predictions of Pearson's theory of hard and soft acids and bases. The hard base, hydroxide ion preferentially attacks the phosphoryl group of trialkylphosphate and results in P – O cleavage. C – O bond cleavage is expected when a soft base, water, attacks the soft acid,  $R^+$ .<sup>17</sup>

In phosphonates and phosphinates, the alkyl groups do not participate in  $\pi$  bond and thus increases the positive charge on phosphorus in comparison to the trialkyl phosphate. Hence, alkaline hydrolysis is favored and acid hydrolysis becomes more difficult.<sup>18</sup> In fact, experimentally, a decreasing alkaline and an increasing acid stability are found in the order: phosphates, phosphonates and phosphinates.

#### 1.1.3.2. Nucleophiles other than hydroxyl ion

Transesterification of trialkyl phosphate can be easily achieved by the nucleophilic attack of alkoxide ion on P. Even though this process has been used for the synthesis of different trialkyl phosphates, the mechanism of this reaction has not been studied extensively. This reaction is likely to proceed in the same manner as the hydrolysis.<sup>19</sup> This is also a fundamental reaction in enzyme inhibition by organophosphates.

Ammonia always reacts with triesters by C – O cleavage with the exception of triaryl phosphates. A nucleophilic attack of ammonia displaces a phenoxide ion from triaryl phosphates to form phosphoramides.<sup>20</sup> Amines react in  $S_N2$  fashion at ester carbon of phosphate esters



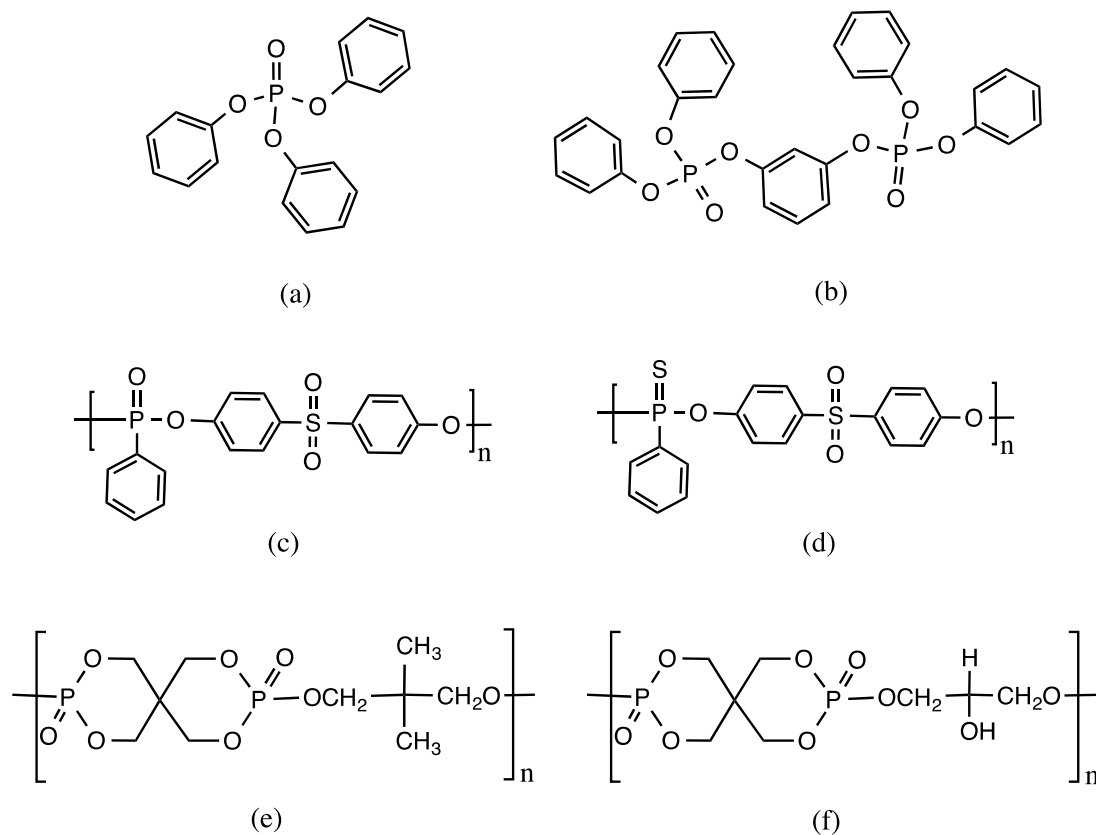
be compounds containing borax or nanocomposite.<sup>25,26</sup> Although the halogen-containing compounds are constantly considered to be very effective FRs, emission of dense and toxic smokes as well as corrosive gases during their combustion is the main concern. Brominated FRs are toxic to humans and animals. Also, they are known to be persistent and bio-accumulative in the environment. Phosphorus flame retardants are considered suitable alternatives for brominated flame retardants.<sup>27</sup>

The range of phosphorus-containing flame retardants is extremely wide since the element exists abundantly. There are three main groups of phosphorus flame retardants.<sup>26</sup> The first group contains inorganic phosphorus flame retardants. Red phosphorus and ammonium polyphosphate are some examples of inorganic flame-retardants. An organic phosphonate is a second type of flame retardant. Phosphines, phosphine oxides, phosphonium compounds, phosphonates, phosphites, and phosphate are all used as flame retardants in polymer. The third group is comprised of halogenated phosphates.

The basic mechanisms of flame retardancy vary depending on the specific flame retardant.<sup>25</sup> Halogenated flame retardants function in the gas phase. Chlorine and bromine atoms from these FRs react with  $H\cdot$  and  $OH\cdot$  radicals from the flammable gas phase resulting in a slowing of the burning process. Another way to inhibit combustion is to provide a thermal insulation barrier between the burning material and the unburned part. Phosphorus flame retardants mainly act through this mechanism in the solid phase of the burning material. The capability of organophosphorus flame retardants to inhibit ignition and promote char formation is maximized in the solid or condensed phase. Upon heating, they react to form a polymeric form of phosphoric acid that causes a char layer. Organophosphorus flame retardants are more

effective in oxygenated polymers like wood, cotton, polyurethanes, polyesters, etc. where char formation is an effective means to limit further burning.<sup>27</sup>

Aliphatic phosphates and phosphonates, particularly spirocyclic bisphosphate derived from pentaerythritol, are commonly used as flame retardants in poly(ethylene terephthalate) (PET), polyurethane foam (PUF), and epoxy resin.



#### 1.1.4.2. Plasticizers

Organophosphate compounds can be incorporated in plastics to increase flexibility or workability. The first commercial use of an OP plasticizer took place before World War I where triaryl phosphate was used in plasticizing cellulose nitrate and cellulose acetate.<sup>1</sup> The more important phosphate plasticizers are trioctyl phosphate (tri-2-ethylhexyl phosphate) and octyl diphenyl phosphate (2-ethylhexyl diphenyl phosphate), which are used in PVC. In addition, tri-*n*-butyl phosphate, triethyl phosphate, tributoxyethyl phosphate, tri(*p*-*tert*-butylphenyl) phosphate, and hexnyl diphenyl phosphate have been used commercially.<sup>28</sup>

Phosphates plasticizers, are generally high-boiling liquids, which when added to polymers, reduce polymer-polymer interactions at the expense of polymer-plasticizer interactions. This increases segmental mobility (movement of small chain of segments due to correlated motion of several consecutive bonds) and polymer flexibility. There are two theories, which have been put forward to explain the mechanism of plasticization.<sup>28</sup> According to the Lubricity Theory the small plasticizer molecules act as a lubricant between adjacent macromolecules and separate polymer chains. Gel Theory considers a plastic as a three dimensional gel. According to this theory, plastic brittleness and stiffness due to a closely packed three-dimensional network structure formed by secondary bonding between macromolecules. Plasticizer molecules eliminate the secondary preferential interaction with these sites. This reduces the extent of the gel structure of plastic.

Phosphate plasticizers are generally preferred over the other types of plasticizers like phthalates and citrates because they exhibit some unique desirable characteristics. The phosphate plasticizers are known to increase the low temperature flexibility of plastics. Trioctyl phosphate is particularly useful for imparting low temperature flexibility to plastic. The phosphates are also used as flame-retardants for polymer systems.

### 1.1.4.3. Pesticides

OP is a very effective and widely used class of pesticides. OP pesticides have replaced organochlorine pesticides, which are more persistent in environment. OP pesticides are esters of phosphoric or phosphorothionic acid that exist in two forms: thion (sulfur containing, P=S) and -oxon (oxygen containing, P=O).<sup>29</sup> The -oxon OPs have a greater toxicity than -thion OPs. However, -thion OPs are readily hydrolysed to -oxons once they are in the environment. The majority of OP pesticides in use are dimethyl compounds (two [-OCH<sub>3</sub>] groups attached to the phosphorus) or diethyl compounds (two [-OC<sub>2</sub>H<sub>5</sub>] groups attached to the phosphorus). The general structure of organophosphate pesticides is shown in Figure 1.6.

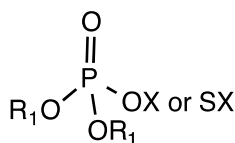
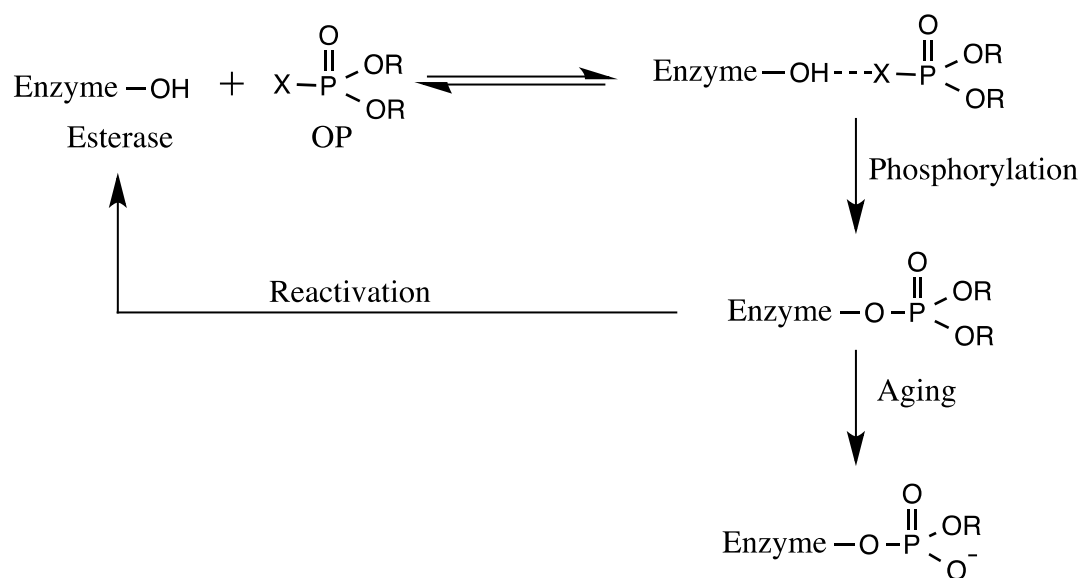


**Figure 1.6. General structure of organophosphate pesticides (X is leaving group)**

OP pesticides were first synthesized in Germany in the late 1930s. Many of the first OPs were extremely toxic and some were developed into potential warfare agents during World War II (e.g. soman, sarin, and tabun). Tetraethylpyrophosphate (TEPP) was first reported as an OP pesticide. It was extremely toxic and highly unstable to hydrolysis under aqueous conditions.<sup>30</sup>

Parathion (O, O-diethyl-O-p-nitrophenyl phosphorothioate) was the first OP to be marketed commercially. Subsequently, its oxygen analog, paraoxon (O, O-diethyl-O-p-nitrophenyl phosphate) was synthesized. Other OPs that are frequently used include phosmet, methyl parathion, chlorpyrifos, diazinon, and malathion. Presently, there are 49 organophosphate compounds registered as pesticides with the Environmental Protection Agency (EPA).<sup>31</sup>

OPs attack the nerve system to kill target pests, usually insects. However, they can also attack the nervous systems of humans. Exposure to OPs can cause both acute and chronic health effects. Acute exposure of OPs affects the parasympathetic, sympathetic, and central nervous systems.<sup>32</sup> The primary reason for OP toxicity is its inhibition of the acetylcholinesterase (AChE), enzyme responsible for hydrolysis of neurotransmitter acetylcholine. The inhibition of the enzyme, AChE by OP mimics the reaction of AChE with Ach, except that formation of phosphorylated enzyme results instead of the acetylation. The phosphorylated enzyme is quite stable towards hydrolysis, causing loss of catalytic activity. This results in the accumulation of ACh at neural junctions and subsequent overstimulation of nerve fibers.<sup>33</sup> Phosphorylated AChE can undergo two possible reactions: recovery and aging. Recovery of the enzyme occurs by hydrolytic removal of the OP, but the rate of hydrolysis is very slow. In the case of pesticides, the half-life of the AChE-OP adduct is several hours. Aging occurs when the enzyme-bound OP is dealkylated. Once aging takes place, the inhibited enzyme cannot be reactivated.



**Scheme 1.5. Inhibition of acetyl cholinesterase by organophosphate pesticide**

### **1.1.5. Chemical Warfare Agents**

Chemical warfare agents (CWAs) have long been considered the “poor man’s atomic bomb”.<sup>34</sup> Among weapons of mass destruction, CWAs are considered the most lethal and brutal weapons made by the man. CWAs are inexpensive and relatively easy to produce, even by small terrorist groups, although their extreme toxicity makes handling difficult. The potential use of chemical warfare agents could be for various purposes, including causing mass casualties, warfare, terrorism, assassination, deterrence, or special purposes. Based on the structure, CWAs can be classified as organophosphorous (OP), organosulfur, organofluorine or arsenicals. Based on their biological effects they can be divided into several types; nerve agents, vesicants, blood agents, pulmonary agents and incapacitating agents.

#### **1.1.5.1. Nerve Agents**

Nerve agents (NA), which are organophosphorous derivatives, are the most significant among different types of CWAs with respect to their toxicity, past use, mode of action, and military capacity. There are two main groups of NAs, G and V agents.<sup>35</sup> G agents, the first generation of NAs, contain a typical P-F or P-CN bond. They include the cyanophosphoramidate, tabun (GA), and the methylfluorophosphonates, sarin (GB), soman (GD), and cyclosarin (GF) (Figure 1.7). G agents can enter into the body through inhalation. However, venomous agents, which are abbreviated as V agents, are more persistent in the environment and can be absorbed through skin. This group of methylphosphothioates includes VX (Great Britain), RVX (Russian VX), and CVX (Chinese VX) (Figure 1.7).

**Table 1.1. Abbreviations and chemical names of nerve agents<sup>35</sup>**

Acronym	Chemical Name
GA (Tabun)	<i>o</i> -Ethyl <i>N,N</i> -dimethyl phosphoramidocyanidate
GB (Sarin)	<i>o</i> -Isopropyl methylphosphonofluoridate
GD (Soman)	<i>o</i> -Pinacolyl methylphosphonofluoridate
GF (Cyclosarin)	<i>o</i> -Cyclohexyl methylphosphonofluoridate
VX	<i>o</i> -Ethyl <i>S</i> -2-diisopropylaminoethyl methylphosphonothioate
RVX	<i>o</i> -Isobutyl <i>S</i> -2-diethylaminoethyl methylphosphonothioate
CVX	<i>o</i> -butyl <i>S</i> -2-diethylaminoethyl methylphosphonothioate

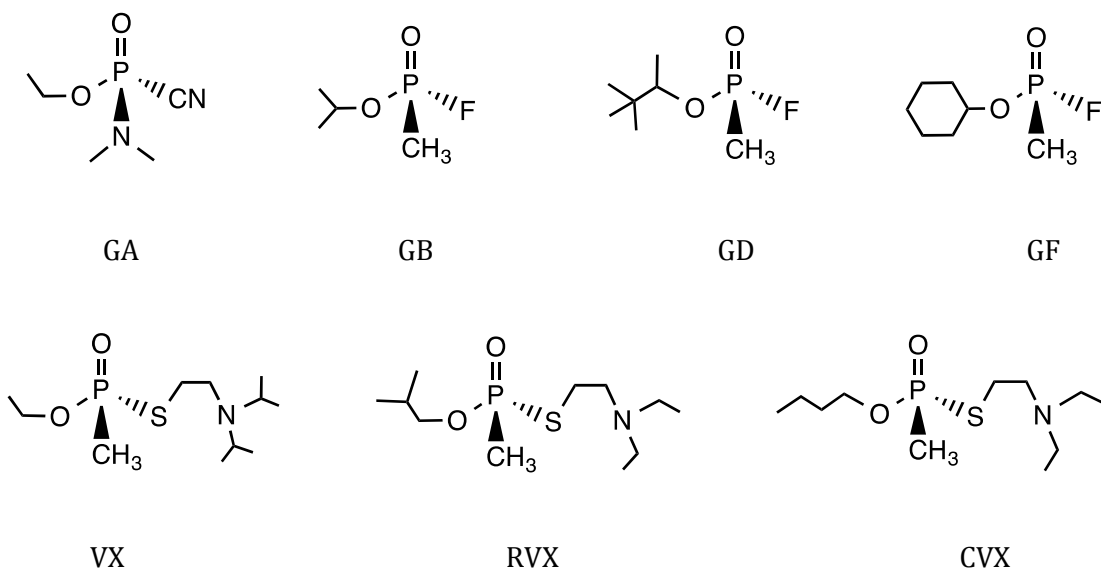


**Figure 1.7. Structures of nerve agents**

### 1.1.5.2. Biological Effects

NAs are more toxic than non-OP CW agents. NAs are extremely toxic and they have very rapid effect. If a person is exposed to high concentration of NA, e.g., 200 mg of sarin/m<sup>3</sup> death can occur within a minute of exposure. The recent use of NAs was the use of sarin gas during the Iraq-Iran conflict in the Gulf War, and during the terrorist attack in the Japanese subway. The most recent use was in Damascus, Syria on Aug 21 2013, when around 1400 people were killed in a sarin attack.<sup>36</sup>

**Table 1.2. Toxicity of the most important nerve agents<sup>37</sup>**

	<b>LC<sub>50</sub> Inhalation</b> <b>mg.min/m<sup>3</sup></b>	<b>LD<sub>50</sub> Skin</b> <b>mg/ individual</b>
Tabun	70	4000
Sarin	35	1700
Soman	35	300
VX	15	10

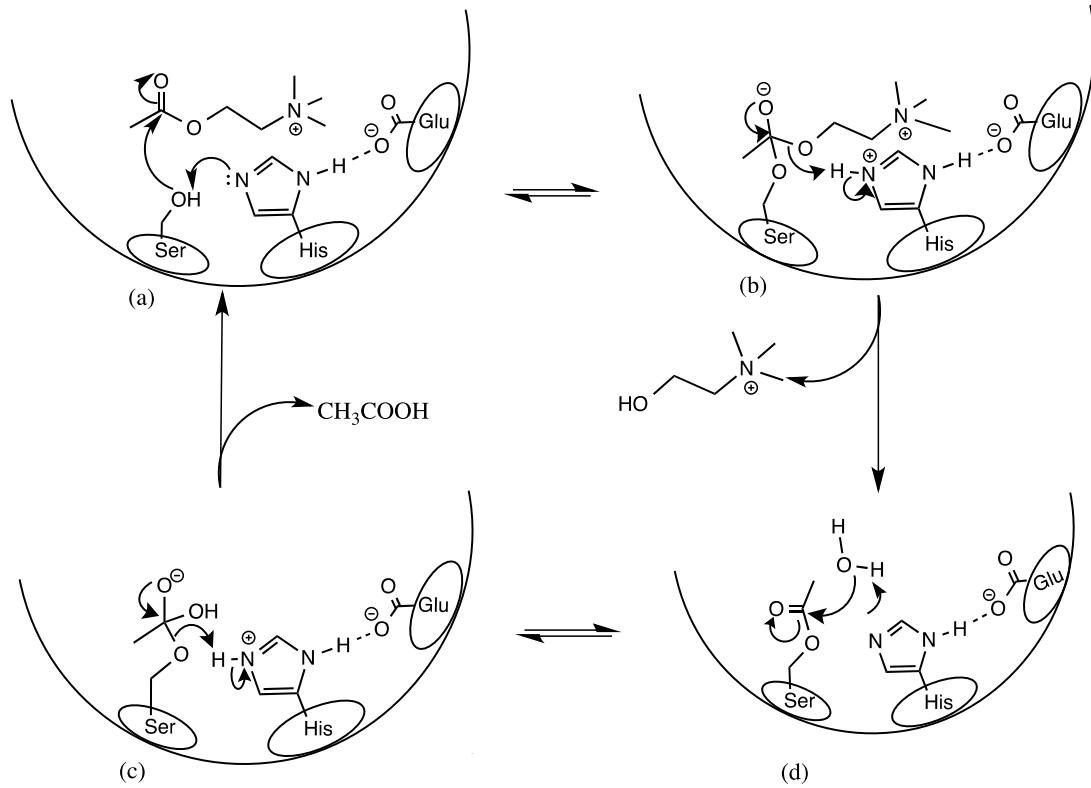
NA poisoning causes contraction of pupils, profuse salivation, convulsions, involuntary urination and defecation, and eventual death by asphyxiation as control is lost over respiratory muscles. In Syria, victims of a sarin attack experienced headaches and nausea, excessive saliva, and redness and itching of the eyes. The symptoms reported by doctors and witnesses included vomiting, foamy salivation, severe agitation, dyspnea (Impaired breathing), neurological convulsions, respiratory and heart failure, and blood out of the nose and mouth. In some cases, hallucinations and memory loss were also observed.<sup>38</sup> The effects of NAs are very long lasting and increase with successive exposures. Survivors of NA poisoning almost invariably suffer chronic neurological damage. This neurological damage can also lead to continuing psychiatric effects.

NAs prove so fatal because they inhibit an enzyme called acetylcholinesterase (AChE). Inhibition occurs through the irreversible binding of an OP to a catalytic site of the enzyme.<sup>39-</sup>  
<sup>41</sup>This enzyme is responsible for hydrolysis of neurotransmitter acetylcholine, a key-signaling molecule that has numerous functions in the body, including facilitating cognitive functioning and triggering muscle contraction. The inhibition of AChE leads to an accumulation of acetylcholine, resulting in continuous stimulation of nerve fibers.

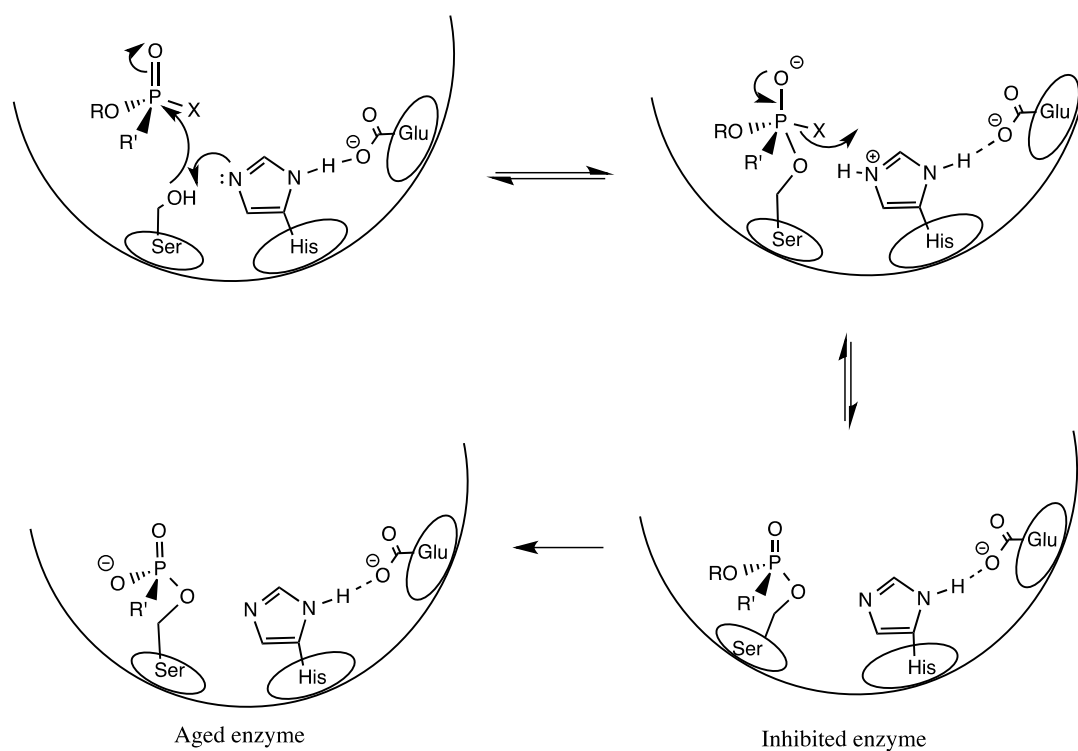
During normal functioning of AChE, a catalytic triad of three amino acids, serine, glutamic acid, and histidine, located in an active site of enzyme, catalyzes the hydrolysis of acetylcholine.<sup>42,43</sup> The catalytic mechanism consists of two steps: (1) nucleophilic serine hydroxyl group attacks acetylcholine (Ach) to form an acetylated enzyme with the release of choline (Scheme 1.6 a & b); (2) nucleophile attack of a water molecule, activated by a histidine molecule, on an acetylated enzyme to give a free enzyme and acetic acid (Scheme 1.6 c& d). Catalytic efficiency of AChE is very high. AChE hydrolyzes more than  $10^4$  molecules of Ach per second.<sup>44</sup>

The mechanism of AChE inhibition by OP is similar to the initial steps of the reaction of an enzyme with Ach. Nucleophilic serine attacks the phosphorous atom of an OP molecule to form a phosphorylated enzyme with the loss of a leaving group from OP. However, in the second step, the catalytic histidine cannot activate a water molecule due to the loss of a favorable conformation triad.<sup>45,46</sup> Therefore, the rate of hydrolysis of a phosphorylated enzyme is extremely slow compared to acetylated enzyme.<sup>47</sup> Hence, phosphorylated enzymes can no longer hydrolyze ACh leading to the accumulation of ACh in cholinergic receptors.

Without functioning AChE, muscle fibers twitch uncontrollably and neurons in the brain become hyperactive, leading to seizures. If untreated, people exposed to sarin typically die of asphyxiation, as the muscles involved with breathing proceed to fire nonstop.



**Scheme 1.6. Mode of action of the enzyme acetylcholinesterase**



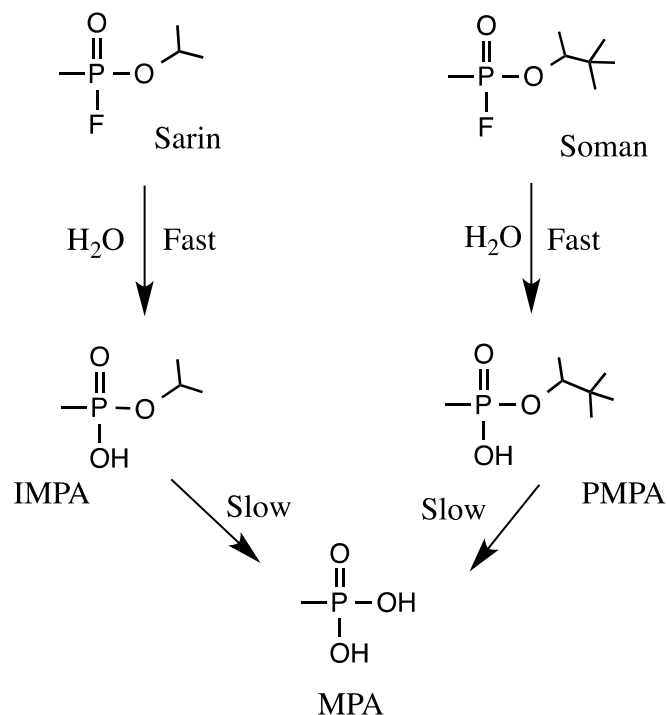
**Scheme 1.7. Inhibition and aging of AChE with organophosphate nerve agents**

### 1.1.5.3. Reactions

#### 1.1.5.3.1. Hydrolysis

##### 1.1.5.3.1.1 G agents

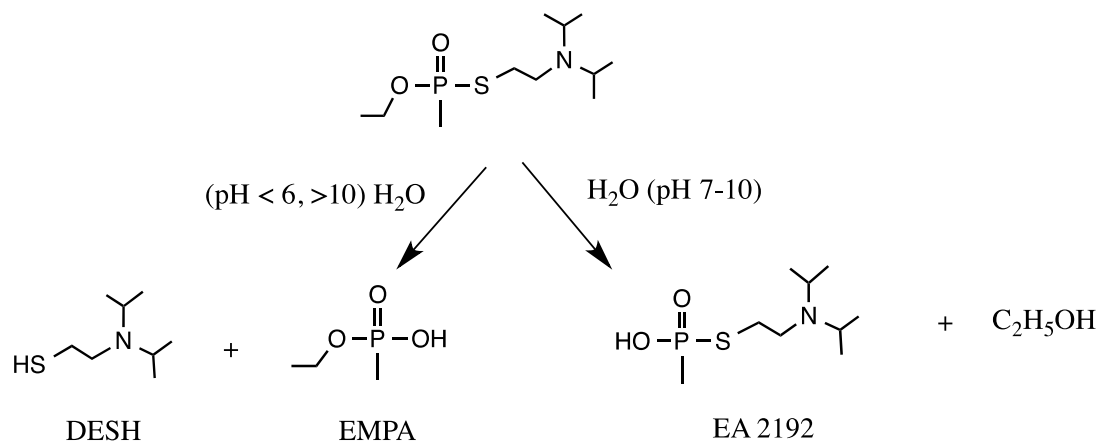
Hydrolysis of NAs is considered a basic method of detoxification.<sup>48</sup> G agents are soluble in water, and their hydrolysis is studied under different pH conditions.<sup>49-51</sup> Hydrolysis of G agents is temperature- and pH-dependent, and proceeds via  $S_N2$  nucleophilic attack at phosphorus. The rate constant is much smaller for hydrolysis at neutral pH compared to the rate constant of acidic and basic hydrolysis. At a pH value greater than 10, both GB and GD hydrolyzed within a few minutes to their corresponding phosphonic acids (Scheme 1.8). Acid decreases the pH of the reaction, which results in a decrease in the rate of hydrolysis. Hence, an excess of the base is required to maintain the reaction rate.



**Scheme 1.8. Hydrolysis of soman and sarin**

#### 1.1.5.3.1.2 VX

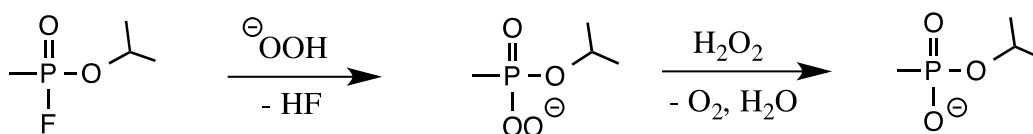
Hydrolysis of VX is more complex, and the mechanism of hydrolysis depends on pH and temperature. It involves several pathways (Scheme 1.9).<sup>52</sup> It proceeds either via P-C or P-S bond cleavage. At a pH value less than 6 and greater than 10, cleavage of the P-S bond is the predominant process, resulting in the formation of ethyl methylphosphonic acid (EMPA) and diisopropylethyl mercaptoamine (DESH). The rate of hydrolysis is very slow at neutral or weakly basic conditions (Half life of 60 h). As shown in Scheme 1.9, one of the reaction paths leads to the formation of the stable but extremely toxic compound, S-(2-diisopropylaminoethyl)methylphosphonothioic acid (EA-2192). Therefore, unlike the G agents, VX cannot be detoxified by base-catalysed hydrolysis. EA-2192 can be hydrolyzed to DESH and methyl phosphonic acid, but at room temperature, the rate of hydrolysis is extremely slow.



### Scheme 1.9. Hydrolysis of VX

#### 1.1.5.3.2. Reaction with H<sub>2</sub>O<sub>2</sub>

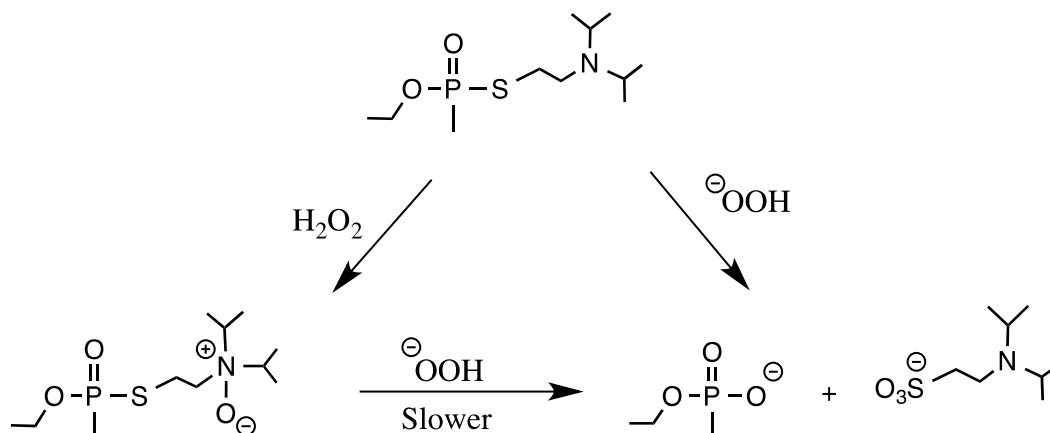
Basic peroxide has been known to decontaminate GB or sarin for decades<sup>53,54</sup> via the formation of strong nucleophilic peroxy anion, HOO<sup>-</sup>. The reaction proceeds through the formation of a peroxyphosphonate intermediate (Scheme 1.10).<sup>55</sup> The reaction of G agents<sup>56,57</sup> and VX<sup>58</sup> with H<sub>2</sub>O<sub>2</sub> is kinetically more favored compared to simple hydroxide. Although, perhydrolysis is fast, G agents can be easily decontaminated by a dilute alkali. Hence, peroxide offers no real advantage for these agents.



### Scheme 1.10. Perhydrolysis of sarin

It was shown that VX also undergoes rapid perhydrolysis to give selectively P-S cleavage.<sup>55,59</sup> Unlike a base hydrolysis of VX, a reaction with peroxide gives non-toxic ethyl methyl phosphonic acid (EMPA). The N-oxide of VX also forms and similarly undergoes perhydrolysis to give EMPA (Scheme 1.11) Hence, perhydrolysis of VX is a much more effective decontamination reaction compared to the reaction with alkali, as toxic S-(2-

diisopropylaminoethyl)methylphosphonothioic acid (EA-2192) is avoided. The reaction is dependent on pH and an addition of bicarbonate as a buffer is required to avoid slowing of the reaction due to the formation of an acid product.<sup>55</sup>



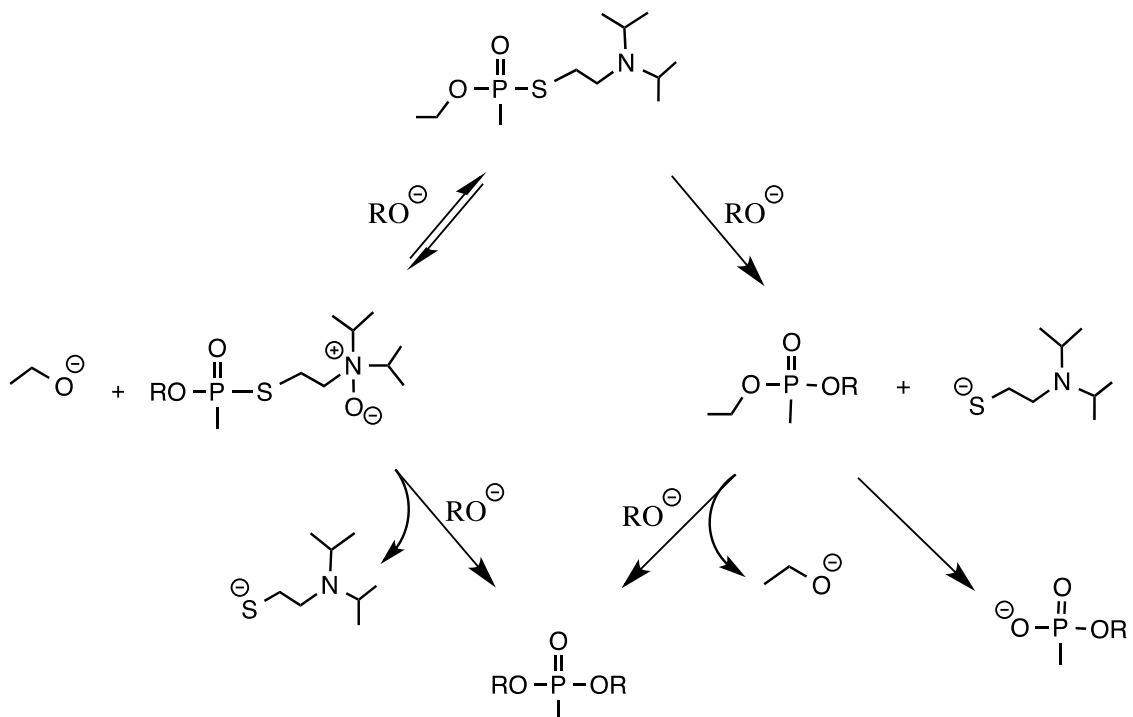
### Scheme 1.11. Perhydrolysis of VX

#### 1.1.5.3.3. Reaction with Alkoxide Anions

Alkoxide anion in alcohol is an attractive system for dissolution and destruction of NAs. An alkoxide solution can be prepared by simple mixing of alcohol with Na or K metal. Reactivity of alkoxide anion increases with an increase in size of the alkyl group (R) of alcohol. The reaction of VX with alkoxide proceeds with P-S cleavage and it involves displacement of thiolate by the alkoxide ion (Scheme 1.12). However, unlike perhydrolysis of VX, alkoxide does not give exclusive P-S cleavage. Cleavage of some of the P-O bonds is also observed to give thioate ester intermediate,  $\text{CH}_3\text{P}(\text{O})(\text{OR})\text{O}^-$ , which is similar to VX. It further undergoes reaction with another alkoxide ion to form  $\text{CH}_3\text{P}(\text{O})(\text{OR})_2$ .<sup>60</sup> Diols (e.g., ethylene diglycol), ether alcohols, or amino alcohols (monoethanolamine, MEA) are also used to generate an alkoxide anion. The reactivity of an alkoxide ion increases as the solvent becomes less protic.<sup>59</sup>

When NaOH or KOH is used to generate an alkoxide ion or when water is present in the reaction system, the hydroxide anion  $\text{OH}^-$  competes with  $\text{RO}^-$  to react with VX. This reaction will

produce toxic thionic acid species  $[\text{MeP}(\text{O})(\text{SCH}_2\text{CH}_2\text{Ni-Pr}_2)_2\text{OH}]$ , which react with an alkoxide ion very slowly.<sup>59</sup> ( $t_{1/2} = 140\text{h}$  at  $0.30\text{ M CH}_3\text{O}^-$ ,  $22^\circ\text{C}$ )



**Scheme 1.12. Reaction of VX with alkoxide anion**

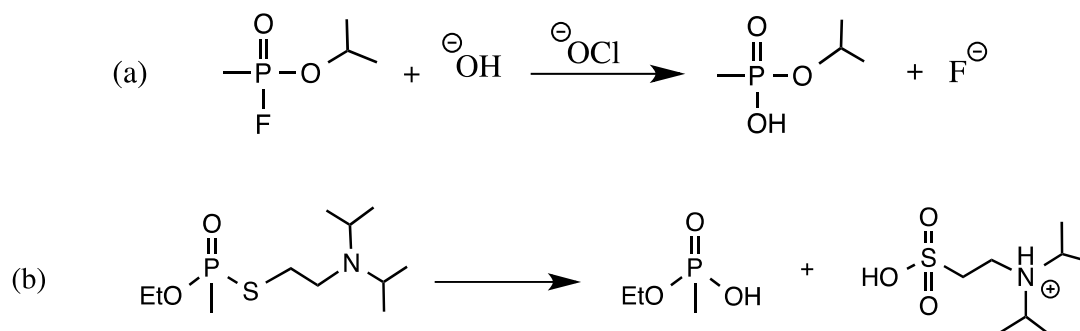
#### 1.1.5.3.4. Other Reactions

##### 1.1.5.3.4.1 Metal Ion Catalyzed Hydrolysis

The kinetic study of hydrolysis of sarin shows that  $\text{Cu}(\text{II})$  is a better catalyst compared to a number of metals (e.g., cerous, manganous ion) studied.<sup>49,61</sup> Two mechanisms for the activation step are possible. The catalytic species could be the hydroxometal complex,  $\text{CuOH}^+$ , or  $\text{Cu}(\text{II})$  could act as a Lewis acid by complexing with the substrate at the phosphoryl oxygen center followed by the attack of the hydroxide ion on the phosphate-Cu complex.<sup>62</sup> Very few reports are available on hydrolysis of VX catalyzed by  $\text{Cu}(\text{II})$ . The diethylamino group of VX competes with phosphoryl oxygen for complexing with copper. Thus, the reaction is expected to be inhibited if  $\text{Cu}(\text{II})$  complexes with diethylamino group instead of phosphoryl group.<sup>52</sup>

#### 1.1.5.3.4.2 Oxidation

Since G-type nerve agents can be easily hydrolysed in basic media, an oxidation study is more useful for V-type nerve agents. A solution or solid form of bleach is more commonly used for decontamination of nerve agents. The representative reaction of nerve agents with bleach is shown in (Scheme 1.13). In an acidic solution, tertiary amine nitrogen gets protonated, and oxidation takes place at sulfur followed by hydrolysis of the P-S bond. At high pH, the tertiary amine is oxidized to the stable N-oxide more rapidly than the sulfur is oxidized. In this case, where nitrogen is only oxidized, detoxification is not effective since an N-oxide product is also toxic and an excess of active chlorine is required for oxidation at sulfur.<sup>52</sup>



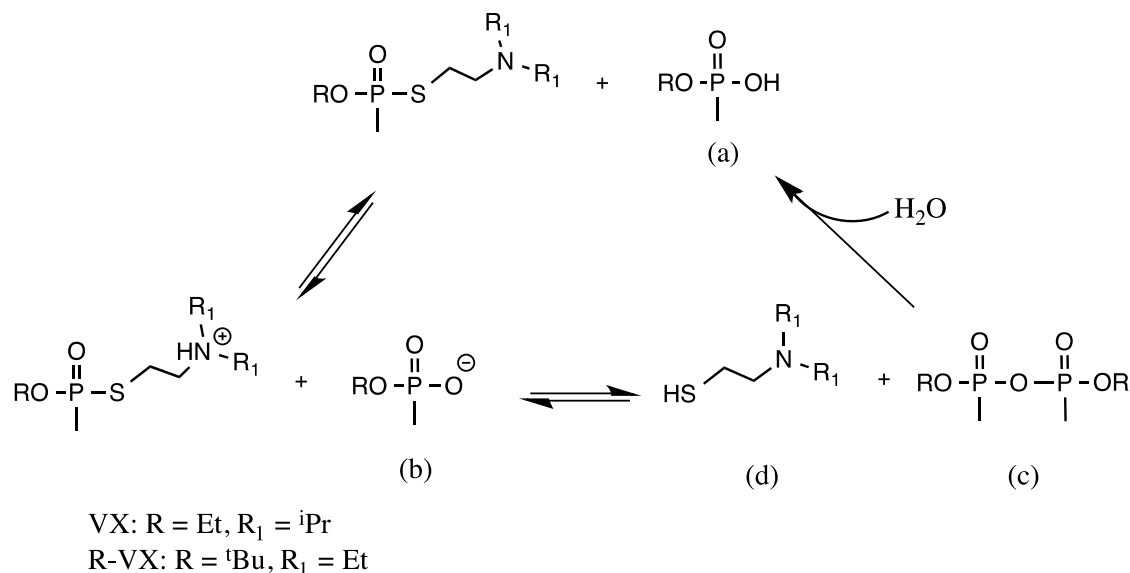
**Scheme 1.13. Reaction of GB (a) and VX (b) with hypochlorite**

The rate of the reaction of sarin with hypochlorite can be increased by the addition of a surfactant. For example, sarin can be completely oxidized within 10 minutes at a sarin/hypochlorite ratio of 20:1 in the presence of CTABr (cetyl trimethylammonium bromide). In the absence of a surfactant, it takes more than 70 minutes.<sup>63</sup>

The number of oxidants containing peroxygen such as *m*-CPBA (*m*-chloroperoxybenzoic acid), peroxyacetic acid, and MMPP (magnesium monoperoxyphthalate) were found to be effective in the oxidation of VX in an aqueous solution.

#### 1.1.5.3.4.3 Autocatalytic Hydrolysis

The V-agents, VX and R-VX, can be completely hydrolyzed within 1-2 months at room temperature to non-toxic products (a) and (d) (Scheme 1.14) in the presence of a stoichiometric amount of water.<sup>64</sup> The reaction is initiated by the attack of the deprotonated phosphonate (b) on protonated VX ( $VXH^+$ ) to produce the diphosphonate intermediate (c). Toxic diphosphonate rapidly undergoes hydrolysis to give acid (a), which is a carrier of the chain reaction.



**Scheme 1.14. Autocatalytic hydrolysis mechanism of VX and R-VX**

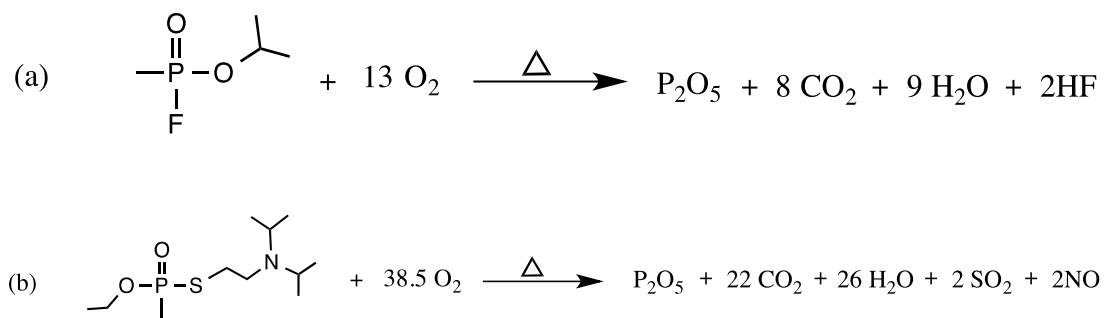
#### 1.1.5.4. Deactivation and Destruction

After World War I and II, large numbers of stockpiled weapons and significant quantities of bulk agents were disposed of or destroyed. Volatile or gaseous chemicals such as phosgene were released into the atmosphere, and chemical weapons were disposed of by burning in an open-pit. The most commonly used methods included dumping them into the sea, and land burial. A very slow release of these chemicals due to containment corrosion led to the contamination of soil and ground water. Also, there is a possibility of a sudden release of nerve agents due to an explosion of sunken munitions. Hence, these methods represent long-term

environmental threats and according to the Chemical Weapons Convention, which was signed on April 29, 1997, these methods are no longer acceptable methods for the destruction of chemical weapons.<sup>65</sup> Other disposal techniques were studied and many of them are still under consideration.<sup>65-67</sup> There are two common methods that the United States uses to dispose of chemical warfare agents and weapons. The primary method is incineration and another method is hydrolysis with supercritical oxidation.

#### 1.1.5.4.1. Incineration

Incineration is an environmentally safe method for toxic waste disposal, provided that the temperature used is sufficiently high for complete decomposition of organic chemicals to simple inorganic chemicals. Incineration of chemical warfare agents will produce hydrogen fluoride (GB), nitrogen oxide (GA and VX), phosphorus pentoxide (GA, GB and VX), and sulfur dioxide (VX). All of these can be removed by scrubbing. The incineration process for GB and VX is shown in Scheme 1.15.



**Scheme 1.15. Incineration process for sarin (a) and VX (b)**

#### 1.1.5.4.2. Neutralization by Base Hydrolysis

Incineration is always an attractive destruction method, but there is always possible danger of emission from the incineration facility. Neutralization is considered the best

alternative to the incineration approach. Neutralization process conditions vary depending on the type of agent to be destroyed. The US army is currently employing two neutralization techniques for stockpile destruction: water hydrolysis followed by biotreatment and water hydrolysis followed by supercritical oxidation.

Water hydrolysis followed by biotreatment was successfully employed at various US army depots including Pueblo Chemical Depot.<sup>68</sup> Mustard gas agents were hydrolyzed using hot water followed by biotreatment, where ordinary bacteria consume neutralization byproducts. In 2003, neutralization followed by supercritical water oxidation was selected as technology to destroy the chemical stockpile at the Blue Grass army Depot in Kentucky.<sup>68</sup> After neutralization and chemical analysis, the hydrolysate was heated to 600-650°C in the presence of air or oxygen (oxidizing agent). Reaction mechanism generally follows free radical pathways that involve oxidative radicals, such as  $\cdot\text{OH}$  and  $\cdot\text{OOH}$ . An organic compound is oxidized to water and sodium carbonate, phosphate, and sulfate. The resulting reaction mass also contains a mixture of gases,  $\text{N}_2$ ,  $\text{O}_2$ ,  $\text{CO}_2$ . Salt separated from an aqueous solution by distillation of water followed by filtration, is then sent to a landfill for disposal.

#### 1.1.5.4.3. Dealkylation

Dealkylation of organophosphate compounds by cleavage of the C-O bond is one of the effective ways of deactivation of OP compounds. The Salen compounds,  $\text{salben}(\text{tBu})[\text{BBr}_2]_2$  and  $\text{salen}(\text{tBu})\text{AlBr}$  (Figure 1.8) can dealkylate CWAs, pesticides and their simulants under very mild conditions.<sup>69</sup> The reactions were conducted in NMR tubes and monitored by the disappearance of the alkoxy peak of the phosphate and appearance of the alkyl peak of the alkyl bromide in the  $^1\text{H}$  NMR spectrum. The percent conversion was calculated from the integration values. For example, with VX the  $\alpha$ -ethoxy proton peak appears as a multiplet centered near  $\delta$  4.15 ppm

prior to reaction with  $\text{salben}(\text{tBu})[\text{BBr}_2]_2$ . After 0.7 h this peak is observed along with the  $\alpha$ -methylene proton peak of ethyl bromide at  $\delta$  3.45 ppm.

$\text{Salben}(\text{tBu})[\text{BBr}_2]_2$  was effective in cleaving only VX whereas GB (Sarin) and GD (Soman) remained practically uncleaved in the 1:1 stoichiometric combinations.  $\text{Salen}(\text{tBu})\text{AlBr}$  showed significant dealkylation for VX, GB, and GD. All of these reactions were conducted in equimolar quantities. It would be expected that much greater dealkylation would take place in shorter periods of time using an excess of the salen reagent.

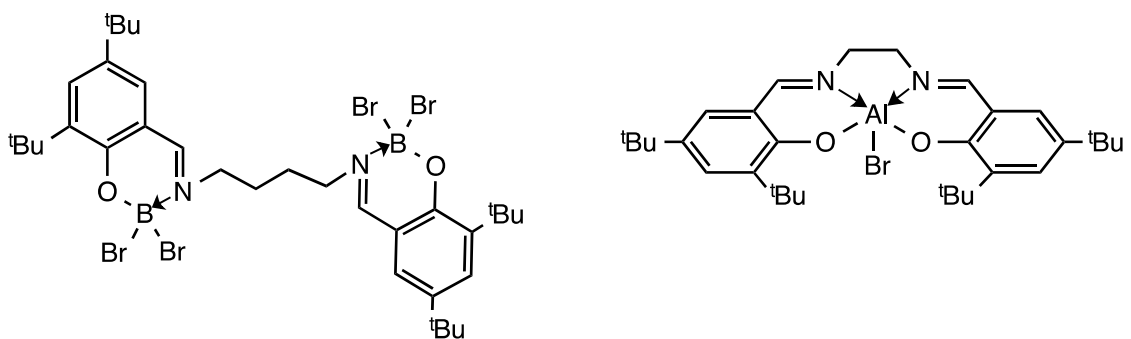
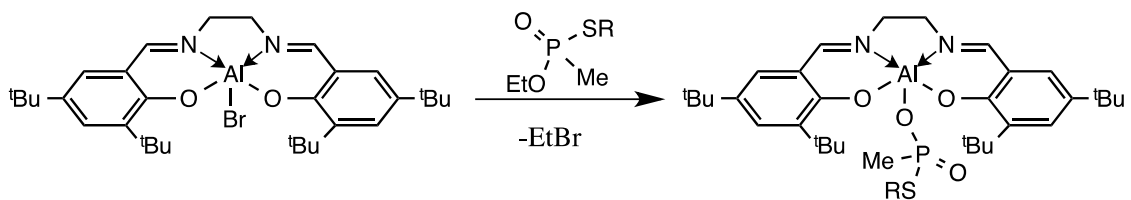


**Figure 1.8.**  $\text{Salben}(\text{tBu})\text{BBr}_2$  and  $\text{salen}(\text{tBu})\text{AlBr}$



**Scheme 1.16.** Dealkylation of VX by  $\text{salen}(\text{tBu})\text{AlBr}$

## Chapter 2 Salen-Supported Aluminum Phosphate Compounds

### 2.1. Introduction

Aluminum phosphate based material have been a subject of recent studies with respect to their potential application as catalysts or catalyst supports, reactive fillers in polymeric composites, analytical and industrial absorbent, flame retardants, etc.<sup>1,70</sup> Polymeric structures formed by self-assembly pathways of aluminophosphate species leading to one-dimensional chain, two-dimensional porous layer, and three-dimensional open-framework materials are of special interest.<sup>71</sup> The synthesis of aluminophosphate polymers is typically carried out by a hydrothermal reaction of  $\text{H}_3\text{PO}_4$  with  $\text{Al}(\text{O}^i\text{Pr})_3$  or aluminumoxohydride in the form of pseudoboehmite, which is a source of aluminum.<sup>72</sup> However, several aluminophosphates of well-defined structures have been obtained by nonaqueous method.<sup>73-75</sup> The dealkylation reaction between trialkylaluminum and diphenylphosphoric acid has been used to synthesize molecular aluminum phosphate.<sup>76</sup> Also, trialkyl aluminum undergoes adduct formation with  $\text{OP}(\text{OSiMe}_3)$  and the subsequent dealkylsilylation reaction to produce molecular aluminophosphate.<sup>77</sup> Most of molecular aluminum phosphate contains a four-coordinated aluminum.  $[(\text{AlO}^i\text{Pr})_2\text{O}_2\text{P}(\text{O}^t\text{Bu})_2]_4$  (five coordinated aluminum)<sup>78</sup> and  $[\text{Al}(\text{O}_2\text{P}(\text{OC}_6\text{H}_5)_2)_3]_n$  (six coordinated aluminum)<sup>76</sup> are some of the examples of higher coordinated aluminum compounds reported in the literature.

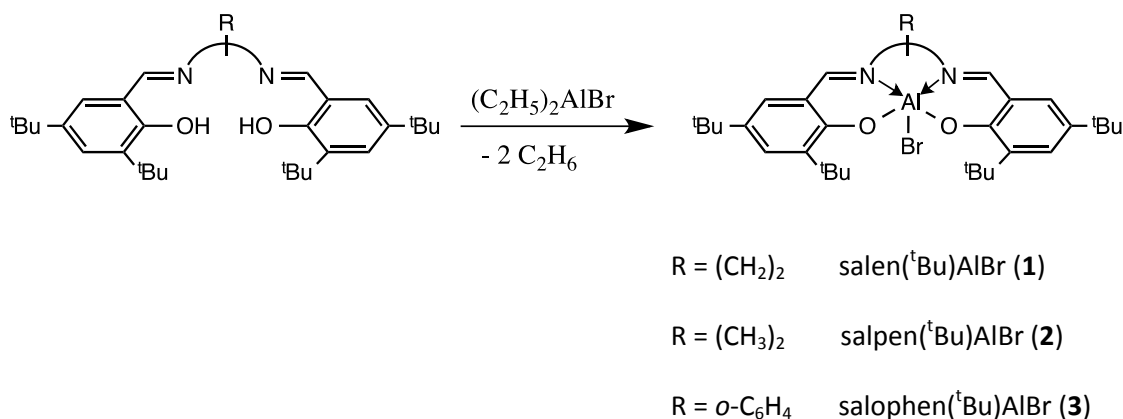
Previously, our research group has shown that mononuclear aluminum Schiff base compounds, Salen(<sup>t</sup>Bu)AlBr (SAB) can effectively dealkylate a wide range of organophosphate compounds<sup>79</sup> including the chemical weapon agents (CWA), VX, GB (sarin) and GD (soman).<sup>69</sup> As one example, the compound salen(<sup>t</sup>Bu)AlBr (SAB-1) cleaved 62% of the phosphate ester groups in GD in just a 1:1 combination. The compound was also active in dealkylating VX and GB.

Dealkylation of phosphate esters using SAB can be viewed as new method for deactivation and decontamination of these compounds.

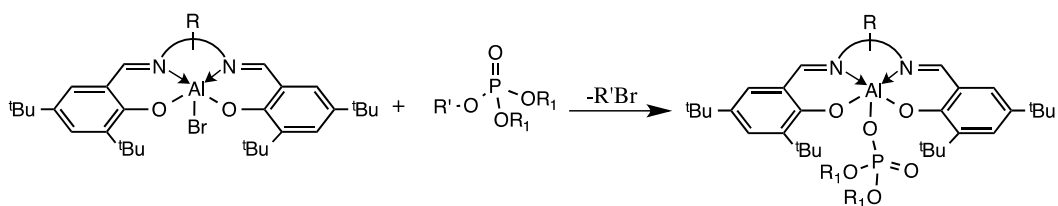
It would be interesting to elucidate the structures of the dealkylated products resulting from the dealkylation of different phosphates with different SAB compounds. In this chapter the synthesis, isolation, structural characterization, and the stability of the dealkylated products is described. Dealkylation reactions were carried out using different stoichiometric ratio of SAB reagent and trialkylphosphate. In these reactions the resulting product is a compound where the dealkylated phosphate ester is covalently bound to the aluminum through Al-O-P linkage.

## 2.2. Synthesis

The salen aluminum bromide compounds **1-3** were prepared by combining diethylaluminum bromide and appropriate salen(<sup>t</sup>Bu)<sub>2</sub>H<sub>2</sub> ligand, according to literature procedure (Scheme 2.1).<sup>79</sup> Dealkylation of different alkyl phosphates was carried out using compounds **1-3** in equimolar ratio to give six coordinated aluminum phosphates, **4-8** (Scheme 2.2). The compounds were isolated by removing solvent under vacuum and purified by recrystallization from hot toluene.



**Scheme 2.1. Synthesis of Salen(<sup>t</sup>Bu)AlBr**



R	R <sub>1</sub>	R'	
(CH <sub>2</sub> ) <sub>2</sub>	CH <sub>3</sub>	CH <sub>3</sub>	[salen( <sup>t</sup> Bu)AlOP(O)(OCH <sub>3</sub> ) <sub>2</sub> ] <sub>n</sub> ( <b>4</b> )
(CH <sub>2</sub> ) <sub>2</sub>	CH <sub>3</sub> CH <sub>2</sub>	CH <sub>3</sub> CH <sub>2</sub>	[salen( <sup>t</sup> Bu)AlOP(O)(OCH <sub>2</sub> CH <sub>3</sub> ) <sub>2</sub> ] <sub>n</sub> ( <b>5</b> )
(CH <sub>2</sub> ) <sub>2</sub>	C <sub>6</sub> H <sub>5</sub>	(CH <sub>2</sub> ) <sub>5</sub> CH <sub>3</sub>	[salen( <sup>t</sup> Bu)AlOP(O)(OPh) <sub>2</sub> ] <sub>n</sub> ( <b>6</b> )
<i>o</i> -C <sub>6</sub> H <sub>4</sub>	CH <sub>3</sub>	CH <sub>3</sub>	[salophen( <sup>t</sup> Bu)AlOP(O)(OCH <sub>3</sub> ) <sub>2</sub> ] <sub>n</sub> ( <b>7</b> )
(CH <sub>2</sub> ) <sub>3</sub>	CH(CH <sub>3</sub> ) <sub>2</sub>	CH(CH <sub>3</sub> ) <sub>2</sub>	[salpen( <sup>t</sup> Bu)Al(O)P(O)(O <sup>i</sup> Pr) <sub>2</sub> ] <sub>2</sub> ( <b>8</b> )

## Scheme 2.2. Formation of Salen aluminum phosphate

### 2.3. Characterization

#### 2.3.1. Spectroscopy

Compounds **4-8** were characterized by NMR, IR, and MS. In <sup>27</sup>Al NMR, no peak was detected for compounds **4-7**. The <sup>27</sup>Al NMR for compound **8** shows two broad peaks. The peak at δ 0.1 ppm represents six-coordinate aluminum and the peak at δ 30 ppm corresponds to five-coordinate aluminum. However, solid-state structure of **8** shows presence of six-coordinate aluminum only. Hence, one phosphate linkage from one of the aluminum atoms dissociate in solution phase making it five-coordinate. This is confirmed by variable-temperature <sup>27</sup>Al NMR. As a temperature of the sample is lowered, intensity of a peak at δ 30 ppm decreased, and eventually disappears at -50°C. The <sup>1</sup>H NMR spectra of **4-8** were very close to the salen aluminum phosphinate analogue, reported previously.<sup>80</sup> <sup>1</sup>H spectra of **4-8** show two singlets for <sup>t</sup>Bu groups of the ligand in the range of δ 1.29 to 1.50 ppm with each peak corresponding to 18 protons. However, there is only one imine singlet in the range of δ 8.3 – 8.8 that indicates

symmetric geometry around ligand backbone for these compounds in solution. There are multiple CH<sub>2</sub> peaks corresponding to the alkylene backbone protons from the ligand. For **4**, **5** and **6** two methylene peaks corresponding to the backbone protons appear at  $\delta$  3.7 and 4.20 ppm. <sup>1</sup>H NMR spectra of compound **8** show multiplet at  $\delta$  2.11, 2.29 and 4.19 corresponding to protons from the ligand backbone (CH<sub>2</sub>CH<sub>2</sub>CH<sub>2</sub>). The <sup>31</sup>P NMR spectra of **4-8** show single peaks at  $\delta$  - 6.58, -8.00, -19.87, -6.94 and -11.16, respectively. These <sup>31</sup>P NMR shifts are upfield from the chemical shifts of corresponding starting trialkylphosphate (Table 2.1), which indicate the shielding of the phosphorus due to coordination to electropositive aluminum. The mass spectra (EI) of **4-8** contained molecular ion peaks for corresponding monomer units. All the compounds have a peak corresponding to the molecular ion minus one of the <sup>t</sup>Bu group, and for compounds **4-6** this is the most abundant peak. The most abundant peak for compound **7** was one corresponding to the molecular ion minus one of the <sup>t</sup>Bu group and phosphate unit, [OP(O)(OMe)<sub>2</sub>]. Mass spectra of compound **8** showed base ion peak form by loss of phosphate unit, [OP(O)(O<sup>i</sup>Pr)<sub>2</sub>] from the molecular ion.

**Table 2.1.** <sup>31</sup>P NMR shifts

Compound	$\delta$ <sup>31</sup> P	Starting alkyl phosphate	$\delta$ <sup>31</sup> P
<b>4</b>	- 6.58	Trimethyl Phosphate	3.01
<b>5</b>	- 8.00	Triethyl Phosphate	- 0.24
<b>6</b>	- 19.88	2-ethylhexyldiphenyl phosphate	- 11.09
<b>7</b>	- 6.94	Trimethyl Phosphate	3.01
<b>8</b>	11.16	Triisoprpyl phosphate	- 3.43

## 2.3.2. Structures

### 2.3.2.1. Polymeric Salen Aluminum Phosphates

The solid-state structures of compounds **5-8** were determined by single-crystal X-ray diffraction. Single crystal suitable for X-ray crystallography was obtained by slow evaporation of either dichloromethane or chloroform solution. Table 2.2 lists selected bond lengths and angles while the data collection parameters are contained in Table A 1. The molecular structure of **7** reveals the formation of polymeric chains of SalenAl unit connected by an O-P-O link (Figure 2.1). A similar kind of polymer formation was observed for compounds **5** and **6**.

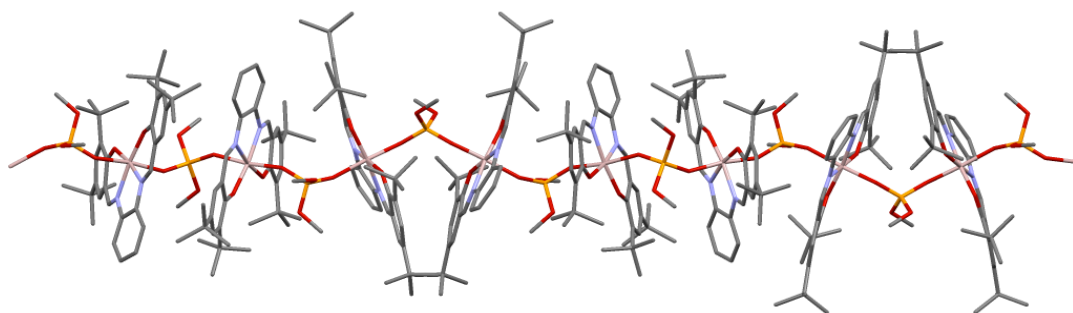


**Figure 2.1. Crystal structure of 7 showing formation of polymer chain**

Compounds **5** and **6** crystallize in orthorhombic space group  $P 2_1 2_1 2_1$  and  $F d d d$ , respectively whereas compound **7** crystallizes in tetragonal space group  $P 4_1 2 2$ . These structures consist of a six-coordinated aluminum atom in a distorted octahedral geometry (Figure 2.2, 2.3 and 2.4). The axial Al-O distances ( $\sim 1.90 - 1.92 \text{ \AA}$ ) are longer than equatorial Al-O distances ( $\sim 1.80 - 1.82 \text{ \AA}$ ) due to the greater steric requirements of the axial groups. The axial O-Al-O bond angles are distorted ( $\sim 171.7 - 174.5^\circ$ ) from ideal linearity. The ligand occupies four equatorial positions and bridging phosphate molecules occupy the two axial positions. Adjacent <sup>t</sup>Bu groups on ligands are arranged in staggered confirmation to reduce steric contact (Figure 2.5). All P atoms have distorted tetrahedral geometry with bond angles ranging from about



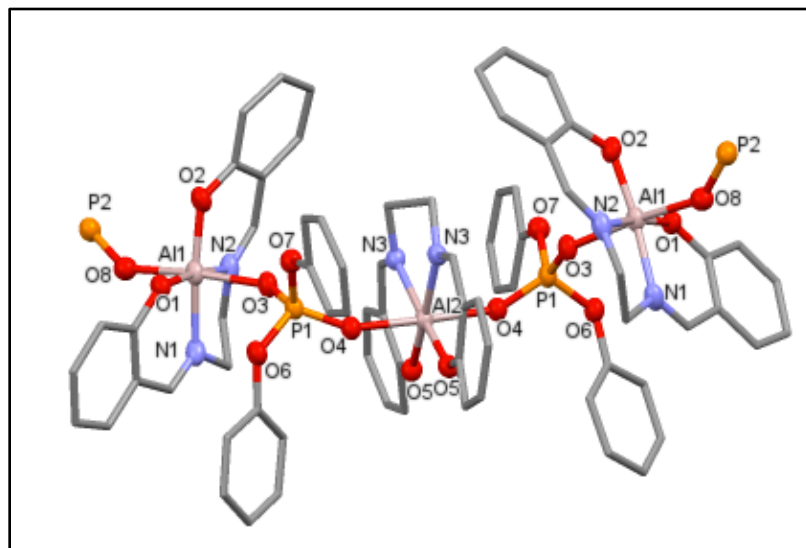


Figure 2.3. Crystal structure of 6 (<sup>t</sup>Bu groups omitted for clarity)

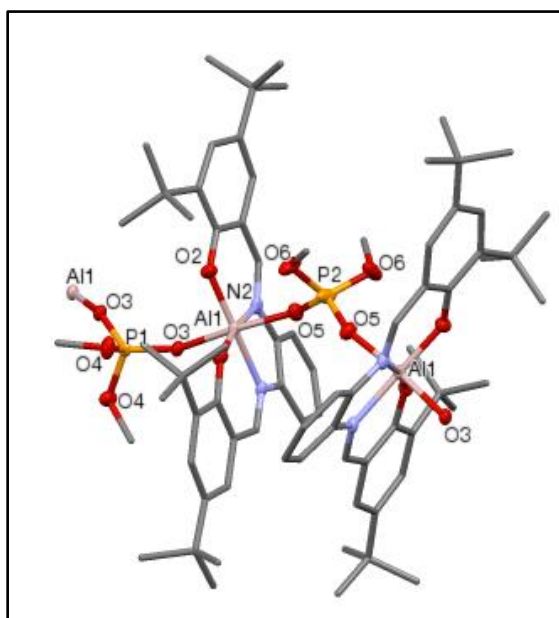
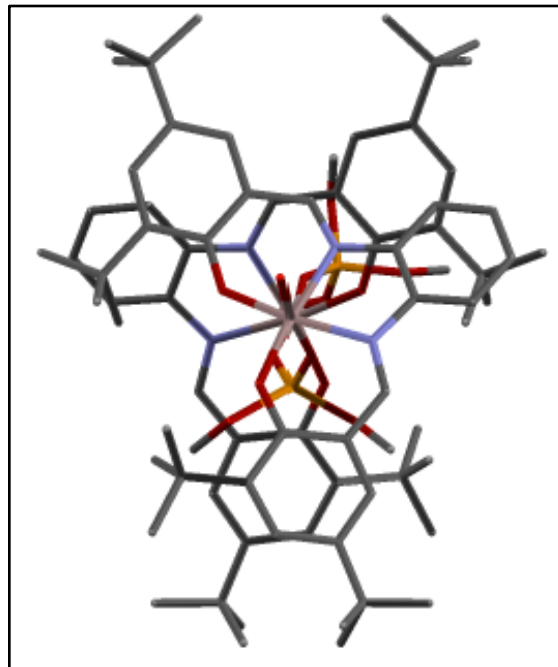


Figure 2.4. Crystal structure of 7



**Figure 2.5. Unit cell of 7 viewed down the c-axis showing staggered confirmation of <sup>t</sup>Bu groups**

### 2.3.2.2. Dimeric Salpen Aluminum Phosphate

The dimeric compound  $[\text{salpen}(\text{tBu})\text{AlOP}(\text{O})(\text{O}^i\text{Pr})_2]_2$  (**8**) resulted from the dealkylation reaction of  $\text{salpen}(\text{tBu})\text{AlBr}$  with triisopropyl phosphate in toluene at room temperature. Selected bond lengths and angles are listed in Table 2.2 and the crystal data collection parameters are shown in Table A 1. Compound **8** crystallizes in the monoclinic space group  $P2_1/c$ . The molecular structure of **8** contains an aluminum-phosphate ring formed by two salen aluminum units and two mono-dealkylated phosphate units (Figure 2.6). Apparently, the flexible nature of the ligand backbones in these compounds allows for the dimerization to occur rather than polymerization. The ring P-O bond distances P1-O3 and P1-O4 (1.4856 and 1.4886 Å respectively) are essentially equal and have double bond character (Table 2.2). The other P-O distances P1-O5 and P1-O6 (1.5735 and 1.5805 Å) are longer and in the range of P-O single bonds.

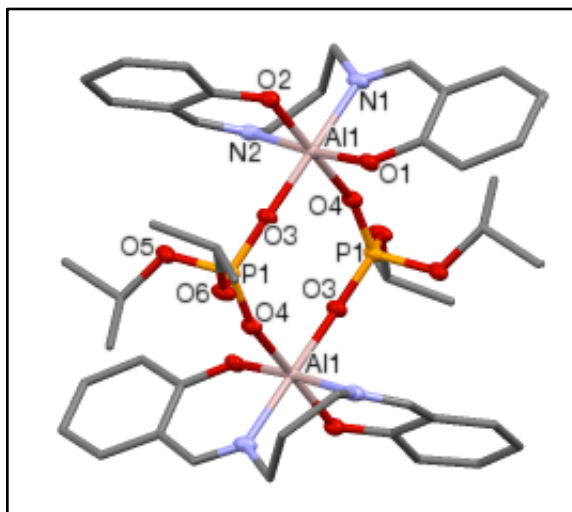


**Figure 2.6. Crystal structure of 8**

Each phosphorus atom is in a distorted tetrahedral geometry. The biggest distortion is found in the O-P-O bond angle ( $118.81^\circ$ ) inside the aluminophosphate ring. Each aluminum atom is six coordinated with distorted octahedral geometry. The phosphate oxygen atoms occupy two of the equatorial positions. A nitrogen atom and an oxygen atom from the ligand occupy the other two equatorial positions. Another pair of nitrogen and oxygen from ligand occupies the axial positions. This is in contrast to polymeric structures discussed in previous section where the phosphate oxygen atoms occupy axial positions, and nitrogen and oxygen atoms from the ligand occupy equatorial positions. The axial Al-O distance ( $1.8277 \text{ \AA}$ ) is slightly shorter than equatorial Al-O distances ( $1.8507$ ,  $1.8625$ ,  $1.8944 \text{ \AA}$ ). However, the axial Al-N2 distance ( $2.0380 \text{ \AA}$ ) is almost equal to the equatorial Al1-N1 ( $2.0356 \text{ \AA}$ ) distance. In Al-O-P linkage, the Al-O-P angles are not equal. Al1-O3-P1 ( $164.11^\circ$ ) is larger than Al1O4-P1 ( $160.31^\circ$ ).

**Table 2.2. Selected bond distances (Å) and angles (°) for compounds 5-8**

<b>Salen(<sup>t</sup>Bu)AlOP(O)(OEt)<sub>2</sub> (5)</b>			
Al(1)-O(2)	1.809(2)	O(2)-Al(1)-O(1)	97.95(9)
Al(1)-O(1)	1.8105(19)	O(2)-Al(1)-O(5)	90.46(9)
Al(1)-O(5)	1.917(2)	O(5)-Al(1)-O(9)	174.50(9)
Al(1)-O(9)	1.9218(19)	O(10)-Al(2)-O(6)	174.58(9)
Al(2)-O(3)	1.802(2)	O(5)-P(1)-O(6)	115.02(11)
Al(2)-O(4)	1.818(2)	O(5)-P(1)-O(7)	111.05(12)
Al(2)-O(10)	1.917(2)	P(1)-O(5)-Al(1)	162.55(14)
Al(2)-O(6)	1.926(2)	P(1)-O(6)-Al(2)	143.86(12)
P(1)-O(5)	1.485(2)	O(10)-P(2)-O(9)	116.03(12)
P(1)-O(6)	1.492(2)	O(10)-P(2)-O(11)	111.09(12)
P(1)-O(8)	1.565(2)	O(9)-P(2)-O(11)	105.98(12)
P(1)-O(7)	1.574(2)	O(10)-P(2)-O(12)	105.3(2)
P(2)-O(10)	1.4850(19)	O(9)-P(2)-O(12)	108.7(4)
P(2)-O(9)	1.485(2)	O(11)-P(2)-O(12)	109.7(3)
P(2)-O(11)	1.576(2)		
P(2)-O(12)	1.582(5)		

**Table 2.2 (Continued)**

<b>Salen(<sup>t</sup>Bu)AlOP(O)(OPh)<sub>2</sub> (6)</b>			
Al(1)-O(1)	1.8028(17)	O(1)-Al(1)-O(2)	96.97(8)
Al(1)-O(2)	1.8034(19)	O(1)-Al(1)-O(3)	93.45(8)
Al(1)-O(8)	1.9460(17)	O(8)-Al(1)-O(3)	171.68(8)
Al(1)-O(3)	1.9524(17)	O(3)-P(1)-O(4)	116.94(9)
Al(2)-O(4)	1.9289 (15)	O(3)-P(1)-O(7)	106.01(10)
Al(2)-O(5)	1.8143 (17)	O(4)-P(1)-O(7)	110.56(9)
P(1)-O(3)	1.4834(17)	O(3)-P(1)-O(6)	111.51(9)
P(1)-O(4)	1.4841(17)	O(4)-P(1)-O(6)	110.07(9)
P(1)-O(7)	1.5843(17)	O(7)-P(1)-O(6)	100.40(9)
P(1)-O(6)	1.5848(17)	P(1)-O(3)-Al(1)	140.04(10)
		P(1)-O(4)-Al(2)	150.25(11)
<b>Salophen(<sup>t</sup>Bu)AlOP(O)(OCH<sub>3</sub>)<sub>2</sub> (7)</b>			
Al(1)-O(1)	1.8161(13)	O(1)-Al(1)-O(2)	96.72(6)
Al(1)-O(2)	1.8234(13)	O(3)-Al(1)-O(5)	172.09(7)
Al(1)-O(3)	1.8999(13)	P(1)-O(3)-Al(1)	150.06(8)
Al(1)-O(5)	1.9000(13)	P(2)-O(5)-Al(1)	148.87(10)
O(3)-P(1)	1.4829(12)	O(3)-P(1)-O(4)	106.62(7)
P(1)-O(4)	1.5730(14)	O(3)-P(1)-O(3)	119.27(10)
O(5)-P(2)	1.4794(13)	O(5)-P(2)-O(6)	104.57(14)
P(2)-O(6)	1.591(4)	O(5)-P(2)-O(5)	119.86(11)
		O(6)-P(2)-O(6)	123.9(3)

**Table 2.2 (Continued)**

<b>Salpen(<sup>t</sup>Bu)AlOP(O)(O<sup>i</sup>Pr)<sub>2</sub> (<b>8</b>)</b>			
Al(1)-O(1)	1.8277(11)	O(1)-Al(1)-O(2)	91.91(5)
Al(1)-O(2)	1.8507(10)	O(1)-Al(1)-O(3)	93.01(5)
Al(1)-O(3)	1.8625(10)	O(3)-Al(1)-O(4)	90.51(5)
Al(1)-O(4)	1.8944(10)	O(2)-Al(1)-O(4)	173.57(5)
Al(1)-N(1)	2.0356(13)	O(3)-Al(1)-N(1)	175.54(5)
Al(1)-N(2)	2.0380(13)	O(1)-Al(1)-N(2)	175.97(5)
O(3)-P(1)	1.4856(10)	O(3)-P(1)-O(4)	118.81(6)
O(4)-P(1)	1.4886(10)	O(3)-P(1)-O(5)	106.60(6)
P(1)-O(5)	1.5735(11)	O(4)-P(1)-O(6)	105.20(6)
P(1)-O(6)	1.5805(10)	O(5)-P(1)-O(6)	106.83(6)
		P(1)-O(3)-Al(1)	164.11(7)
		P(1)-O(4)-Al(1)	160.31(7)

**2.3.2.3. Solution Phase structures**

Gel Permeation Chromatography (GPC) was used to analyze the solution phase structures of compounds **7** and **8**. A GPC chromatogram of **7** (Figure A6 a) showed the formation of dimeric and monomer species in solution phase, in contrast to polymeric or oligomeric species in solid state. However, compound **8** is a dimer in solid state as well as in solution phase (Figure A6 b).

## 2.4. Stability

For effective use of salen aluminum bromide compounds in decontamination of nerve agents, it is necessary that the resulting products of this reaction are nontoxic, easy to handle, and stable in environmental conditions. The significant aspect of the dealkylation of trialkylphosphate using SAB is the formation of the solid compound possessing covalent Al-O-P linkage. The structures of the dealkylated products reported above all show that dealkylated phosphate ester are covalently bound to aluminum center through Al-O bond. Hence, in the decontamination process of nerve agents using SAB reagents, the resulting product would be a compound where the dealkylated nerve agent is bound to the aluminum center through a covalent Al-O-P linkage. Thus, nerve agents can be deactivated and locked into salen units using a dealkylation reaction.

In Al-O-P linkage, the Al-O bond distances (1.86-1.90 Å) are in the range of Al-O covalent bond distance. The P-O bonds (1.48-1.49 Å) have double bond character. The literature reported aluminum (III) meso-tetraphenylporphyrin complex axially bonded to phosphinate has an axial Al-O bond distance of 1.86 Å and is stable in air and moisture.<sup>82</sup> Hence, Al-O-P linkage of resulting dealkylated product would be hydrolytically stable and it is unlikely that the aluminum center will release dealkylated phosphate ester in the presence of water.

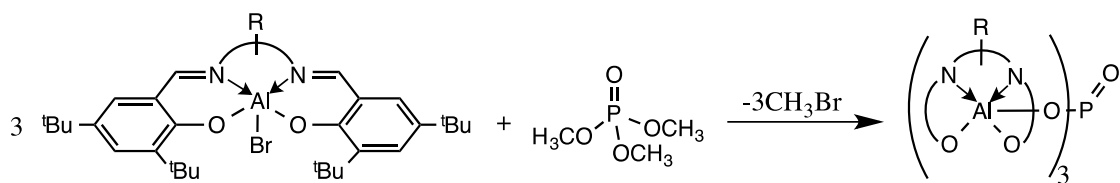
To confirm this assumption, a stability study of the salen aluminum phosphate was carried out. In a typical experiment, compound **4** was suspended in water and resulting yellow slurry stirred for several days. <sup>1</sup>H NMR was used for monitoring the stability of the compound and after three weeks the final compound was isolated by filtration and characterized by <sup>1</sup>H and <sup>31</sup>P NMR, IR, MS (EI, positive), and melting point. The <sup>1</sup>H NMR has peaks corresponding to the

ligand and the methoxy groups of the mono-dealkylated phosphate. No peak corresponding to aldehyde proton was observed suggesting the stability of imine bonds in the ligand backbone. The  $^{31}\text{P}$  NMR has a single peak at  $\delta$  -6.58 which is upfield compared to trimethylphosphate ( $\delta$  3.014) and dimethylphosphonic acid ( $\delta$  6.4).<sup>83</sup> This suggests that phosphorous is coordinated to the electropositive aluminum center through Al-O-P a linkage. Also the presence of only one peak ruled out the release of dealkylated phosphate ester unit by hydrolysis of Al-O bond.

## 2.5. Total Dealkylation

The salen aluminum phosphate compounds discussed in previous sections of this chapter are monodealkylated products. Since the dealkylation reaction was carried out using an equimolar ratio of trialkylphosphate and SAB, only one C-O bond of trialkyl phosphate was cleaved to give monodealkylated product. For the deactivation of nerve agents the breaking of only one C-O bond is required. Hence, the study of the monodealkylated products is important and sufficient enough to explore the possible use of SAB compounds in nerve agent deactivation. However, if a dealkylation reaction is carried out using stoichiometric amounts of the SAB compounds and the trialkylphosphate (3moles of SAB per mole of phosphate), breaking of all three C-O bonds take place to give a fully dealkylated product, [(SalenAlO)<sub>3</sub>PO].

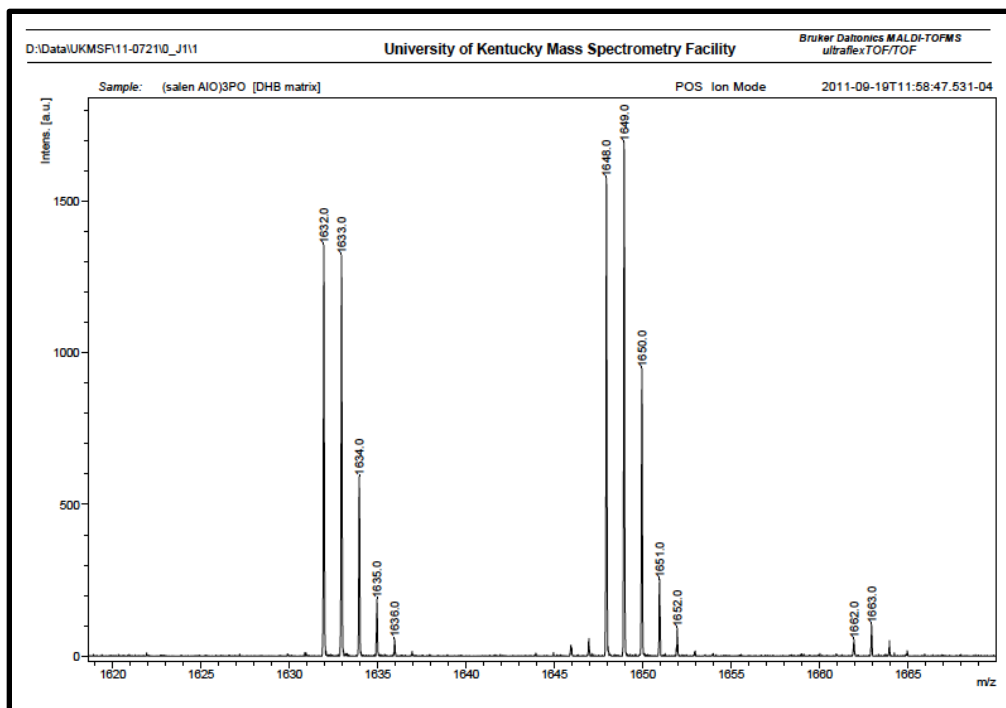
Total dealkylation of trimethyl phosphate was carried out using compounds **1-3** in stoichiometric amounts to give fully dealkylated products, **9-11** (Scheme 2.3). Although attempts to isolate single crystal suitable for X-ray crystallography were not successful,  $^1\text{H}$ , IR, MS (MALDI) analyses support the formation of fully dealkylated phosphate.



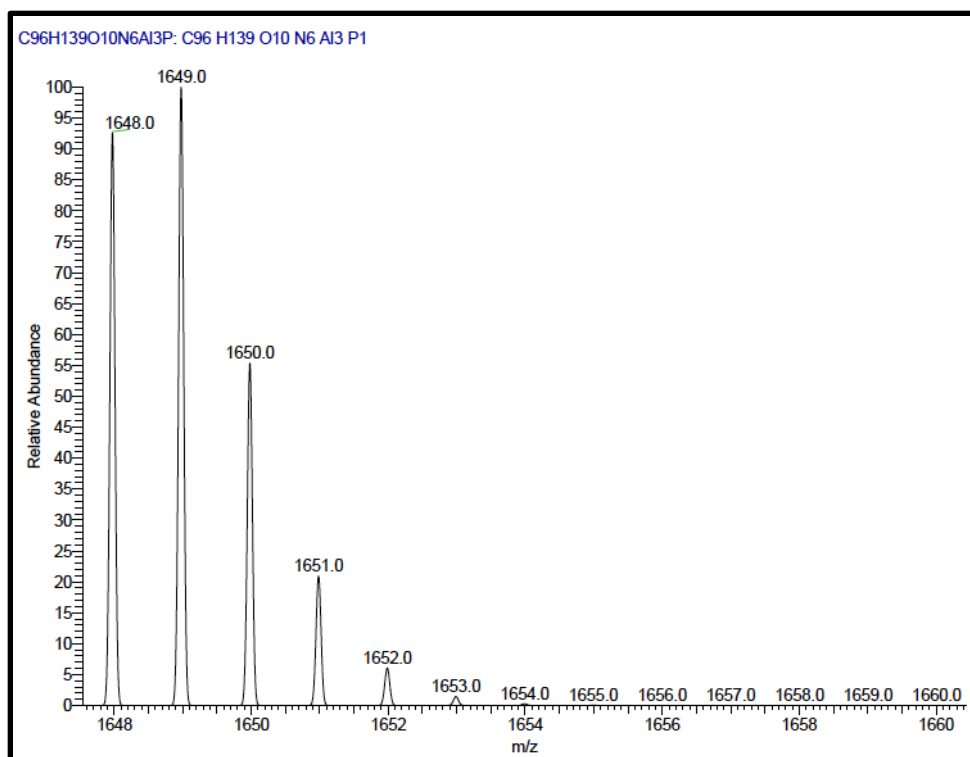
R	
(CH <sub>2</sub> ) <sub>2</sub>	[(Salen( <sup>t</sup> Bu)AlO) <sub>3</sub> PO] ( <b>9</b> )
(CH <sub>2</sub> ) <sub>3</sub>	[(Salpen( <sup>t</sup> Bu)AlO) <sub>3</sub> PO] ( <b>10</b> )
<i>o</i> -C <sub>6</sub> H <sub>4</sub>	[Salophen( <sup>t</sup> Bu)AlO) <sub>3</sub> PO] ( <b>11</b> )

### Scheme 2.3. Total dealkylation of trimethyl phosphate

It was observed that the <sup>1</sup>H NMR spectra have peaks corresponding to the ligand only and no peak corresponding to the methoxy group of phosphate. MALDI mass spectra of the compound **9**, **10**, and **11** show molecular ion peaks at *m/z* 1648, 1705, and 1807, respectively. The isotope pattern from these spectra shows a very good match with the isotope pattern obtained from the simulation experiment. For example, mass spectra of compound **9** (Figure 2.7 A) show six isotope peaks at *m/z* 1648 (93 %), 1649 (100%), 1650 (55 %), 1651 (22 %), 1652 (7 %), and 1653 (2 %), which is in good agreement with isotope simulation for (C<sub>96</sub>H<sub>139</sub>O<sub>10</sub>N<sub>6</sub>Al<sub>3</sub>P), the molecular formula of compound **9** (Figure 2.7 B).



A



B

Figure 2.7. A: MALDI mass spectra of 9; B: Isotope simulation for mol. wt 1648

## 2.6. Conclusion

The resulting products from the dealkylation reaction of a series of trialkylphosphates using Salen(<sup>t</sup>Bu)AlBr compounds have been isolated and fully characterized. These products are soluble aluminum phosphate compounds where salen aluminum complex is axially bonded to dealkylated phosphate molecule. These compounds are building blocks to obtain self-assembled structures. According to the number of methylene units in the salen ligand backbone, resulting products are either chain or ring structures. The dealkylation has an important application in deactivation of nerve agents. This study has highlighted two advantages of this chemistry: 1) In Al-O-P linkage, the Al-O bond distances (1.86-1.90 Å) are in the range of Al-O covalent bond distance. These aluminum phosphate compounds do not decompose in neutral water. Thus, dealkylated OPs will be held strongly by salen units. 2) In packing diagram, both chain and ring structures appear as a column and phosphate units are arranged in the core of this column (Figure A1 and A2). Hence, after deactivation nerve agents can be locked into salen units.

## 2.7. Experimental

**General Remarks.** All air-sensitive manipulations were conducted using standard bench top Schlenk line technique in conjunction with an inert-atmosphere glovebox. All solvents were rigorously dried prior to use. All glassware was cleaned with a base and an acid wash and dried in an oven at 130°C overnight. Compounds Salen(<sup>t</sup>Bu)AlBr (**1**), Salpen(<sup>t</sup>Bu)AlBr (**2**) and Salophen(<sup>t</sup>Bu)AlBr (**3**) were synthesized according to the literature procedure.<sup>79</sup> NMR data were obtained on Varian Inova-400 instrument. Chemical shifts are reported relative to SiMe<sub>4</sub> for <sup>1</sup>H, AlBr<sub>3</sub> in D<sub>2</sub>O for <sup>27</sup>Al and H<sub>3</sub>PO<sub>4</sub> in D<sub>2</sub>O for <sup>31</sup>P and are reported in ppm. Infrared transmission spectra were recorded at room temperature in a potassium bromide pellet on a Fourier transform Smart Omni transmission Nicolet is10 spectrometer.

X-ray data were collected on a Bruker-Nonius X8 Proteum (Cu K $\alpha$  radiation) diffractometer. All calculations were performed using the software package SHELXTL-plus. The structures were solved by direct methods and successive interpretation of difference Fourier maps followed by least squares refinement. All non-hydrogen atoms were refined anisotropically. The hydrogen atoms were included using a riding model with isotropic parameters tied to the parent atom.

Isotopic distribution for the total dealkylated product was calculated using software 'iso2l', 2011 version.

Gel Permeation Chromatography (GPC) analysis was conducted on an Agilent Infinity 1260 HPLC equipped with Polymer Standard Services Suprema Linear S guard column (10  $\mu$ m, 8 X 50 mm) and Suprema Linear S analytical column (10  $\mu$ m, 8 X 300 mm). The eluent was a 1:1 mixture of DMSO: THF at a flow rate of 0.6 mL/min. Relative molecular weights were determined by a calibration curve of polystyrene standards (65,000 Da, 30,000 Da, 13,500 Da, 4,000 Da, 906 Da) as well as phenyl ether (170g/mol). Polystyrene was monitored at a wavelength of 272 nm while diphenyl ether were monitored at 280 nm. Compound **7** and **8** were monitored at 360 nm.

**Synthesis of [Salen(<sup>t</sup>Bu)AlOP(O)(OMe)<sub>2</sub>]<sub>n</sub> (**4**).** To a rapidly stirred solution of Salen(<sup>t</sup>Bu)AlBr (3.0 g, 5.02 mmol) in chloroform trimethyl phosphate (0.7 g, 5.02 mmol) was added. The reaction mixture was stirred for 24 h at room temperature and filtered. The volatiles were removed under vacuum from pale yellow filtrate to give yellow solid, which was purified by recrystallization from toluene. Single crystals suitable for X-ray analysis were grown by slow evaporation of toluene: dichloromethane mixture. Yield: 2.6 g (80.5 %). M.p.: 310-312°C. <sup>1</sup>H NMR (CDCl<sub>3</sub>): 1.27 (s, 18H, C(CH<sub>3</sub>)<sub>3</sub>), 1.46 (s, 18H, C(CH<sub>3</sub>)<sub>3</sub>), 3.08 (d, 6H, phosphate OCH<sub>3</sub>), 3.9 (s,

br, 4H, NCH<sub>2</sub>), 7.04 (d, 2H, Ph-H), 7.53 (d, 2H, Ph-H), 8.38 (s, 2H, N=CH). <sup>31</sup>P[<sup>1</sup>H] NMR(CDCl<sub>3</sub>): δ - 6.58. IR (KBr, cm<sup>-1</sup>): 3041s, 2953w, 2906w, 2867m, 1651w, 1636w, 1550m, 1537m, 1476s, 1464m, 1257w, 1219m, 1075m, 1038w, 974s, 839m, 788m, 752s, 608m, 583m. MS (EI, positive): 642(M<sup>+</sup>, 24%), 585(M<sup>+</sup> - <sup>t</sup>Bu, 100%), 529(M<sup>+</sup> - 2 <sup>t</sup>Bu, 17%), 517(M<sup>+</sup> - OP(O)(OMe)<sub>2</sub>, 7%).

**Synthesis of [Salen(<sup>t</sup>Bu)AlOP(O)(OEt)<sub>2</sub>]<sub>n</sub> (5).** To a rapidly stirred solution of Salen(<sup>t</sup>Bu)AlBr (0.9 g, 1.50 mmol) in chloroform triethyl phosphate (0.27 g, 1.505 mmol) was added. The reaction mixture was stirred for 24 h at room temperature and filtered. The volatiles were removed under vacuum from pale yellow filtrate to give yellow solid, which was purified by recrystallization from toluene. Single crystals suitable for X-ray analysis were grown by slow evaporation of dichloromethane solution. Yield: 0.80 g (80.0%). M.p.: 321°C. <sup>1</sup>H NMR (CDCl<sub>3</sub>): δ 0.84 (t, 6H, phosphate OCH<sub>2</sub>CH<sub>3</sub>), 1.29 (s, 18H, C(CH<sub>3</sub>)<sub>3</sub>), 1.52 (s, 18H, C(CH<sub>3</sub>)<sub>3</sub>), 3.58 (m, 4H, phosphate OCH<sub>2</sub>CH<sub>3</sub>), 3.74 (s, br, 2H, NCH<sub>2</sub>), 4.34 (s, br, 2H, NCH<sub>2</sub>), 7.05 (d, 2H, Ph-H), 7.54 (d, 2H, Ph-H), 8.41 (s, 2H, N=CH). <sup>31</sup>P[<sup>1</sup>H] NMR(CDCl<sub>3</sub>): δ -8.00. IR (KBr, cm<sup>-1</sup>): 3042s, 2956w, 2905w, 2868m, 1648w, 1545w, 1537m, 1477s, 1443m, 1245w, 1169m, 1060m, 965s, 874m, 787m, 753s, 606m, 583m. MS (EI, positive): 670(M<sup>+</sup>, 24%), 613(M<sup>+</sup> - <sup>t</sup>Bu, 100%), 517(M<sup>+</sup> - OP(O)(OEt)<sub>2</sub>, 7%).

**Synthesis of [Salen(<sup>t</sup>Bu)AlOP(O)(OPh)<sub>2</sub>]<sub>n</sub> (6).** To a rapidly stirred solution of salen(<sup>t</sup>Bu)AlBr (1.05 g, 1.75 mmol) in chloroform 2-ethylhexyldiphenyl phosphate (0.636 g, 1.75 mmol) was added. The reaction mixture was stirred for 24 h at room temperature and filtered. The volatiles were removed under vacuum from pale yellow filtrate to give yellow solid. Yield: 0.82 g (61.2%). M.p.: 262°C. <sup>1</sup>H NMR (CDCl<sub>3</sub>): δ 1.32 (s, 18H, C(CH<sub>3</sub>)<sub>3</sub>), 1.48 (s, 18H, C(CH<sub>3</sub>)<sub>3</sub>), 3.68 (s, br, 2H, NCH<sub>2</sub>), 4.25 (s, br, 2H, NCH<sub>2</sub>), 6.75 – 7.02 (m, 10H, P-O-C<sub>6</sub>H<sub>5</sub>), 7.01(d, 2H, Ph-H), 7.55 (d, 2H, Ph-H), 8.32 (s, br, 0 2H, N=CH). <sup>31</sup>P[<sup>1</sup>H] NMR(CDCl<sub>3</sub>): δ -19.88. IR (KBr, cm<sup>-1</sup>): 3064s, 3043s, 2954w,

2903m, 2867m, 1643w, 1594w, 1538w, 1492m, 1477s, 1442m, 1235w, 1207m, 1122m, 941s, 814m, 753,m, 607m. MS (EI, positive): 760(M<sup>+</sup>, 30%), 709(M<sup>+</sup> - <sup>t</sup>Bu, 100%), 633(M<sup>+</sup> - <sup>t</sup>Bu - Ph, 15%), 517(M<sup>+</sup> - OP(O)(OPh)<sub>2</sub>, 18%).

**Synthesis of [Salophen(<sup>t</sup>Bu)AlOP(O)(OMe)<sub>2</sub>]<sub>n</sub> (7).** To a rapidly stirred solution of Salophen(<sup>t</sup>Bu)AlBr (0.84 g, 1.30 mmol) in chloroform trimethyl phosphate (0.18 g, 1.30 mmol) was added. The reaction mixture was stirred for 24 h at room temperature and filtered. The volatiles were removed under vacuum from pale yellow filtrate to give yellow solid, which was purified by recrystallization from toluene hexane mixture. Single crystals suitable for X-ray analysis were grown by slow evaporation of chloroform solution. Yield: 0.68 g (75.8%). M.p.: 344°C. <sup>1</sup>H NMR (CDCl<sub>3</sub>): δ 1.36 (s, 18H, C(CH<sub>3</sub>)<sub>3</sub>), 1.53 (s, 18H, C(CH<sub>3</sub>)<sub>3</sub>), 3.04 (d, 6H, phosphate OCH<sub>3</sub>), 7.191 (d, 2H, Ph-H), 7.37(m, 4H, Ph-H), 7.61 (d, 2H, Ph-H), 8.81 (s, br, 2H, N=CH). <sup>31</sup>P[<sup>1</sup>H] NMR(CDCl<sub>3</sub>): δ -6.94. IR (KBr, cm<sup>-1</sup>): 2950w, 2904m, 2866m, 2359s, 1617w, 1584w, 1531m, 1475s, 388m, 1218w, 1196m, 1051m, 863s, 846m, 594,m, 564s. MS (EI, positive): 690(M<sup>+</sup>, 63%), 675(M<sup>+</sup> - CH<sub>3</sub>, 96%), 550(M<sup>+</sup> - CH<sub>3</sub> - OP(O)(OCH<sub>3</sub>)<sub>2</sub>, 100%).

**Synthesis of [Salpen(<sup>t</sup>Bu)AlOP(O)(O<sup>i</sup>Pr)<sub>2</sub>]<sub>2</sub> (8).** To a rapidly stirred solution of salpen(<sup>t</sup>Bu)AlBr (1.43 g, 2.33 mmol) in chloroform triisopropyl phosphate (0.52 g, 2.33 mmol) was added. The reaction mixture was stirred for 24 h at room temperature and filtered. The volatiles were removed under vacuum from pale yellow filtrate to give yellow solid, which was purified by recrystallization from toluene. Yield: 1.0 g (60.24 %). M.p.: 248 °C. <sup>1</sup>H NMR (CDCl<sub>3</sub>): δ 0.91 (d, 12H, phosphate OCH(CH<sub>3</sub>)<sub>2</sub>), 1.29 (s, 18H, C(CH<sub>3</sub>)<sub>3</sub>), 1.48 (s, 18H, C(CH<sub>3</sub>)<sub>3</sub>), 2.21 (m, 1H, CH<sub>2</sub>CH<sub>2</sub>CH<sub>2</sub>), 2.29 (m, 1H, CH<sub>2</sub>CH<sub>2</sub>CH<sub>2</sub>), 3.68 (m, 2H, phosphate OCH(CH<sub>3</sub>)<sub>2</sub>), 4.19 (m, 4H, NCH<sub>2</sub>), 7.02 (d, 2H, Ph-H), 7.50 (d, 2H, Ph-H), 8.27 (s, 2H, N=CH). <sup>31</sup>P [<sup>1</sup>H] NMR (CDCl<sub>3</sub>): δ -11.16. IR (KBr, cm<sup>-1</sup>): 3064s, 3031s, 2958w, 2898m, 2869m, 1640w, 1626w, 1551m, 1467s, 1441m, 1325w,

1263w, 1171m, 1013m, 994s, 840m, 540s. MS (EI, positive): 712( $M^+$ , 7%), 530( $M^+$  - OP(O)( $O^iPr$ )<sub>2</sub>, 100%).

**Synthesis of (Salen(<sup>t</sup>Bu)AlO)<sub>3</sub>PO (9).** To a rapidly stirred solution of salen(<sup>t</sup>Bu)AlBr (0.42 g, 0.70 mmol) in chloroform trimethyl phosphate (0.033 g, 0.23 mmol) was added. The reaction mixture was stirred for 24 h at room temperature and filtered. The volatiles were removed under vacuum from pale yellow filtrate to give yellow solid, which was purified by recrystallization from toluene hexane mixture. Yield: 0.3 g (76.92 %). <sup>1</sup>H NMR (CDCl<sub>3</sub>): δ 1.30 (s, 18H, C(CH<sub>3</sub>)<sub>3</sub>), 1.48 (s, 18H, C(CH<sub>3</sub>)<sub>3</sub>), 3.80 (s, br, 4H, NCH<sub>2</sub>), 7.05 (d, 2H, Ph-H), 7.52 (d, 2H, Ph-H), 8.3 (s, 2H, N=CH). IR (KBr, cm<sup>-1</sup>): 2962m, 2905m, 2866m, 1648s, 1628s, 1544m, 1475m, 1444m, 1421w, 1390w, 1361w, 1310w, 1257w, 1180w, 867w. MS (MALDI, positive): 1648( $M^+$ , 100%), 1632( $M^+$  - CH<sub>3</sub>, 90%).

**Synthesis of (Salpen(<sup>t</sup>Bu)AlO)<sub>3</sub>PO (10).** To a rapidly stirred solution of salpen(<sup>t</sup>Bu)AlBr (0.95 g, 1.55 mmol) in chloroform trimethyl phosphate (0.072 g, 0.52 mmol) was added. The reaction mixture was stirred for 24 h at room temperature and filtered. The volatiles were removed under vacuum from pale yellow filtrate to give yellow solid, which was purified by recrystallization from toluene hexane mixture. Yield: 0.6 g (68.96 %). <sup>1</sup>H NMR (CDCl<sub>3</sub>): δ 1.30 (s, 18H, C(CH<sub>3</sub>)<sub>3</sub>), 1.50 (s, 18H, C(CH<sub>3</sub>)<sub>3</sub>), 2.23 (m, 2H, CH<sub>2</sub>CH<sub>2</sub>CH<sub>2</sub>), 3.65 (s, br, 2H, NCH<sub>2</sub>), 4.02 (s, br, 2H, NCH<sub>2</sub>), 7.02 (d, 2H, Ph-H), 7.50 (d, 2H, Ph-H), 8.23 (s, 2H, N=CH). IR (KBr, cm<sup>-1</sup>): 3064s, 3031s, 2956w, 2908m, 2866m, 1640w, 1626w, 1551m, 1467s, 1441m, 1325w, 1263w, 1171m, 1013m, 994s, 840m, 540s. MS (MALDI, positive): 1750 ( $M^+$  + CH<sub>3</sub>, 100%), 1188 ( $M^+$  - salen, 10%), 531 (SalenAl, 15%).

**Synthesis of (Salophen(<sup>t</sup>Bu)AlO)<sub>3</sub>PO (11).** To a rapidly stirred solution of salophen(<sup>t</sup>Bu)AlBr (0.77 g, 1.2 mmol) in chloroform trimethyl phosphate (0.056 g, 0.40 mmol) was added. The reaction

mixture was stirred for 24 h at room temperature and filtered. The volatiles were removed under vacuum from pale yellow filtrate to give yellow solid, which was purified by recrystallization from toluene hexane mixture. Yield: 0.5 g (70.4%).  $^1\text{H NMR}$  ( $\text{CDCl}_3$ ):  $\delta$  1.25 (s, 18H,  $\text{C}(\text{CH}_3)_3$ ), 1.42 (s, 18H,  $\text{C}(\text{CH}_3)_3$ ), 6.80 (m, 2H, Ph-H), 7.20 (d, 2H, Ph-H), 7.40 (m, 2H, Ph-H), 7.55 (d, 2H, Ph-H), 8.4 (s, 2H, N=CH). IR (KBr,  $\text{cm}^{-1}$ ): 3064s, 3031s, 2961w, 2905m, 2869m, 1635w, 1626w, 1445, 1441m, 1325w, 1263w, 1171m, 1013m, 994s, 865w, 847m, 785s, 757w, 610m. MS (MALDI, positive): 1807 ( $\text{M}^+ + \text{CH}_3$ , 20%), 1256 ( $\text{M}^+ - \text{salen}$ , 100%)

**Aqueous Stability study:** Nitrogen was bubbled through deionized water at atmospheric pressure and 25°C for an indicated time. Initial pH was 6.7.  $\text{Salen}(\text{tBu})\text{AlOP}(\text{O})(\text{OMe})_2$  (2.0 g, 3.1 mmol) was added to 20 mL of water and stirred for 3 weeks under  $\text{N}_2$  atmosphere. Yellow slurry was filtered and washed with water. Recovery: 1.9 g (95 %). M.p.: 309° - 312° C.  $^1\text{H NMR}$  ( $\text{CDCl}_3$ ): 1.27 (s, 18H,  $\text{C}(\text{CH}_3)_3$ ), 1.46 (s, 18H,  $\text{C}(\text{CH}_3)_3$ ), 3.08 (d, 6H, phosphate  $\text{OCH}_3$ ), 3.9 (s, br, 4H,  $\text{NCH}_2$ ), 7.04 (d, 2H, Ph-H), 7.53 (d, 2H, Ph-H), 8.38 (s, 2H, N=CH). IR (KBr,  $\text{cm}^{-1}$ ): 3447w, 3041s, 2953w, 2906w, 2867m, 1651w, 1636w, 1550m, 1537m, 1476s, 1464m, 1257w, 1219m, 1075m, 1038w, 974s, 839m, 788m, 752s, 608m, 583m. MS (EI, positive): 642( $\text{M}^+$ , 24%), 585( $\text{M}^+ - \text{tBu}$ , 100%), 529( $\text{M}^+ - 2 \text{tBu}$ , 17%), 517( $\text{M}^+ - \text{OP}(\text{O})(\text{OMe})_2$ , 7%).

## Chapter 3 Water-Soluble Salen Aluminum Compounds

### 3.1. Introduction

Typical Salen ligands prepared by condensation of salicylaldehyde or its derivatives with ethylenediamine or its derivatives are insoluble in water. By incorporating hydrophilic groups, such as a sulfonate group or a carboxylic group, around the phenol portion of the ligand, the ligands can be made highly soluble in water. The first synthesis of water-soluble salen complexes was published in 1955.<sup>84,85</sup> The metal complexes of the salen sulfonate ligand were prepared by first sulfonating the preformed salen ligand with concentrated  $\text{H}_2\text{SO}_4$ , complexing the produced sulfonic acid derivative of salen with the desired metal salt in EtOH, and finally neutralizing the sulfonic acid groups with NaOH to form the disodium salt of the sulfonated complex. The imine bonds in the salen structure are sensitive to hydrolysis in acidic conditions. Hence, very poor yields are observed in this method. In the alternative method, reported in 1956,<sup>86</sup> the sodium salt of the sulfonated salicylaldehyde was used as a starting material. This aldehyde was condensed with ethylenediamine in EtOH– $\text{H}_2\text{O}$  to form the desired ligand directly as disodium salt.

Evans and coworkers have widely used this method for the preparation of sulfonated salen complexes and their analogues, which were used for studies on singlet oxygen in aqueous solutions.<sup>87-89</sup> Co(sulfosalen) complex and its derivatives were prepared in a similar way, and their reactions with dioxygen were studied.<sup>90</sup> Very recently, chiral sulfonato-salen type complexes of Ni(II), Cu(II) and Zn(II) synthesized by using the same strategy were published.<sup>91</sup> In addition to the sulfonate group, other hydrophilic groups like an ammonium group or a carboxylic acid carboxylate group have been reported in the literature to produce a water-soluble salen ligand.<sup>92,93</sup> Water-soluble Schiff base complexes have also been used as DNA

cleavage catalysts. Many anionic and cationic water-soluble salen complexes have been synthesized for these<sup>93,94</sup> and other purposes.<sup>95</sup>

While studying the dealkylation of organophosphates using aluminum Schiff base chelates, our ultimate goal is to make these compounds practically useful in the destruction of nerve agents and pesticides. The series of SAB-X reported earlier is useful only in non-coordinating polar solvents for the dealkylation of phosphates. However, for possible application of these compounds in destruction and decontamination of nerve agents and pesticides, the dealkylation should be carried out in water. A major difficulty in conducting these reactions in water is the hydrophobic nature of salen(<sup>t</sup>Bu)AlBr. So our primary aim is to prepare water-soluble compounds. This chapter describes the preparation and characterization of water-soluble group 13 salen complexes.

Although the salen aluminum bromide compounds dealkylate organophosphates compounds effectively in non-nucleophilic solvents, they might not be very effective in strong donor solvents like methanol or water. It would be interesting to study the dealkylation of organophosphates in different nucleophilic or donor solvents. This chapter also includes the study of dealkylation of phosphate in different Lewis basic solvents using Salen(<sup>t</sup>Bu)AlBr.

### **3.2. Dealkylation in Lewis Basic Solvents**

Previously, we have seen that chelated aluminum compounds, Salen(<sup>t</sup>Bu)AlBr, dealkylate a series of organophosphate esters by cleavage of the P-O-C linkage.<sup>79</sup> However, this study was carried out only in non-coordinating polar solvents (e.g. chloroform). In order to see the effect of coordinating solvents, dealkylation of trimethyl phosphate was carried out in different Lewis basic solvents. Salen(<sup>t</sup>Bu)AlBr and trimethyl phosphate were stirred in different solvents for 24 hours and the resulting product was separated by filtration. Solvents that can

coordinate through oxygen atom, nitrogen atom are used in experiment. To compare the percentage of the dealkylation, the reaction was repeated in chloroform (non-coordinating solvent). Percentage yield is shown in Table 3.1.

**Table 3.1. Percent Dealkylation of trimethyl phosphate in Lewis basic solvents**

Solvent	Trimethyl Phosphate		Nerve Agent VX	
	%	Time (h)	%	Time (h)
CHCl <sub>3</sub>	96	24	57	4
MeCN	57	24	15	9
THF	66	24		
DMF	22	24		
MeCN + H <sub>2</sub> O (1:1)	56	24		

In Lewis basic solvents, dealkylation of trimethyl phosphate is low compared to chloroform. Lower percentage yield of the dealkylated product in Lewis basic solvents can be explained with the help of the mechanism of the reaction. According to the proposed

mechanism,<sup>79</sup> Salen(<sup>t</sup>Bu)AlBr forms a cation through coordination of a Lewis basic phosphate to the aluminum center with the displacement of a bromide anion. This activates the  $\alpha$ -carbon of the phosphate for nucleophilic attack of the bromide (Figure 3.1). When the dealkylation reaction is carried out in Lewis basic solvents, the solvent molecules compete with phosphate molecules to coordinate to the aluminum center. It results in blocking of the coordination site of aluminum. SalenAlX (X = Br<sup>-</sup> or OTs<sup>-</sup>) combinations with Lewis basic solvents, such as H<sub>2</sub>O, methanol, or THF, are known to produce six-coordinated derivatives, several of which have been structurally characterized.<sup>96</sup>

Note that all of these reactions were conducted in equimolar quantities and were stopped after 24 hours. It may be possible that with a longer reaction time and using an excess of the salen chelate we might observe a much greater percent dealkylation.

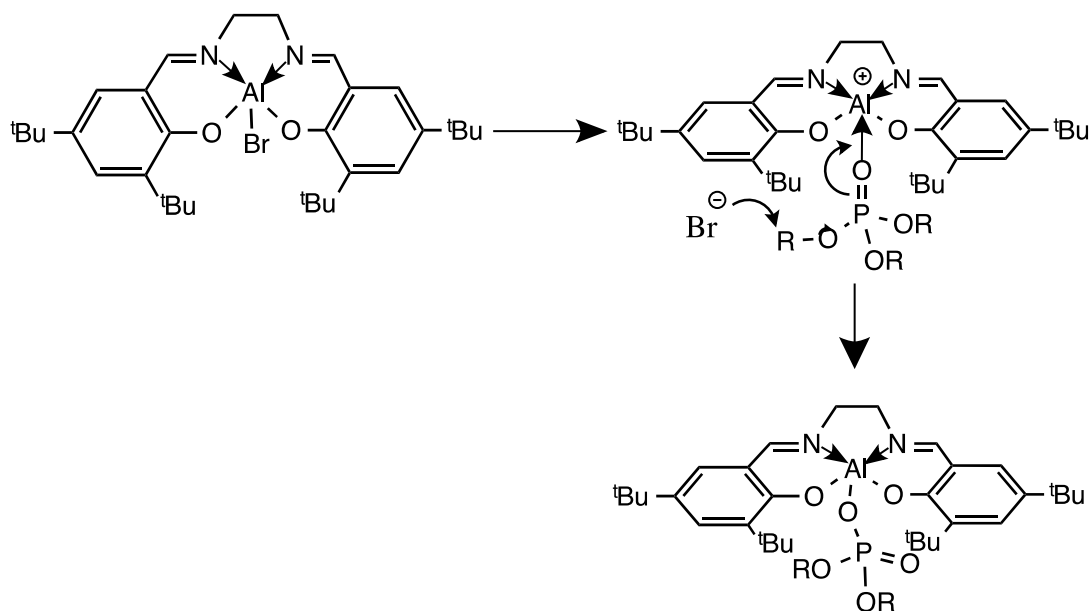


**Figure 3.1.** Dealkylation pathway of organophosphates with Salen(<sup>t</sup>Bu)AlBr compounds

In an attempt to get a preliminary idea of the dealkylation of organophosphate nerve agents in Lewis basic solvents, dealkylation of VX was carried out in acetonitrile. The reaction was carried out in an NMR tube in CD<sub>3</sub>CN by using stoichiometric amounts of the Salen(<sup>t</sup>Bu)AlBr and VX. HMPA was used as an internal standard for <sup>31</sup>P NMR. In an NMR spectrum of a starting reaction mixture, two <sup>31</sup>P peaks were observed at δ 23 and 52 corresponding to VX and HMPA, respectively (Figure 3.2). After 9 hours a new peak at δ 10 was observed. Previously, it was observed that HMPA is inert and Salen(<sup>t</sup>Bu)AlBr does not show any activity towards cleaving a P-N-C bond in HMPA.<sup>69</sup> Hence, formation of the new peak confirms the dealkylation of VX. The percent conversion was calculated from integration of the remaining phosphate and dealkylated product. Only 15% conversion was observed after 9 hours, as opposed to 57% conversion after 4 hours when the reaction was carried out in CDCl<sub>3</sub>. The reaction had to stop due to the formation of a precipitate.

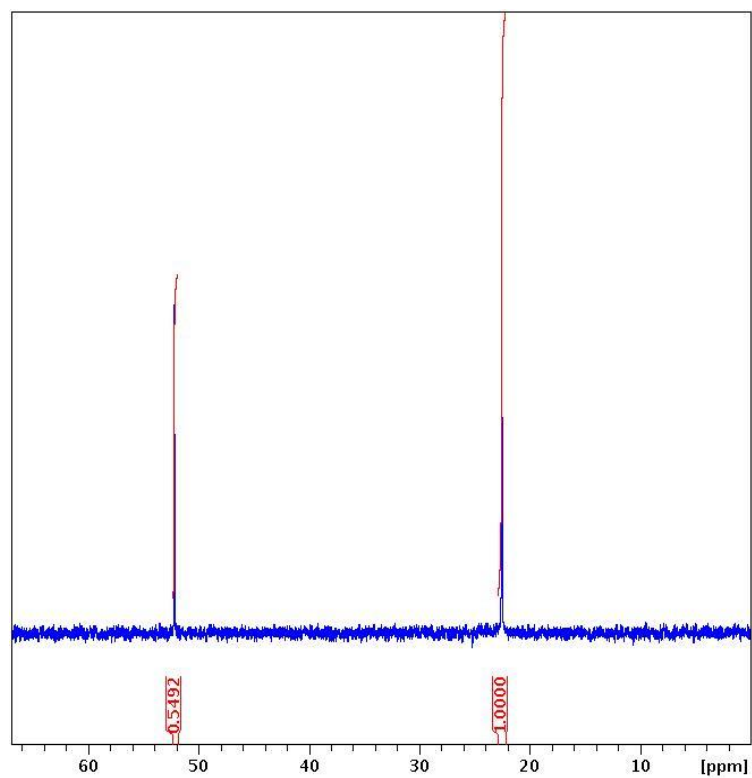
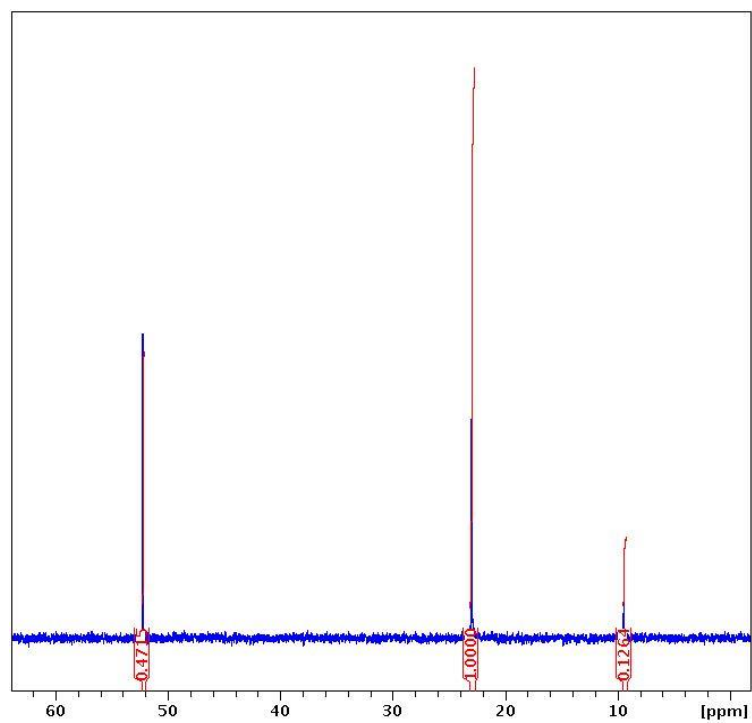


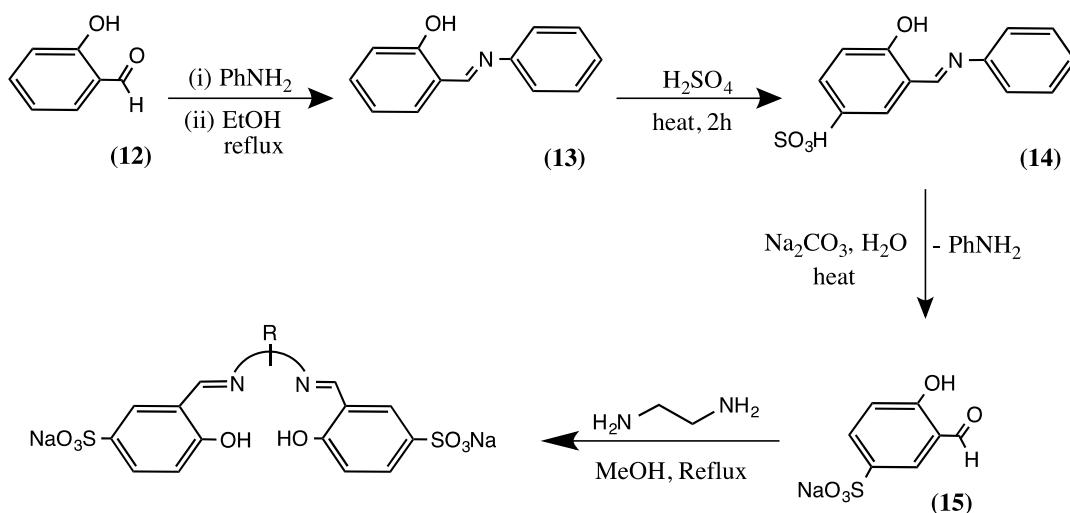
Figure 3.2.  $^{31}\text{P}$  NMR of dealkylation of VX with salen(<sup>t</sup>Bu)AlBr ; top: at t = 0 h; bottom: at t = 9 h

### 3.3. Water-Soluble Salen Compounds

Salen(<sup>t</sup>Bu)AlBr dealkylates organophosphate compounds in non-coordinating polar solvents with high conversion rate at room temperature. However, for possible application of these compounds in destruction and decontamination of nerve agents and pesticides, the dealkylation should be carried out in water. A major difficulty in conducting these reactions in water is the hydrophobic nature of salen(<sup>t</sup>Bu)AlBr. So our primary aim is to prepare water-soluble compounds. This could be achieved by introducing sulfonate groups into salen ligand. In the previous section, we have seen that in an acetonitrile-water mixture, salen(<sup>t</sup>Bu)AlBr dealkylates trimethyl phosphate to some extent. Hence creation of water stable system might prove useful to carry out dealkylation in water.

#### 3.3.1. Synthesis

The water-soluble salen ligands (**16-18**) were prepared by condensation of salicylaldehyde-5-sulfonate (**15**) with appropriate diamine following the literature procedure (Scheme 3.1).<sup>97</sup> Salicylaldehyde-5-sulfonate (**15**) was selectively prepared by sulfonation of protected aldehyde (**14**) and characterized by <sup>1</sup>H NMR, IR, MS (EI positive) and X-ray analyses. Salen group 13 complexes **19-24** were prepared in quantitative yield by combining the Salen(SO<sub>3</sub>Na)<sub>2</sub> (**16-18**) with aluminum and gallium nitrate.

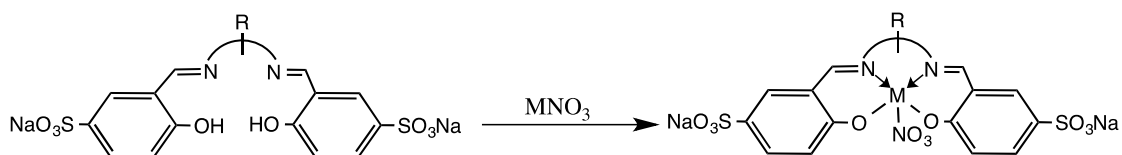


$\text{R} = (\text{CH}_2)_2$     **salen(SO<sub>3</sub>Na)H<sub>2</sub> (16)**

$\text{R} = (\text{CH}_3)_2$     **salpen(SO<sub>3</sub>Na)H<sub>2</sub> (17)**

$\text{R} = o\text{-C}_6\text{H}_4$     **salophen(SO<sub>3</sub>Na)H<sub>2</sub> (18)**

**Scheme 3.1. Synthesis of Salen(SO<sub>3</sub>Na)H<sub>2</sub>**



<b>R</b>	<b>M</b>	
(CH <sub>2</sub> ) <sub>2</sub>	Al	salen(SO <sub>3</sub> Na)AlNO <sub>3</sub> <b>(19)</b>
(CH <sub>2</sub> ) <sub>3</sub>	Al	salpen(SO <sub>3</sub> Na)AlNO <sub>3</sub> <b>(20)</b>
<i>o</i> -C <sub>6</sub> H <sub>4</sub>	Al	salophen(SO <sub>3</sub> Na)AlNO <sub>3</sub> <b>(21)</b>
(CH <sub>2</sub> ) <sub>2</sub>	Ga	salen(SO <sub>3</sub> Na)GaNO <sub>3</sub> <b>(22)</b>
(CH <sub>2</sub> ) <sub>3</sub>	Ga	salpen(SO <sub>3</sub> Na)GaNO <sub>3</sub> <b>(23)</b>
<i>o</i> -C <sub>6</sub> H <sub>4</sub>	Ga	salophen(SO <sub>3</sub> Na)GaNO <sub>3</sub> <b>(24)</b>

**Scheme 3.2. Synthesis of Salen(SO<sub>3</sub>Na)MNO<sub>3</sub>**

### 3.3.2. Characterization

The preparation of water-soluble salen ligand is shown in Scheme 3.1. The approach to ligand **16** requires sulfonation of the salicylaldehyde and then coupling with the ethylenediamine. Sulfonation of protected aldehyde **13** selectively produced the *para*-sulfonated compound **14**, as confirmed by  $^1\text{H}$  NMR. Deprotection of the aldehyde group of compound **14** gave compound **15**, which was characterized by  $^1\text{H}$  NMR, IR, and mass spectrometry. Water-soluble ligands **16-18** were prepared by condensation of two molecules of **15** with a molecule of appropriate diamine. Water-soluble ligands **16-18** were successfully converted into their aluminum and gallium complexes by treatment with corresponding nitrate.

$^1\text{H}$  NMR spectra of compound **15** showed doublet of doublet at  $\delta$  7.65 and two doublets at  $\delta$  6.71 and 7.89 corresponding to protons of a phenyl ring. A singlet corresponding to aldehyde proton was observed at  $\delta$  10.1. The mass spectra (ESI) of **15** show a single peak at  $m/z$  201, which corresponds to the molecular ion minus sodium ion. The solid-state structure of compounds **15** was determined by single-crystal X-ray diffraction. Single crystals suitable for X-ray crystallography were obtained from water by slow evaporation. Table 3.1 lists selected bond lengths and angles while the data collection parameters are contained in Table A 1. Figure 3.3 shows the molecular structure for compound **15**. The structure of **15** contained  $\text{SO}_3\text{Na}$  group in a *para* position with respect to the aldehyde group. Also, it shows two water molecules associated with sodium ion.

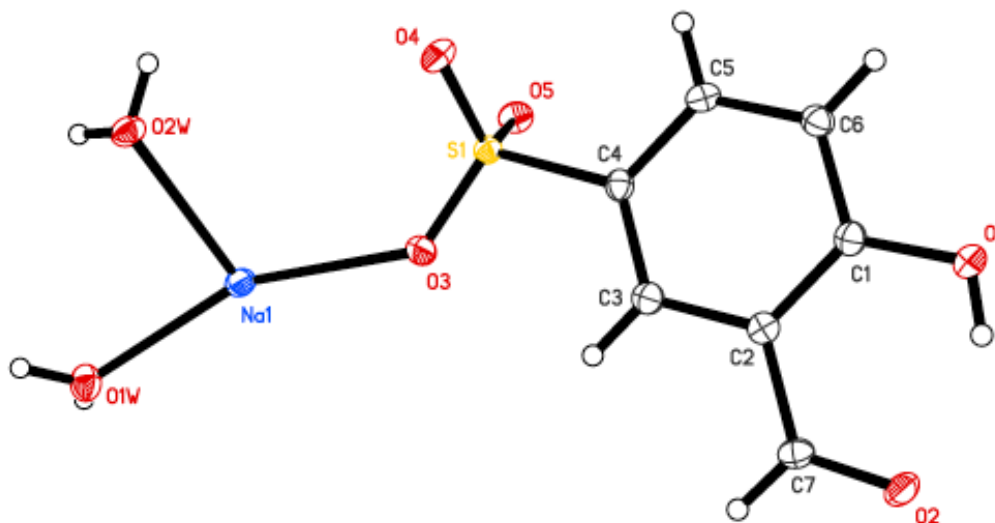


Figure 3.3. Crystal structure of 15

Table 3.1. Selected bond distances (Å) and angles (°) for 15

S(1)-O(3)	1.4541(19)	O(3)-S(1)-O(4)	113.32(11)
S(1)-O(4)	1.4637(19)	O(3)-S(1)-O(5)	112.22(11)
S(1)-O(5)	1.4655(18)	O(4)-S(1)-O(5)	112.41(11)
S(1)-C(4)	1.772(2)	S(1)-O(3)-Na(1)	132.31(11)
Na(1)-O(3)	2.355(2)	O(3)-Na(1)-O(1W)	156.09(8)
Na(1)-O(1W)	2.329(2)	O(3)-Na(1)-O(2W)	107.01(8)
Na(1)-O(2W)	2.347(2)	O(2W)-Na(1)-O(1W)	90.24(8)

Water-soluble ligands (**16-18**) were characterized by  $^1\text{H}$  NMR, IR and MS.  $^1\text{H}$  spectra for **16-18** contained only one imine singlet for each compound in the range of  $\delta$  8.3 – 8.9. For the compounds **16** and **17** the peaks corresponding to the  $\text{CH}_2$  protons of the ligand backbone appears in the range of  $\delta$  1.55 – 4.15. The IR spectra showed strong absorption due to  $\nu_{\text{C=N}}$  at 1634, 1636 and 1621  $\text{cm}^{-1}$  and medium absorption due to  $\nu_{\text{S=O}}$  at 1357, 1367 and 1373 for **16-18**, respectively. In the mass spectra (EI), all three compounds had a peak corresponding to the molecular ion minus sodium. All three ligands show very good water solubility, but are not stable in water. When  $^1\text{H}$  NMR of these compounds was carried out using  $\text{D}_2\text{O}$ , a singlet was observed at  $\delta$  10.1 corresponding to the aldehyde proton. This indicates that the imine bond is susceptible to hydrolysis in the presence of water.

Salen group 13 complexes (**19-24**) show only one imine singlet in the range of  $\delta$  8.45-8.92, which suggest a symmetrical structure in the solution state. For the compound **19, 20, 22** and **23** peaks corresponding to the  $\text{CH}_2$  protons of the ligand backbone appears in the range of  $\delta$  2.2 to 3.98. The IR spectra showed strong absorption due to  $\nu_{\text{C=N}}$  in the range of 1621 to 1637  $\text{cm}^{-1}$  and medium absorption due to  $\nu_{\text{S=O}}$  in the range of 1357 to 1367  $\text{cm}^{-1}$ .

Unlike  $\text{Salen}(\text{SO}_3\text{Na})\text{H}_2$  ligands, their group 13 complexes show very good stability in water.  $^1\text{H}$  NMR of these compounds was recorded in  $\text{D}_2\text{O}$ . Prolong monitoring by  $^1\text{H}$  NMR for possible hydrolysis does not show a peak corresponding to aldehyde even after several days. This suggests that after coordination of group 13 metals, the imine bond of the salen ligand becomes water stable and does not undergo hydrolysis.

Slow evaporation of aqueous solution of **19** gives a colorless, needle shaped crystal suitable for X-ray analysis. Unfortunately, the X-ray structure could not be refined to an acceptable R-value due to the large degree of disorder of sulfonate groups as well as ethylene

backbone. Despite the disorder, we can confirm that the structures consist of a central six-coordinate aluminium atom in a distorted Oh geometry with the Salen(SO<sub>3</sub>Na) ligand occupying the four equatorial positions and the two water molecules in the axial positions.

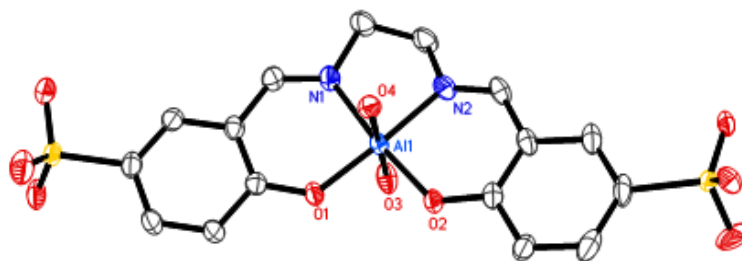


**Figure 3.4. Crystal structure of 19**

### 3.4. Conclusion

Salen(<sup>t</sup>Bu)AlBr shows activity towards dealkylation of the organophosphate in Lewis basic solvents like acetonitrile, tetrahydrofuran, etc. The rate of dealkylation in coordinating Lewis basic solvents is slow compared to that in non-coordinating polar solvents like CHCl<sub>3</sub>. Three water-soluble salen ligands and their group 13 metal complexes have been synthesized. Salen(SO<sub>3</sub>Na)<sub>2</sub> ligand is unstable in water and undergoes hydrolysis to give starting aldehyde and diamine. However, group 13 chelates are stable and do not show any hydrolysis product. Unfortunately, these group 13 metal chelates do not show any activity in dealkylation of organophosphate. This inactivity could be attributed to two coordinated water molecules. Water is stronger Lewis base than trimethyl phosphate therefore phosphate cannot replace the coordinated water molecule to become activated.<sup>96</sup>

### 3.5. Experimental

**General Remarks.** All glassware was cleaned with a base and an acid wash and dried in an oven at 130°C overnight. Starting materials for the synthesis were as follows: Salicylaldehyde (99%, Across Org.), Aniline (99%, Alfa Aesar), ethylenediamine (99%, Across Org.), aluminum nitrate

(98%, Aldrich), and gallium nitrate (99.9%, Alfa Aesar). The listed materials were used as received without further purification. NMR data were obtained on Varian Inova-400 instrument. Chemical shift are reported relative to SiMe<sub>4</sub> for <sup>1</sup>H and <sup>13</sup>C. Infrared transmission spectra were recorded at room temperature in a potassium bromide pellet on a Fourier-transform Smart Omni transmission Nicolet is10 spectrometer.

X-ray data were collected on a Bruker-Nonius X8 Proteum (Cu K $\alpha$  radiation) diffractometer. All calculations were performed using the software package SHELXTL-plus. The structures were solved by direct methods and successive interpretation of difference Fourier maps followed by least squares refinement. All non-hydrogen atoms were refined anisotropically. The hydrogen atoms were included using a riding model with isotropic parameters tied to the parent atom.

**Dealkylation of organophosphate in Lewis Basic solvent.** In a typical experiment salen(<sup>t</sup>Bu)AlBr (0.5 g, 0.84 mmol) was dissolved in acetonitrile (20 mL). The clear solution was obtained after 5 minutes stirring to which trimethylphosphate (98  $\mu$ L, 0.84 mmol), density 1.197g/mL) was added with a syringe. The mixture was stirred for 24 hours at room temperature. Then it was cannula filtered and the pale yellow residue was dried under vacuum. The % dealkylation was calculated from the yield of the reaction.

**Dealkylation of Nerve agents in Lewis Basic solvent.** VX was obtained from Aberdeen Proving Ground (APG). Trained personnel using applicable safety precautions conducted reactions with chemical warfare agents on site at Edgewood Chemical and Biological Center at APG.

<sup>31</sup>P NMR spectra were collected on samples prepared directly in NMR tubes using a Bruker AVANCE 300 MHz NMR spectrometer fitted with 5 mm broadband probe. The reactants were placed in a 4 mm glass NMR sleeve which was flame sealed and placed in a 5 mm glass

NMR tube also flame sealed. The contents of the doubly sealed tube were then vortex mixed and placed in the NMR probe. A 5  $\mu\text{L}$  of VX (18.9  $\mu\text{mol}$ ) was reacted in equimolar quantities with  $\text{salen}(\text{tBu})[\text{AlBr}]$  (11.3 mg, 18.9  $\mu\text{mol}$ ) in at ambient temperature in 1.0 mL each of  $d^3$ -acetonitrile and  $\text{CDCl}_3$ . A 5  $\mu\text{L}$  of hexamethylphosphoramide (HMPA) was added as an internal standard. Percentage conversion was calculated from integration of the remaining phosphate and dealkylated product.

**Synthesis of sodium salicylaldehyde-5-sulfonate (15).** Salicylaldehyde (20 g, 0.16 mol) was charged into a 250 mL round bottom flask containing methanol (60mL). A solution of aniline (14.8 mL, 0.16 mol) in methanol (40 mL) was added slowly over 30 minutes. The reaction mixture was stirred at reflux temperature for 20 hours. The reaction mixture was allowed to cool to room temperature and filtered on a Buchner funnel to isolate yellow crystalline compound. Yield: 28.1 g (89.0 %). Mp: 50°C.  $^1\text{H}$  NMR ( $\text{CDCl}_3$ ):  $\delta$  6.93 (dt, 1H, Ph-*H*), 7.01 (d, 1H, Ph-*H*), 7.28 (m, 3H, Ph-*H*), 7.38(m, 4H, Ph-*H*), 8.6 (s, 1H, N=CH)

This compound (5 g) was charged into a 100 mL round bottom flask containing five times its weight of concentrated sulfuric acid, which gave upon stirring a clear orange solution. This solution was heated for 2 hours at 110°C. The reaction mixture was allowed to cool at 0°C for 30 minutes, then ice pieces were added to induce crystallization of N-phenylsalicylaldehyde-5-sulfonic acid which was filtered on a Buchner funnel and washed with small quantities of ice-water to remove excess sulfuric acid. Recrystallized from boiling water to afford yellow powder. Yield: 6.2 g (88.57 %).  $^1\text{H}$  NMR ( $\text{CD}_3\text{OD}$ ):  $\delta$  6.82 (dd, 1H, Ph-*H*), 7.4 (m, 2H, Ph-*H*), 7.52(m, 3H, Ph-*H*), 7.64 (m, 1H, Ph-*H*), 7.9(s, 1H, N=CH). IR (KBR)  $\nu/\text{cm}^{-1}$ : 3395w, 3055w, 1651s, 1605m, 1361m, 1180s, 1176s, 1113s, 1036s.

This pure compound was dissolved in boiling water, and sodium carbonate (5 g) was added until evolution of carbon dioxide ceased. Reaction mass was heated to boiling and nitrogen gas was passed through reaction mixture to remove aniline. This process was repeated several times until water vapor showed no alkaline response to pH paper. The aqueous solution was evaporated to dryness, dissolved in ethanol and filtered to eliminate inorganic salt impurities. The ethanol layer was evaporated under vacuum to give bright yellow sodium salicylaldehyde. Yield: 3.07 g (61.2 %). Mp: 330 -332°C.  $^1\text{H}$  NMR ( $\text{D}_2\text{O}$ ):  $\delta$  7.05 (d, 1H, Ph-H), 7.95 (dd, 1H, Ph-H), 8.10 (d, 1H, Ph-H), 10.0(s, 1H, CHO). IR (KBR)  $\nu/\text{cm}^{-1}$ : 3461w, 2758s, 1655w, 1598m, 1459w, 1398m, 1195w, 1106m, 840w. MS (EI, positive): 201( $\text{M}^+$  - Na, 100%)

**Synthesis of Salen( $\text{SO}_3\text{Na}$ ) $\text{H}_2$  (16).** To a solution of sodium salicylaldehyde (1.5g, 6.6 mmol) in methanol (50 mL) was added a solution of ethylenediamine (0.25 mL, 3.3 mmol) in a methanol (10 mL). The resulting slurry was stirred at reflux temperature for 2 hours. Reaction mass was allowed to cool to room temperature and filtered to isolate a nice yellow crystalline solid. Yield: 1.4g (80%). Mp: > 380°C.  $^1\text{H}$  NMR ( $\text{CD}_3\text{OD}$ ):  $\delta$  3.98 (s, 4H,  $\text{NCH}_2$ ), 6.8 (dd, 2H, Ph-H), 7.6 (d, 2H, Ph-H), 7.98 (d, 2H, Ph-H), 8.62 (s, 2H,  $\text{N}=\text{CH}$ ). IR (KBR)  $\nu/\text{cm}^{-1}$ : 3537s, 3466s, 3411s, 3042s, 2893w, 1634s, 1611m, 1579m, 1483m, 1357m, 1184s, 1108s, 1053s, 1033s, 843s, 729 m.

**Synthesis of Salpen( $\text{SO}_3\text{Na}$ ) $\text{H}_2$  (17).** To a solution of sodium salicylaldehyde (1.2 g, 5.3 mmol) in methanol (50 mL) was added a solution of 1,3 propylenediamine (0.32 mL, 2.6 mmol) in methanol (10 mL). The resulting solution was stirred at reflux temperature for 2 hours. Reaction mass was allowed to cool to room temperature and filtered to isolate a nice yellow crystalline solid. Yield: 0.6 g (77.9 %). Mp: > 380°C.  $^1\text{H}$  NMR ( $\text{CD}_3\text{OD}$ ):  $\delta$  2.1 (m, 2H,  $\text{CH}_2\text{CH}_2\text{CH}_2$ ), 3.7 (t, 4H,  $\text{NCH}_2$ ), 6.8 (d, 2H, Ph-H), 7.6 (dd, 2H, Ph-H), 7.89 (d, 2H, Ph-H), 8.52 (s, 2H,  $\text{N}=\text{CH}$ ). IR (KBR)  $\nu/\text{cm}^{-1}$

<sup>1</sup>: 3537s, 3466s, 3411s, 3042s, 2942s, 2850s, 1636w, 1610w, 1581m, 1482m, 1367m, 1195w, 1107m, 729m.

**Synthesis of Salophen(SO<sub>3</sub>Na)H<sub>2</sub> (18).** To a solution of sodium salicylaldehyde (1.5 g, 6.6 mmol) in ethanol (50 mL) was added a solution of 1,2-phenylenediamine (0.36 g, 3.3 mmol) in ethanol (20 mL). The resulting solution was stirred at reflux temperature for 2 hours. Reaction mass was allowed to cool to room temperature and filtered to isolate a nice yellow crystalline solid. Yield: 0.7 g (72.1 %). Mp: > 380°C. <sup>1</sup>H NMR (CD<sub>3</sub>OD): δ 6.95 (d, 2H, Ph-H), 7.4 (m, 4H, Ph-H), 7.8 (dd, 2H, Ph-H), 8.00 (d, 2H, Ph-H), 8.92 (s, 2H, N=CH). IR (KBR)  $\nu$ / cm<sup>-1</sup>: 3537s, 3466s, 1638w, 1610w, 1581m, 1482m, 1373m, 1195w, 1107m, 729w.

**Synthesis of Salen(SO<sub>3</sub>Na)AlNO<sub>3</sub> (19).** A rapidly stirred solution of salen(SO<sub>3</sub>Na)H<sub>2</sub> (0.5 g, 0.97 mmol) in methanol (30 mL) was combined with Al(NO<sub>3</sub>)<sub>3</sub>·9H<sub>2</sub>O (458 mg, 0.93 mmol) followed by addition of sodium acetate (380 mg, 2.82 mmol). Clear reaction mass was stirred for 15 hours. Then it was concentrated under vacuum to about one third of its volume. The yellow precipitate was isolated by filtration, washed with cold methanol and dried under vacuum. X-ray quality crystals were grown from slow diffusion of methanol vapor into a concentrated aqueous solution of salen(SO<sub>3</sub>Na)AlNO<sub>3</sub>. Yield: 0.25 g (52%). <sup>1</sup>H NMR (D<sub>2</sub>O): δ 3.98 (s, 4H, NCH<sub>2</sub>), 6.95 (d, 2H, Ph-H), 7.78 (dd, 2H, Ph-H), 7.83 (d, 2H, Ph-H), 8.45 (s, 2H, N=CH). IR (KBR)  $\nu$ / cm<sup>-1</sup>: 3530b, 3040s, 2942s, 2850s, 1636w, 1610w, 1581m, 1482m, 1367m, 1195w, 1107m, 729w.

**Synthesis of Salpen(SO<sub>3</sub>Na)AlNO<sub>3</sub> (20).** A rapidly stirred solution of salpen(SO<sub>3</sub>Na)H<sub>2</sub> (0.5 g, 1 mmol) in methanol (20 mL) was combined with Al(NO<sub>3</sub>)<sub>3</sub>·9H<sub>2</sub>O (412 mg, 1.1 mmol) followed by addition of sodium acetate (390 mg, 2.9 mmol). Clear reaction mass was stirred for 15 hours. Then it was concentrated under vacuum to about one third of its volume. The yellow precipitate was isolated by filtration, washed with cold methanol and dried under vacuum. Yield: 0.36 g

(62%).  $^1\text{H}$  NMR ( $\text{D}_2\text{O}$ ):  $\delta$  2.2 (m, 2H,  $\text{CH}_2\text{CH}_2\text{CH}_2$ ), 3.6 (t, 4H,  $\text{NCH}_2$ ), 6.8 (d, 2H, Ph-*H*), 7.6 (dd, 2H, Ph-*H*), 7.9 (d, 2H, Ph-*H*), 8.5 (s, 2H,  $\text{N}=\text{CH}$ ). IR (KBR)  $\nu/\text{cm}^{-1}$ : 3545 b, 3042s, 2942s, 2850s, 1636w, 1610w, 1581m, 1482m, 1367m, 1195w, 1107m, 729w.

**Synthesis of Salopen( $\text{SO}_3\text{Na}$ )  $\text{AlNO}_3$ (21).** A rapidly stirred solution of salopen( $\text{SO}_3\text{Na}$ ) $\text{H}_2$  (0.5 g, 0.97 mmol) in methanol (20 mL) was combined with  $\text{Al}(\text{NO}_3)_3 \cdot 9\text{H}_2\text{O}$  (400 mg, 1.06 mmol) followed by addition of sodium acetate (378 mg, 2.81 mmol). Clear reaction mass was stirred for 15 hours. Then it was concentrated under vacuum to about one third of its volume. The Yellow precipitated was isolated by filtration, washed with cold methanol and dried under vacuum. Yield: 0.36 g (62%).  $^1\text{H}$  NMR ( $\text{D}_2\text{O}$ ):  $\delta$  6.98 (d, 2H, Ph-*H*), 7.3 (m, 4H, Ph-*H*), 7.8 (dd, 2H, Ph-*H*), 8.00 (d, 2H, Ph-*H*), 8.92 (s, 2H,  $\text{N}=\text{CH}$ ). IR (KBR)  $\nu/\text{cm}^{-1}$ : 3540b, 3042s, 1636w, 1610w, 1581m, 1482m, 1367m, 1195w, 1107m, 729w.

**Synthesis of Salen( $\text{SO}_3\text{Na}$ )  $\text{GaNO}_3$ (22).** A rapidly stirred solution of salen( $\text{SO}_3\text{Na}$ ) $\text{H}_2$  (0.5 g, 1.05 mmol) in methanol (30 mL) was combined with  $\text{Ga}(\text{NO}_3)_3 \cdot 9\text{H}_2\text{O}$  (0.48 g, 1.15 mmol). Clear reaction mass was stirred for 15 hours. Then it was concentrated under vacuum to about one third of its volume. The white precipitated was isolated by filtration, washed with cold methanol and dried under vacuum. Yield: 0.4 g (63.5%).  $^1\text{H}$  NMR ( $\text{D}_2\text{O}$ ):  $\delta$  3.98 (s, 4H,  $\text{NCH}_2$ ), 6.95 (d, 2H, Ph-*H*), 7.78 (dd, 2H, Ph-*H*), 7.83 (d, 2H, Ph-*H*), 8.45 (s, 2H,  $\text{N}=\text{CH}$ ). IR (KBR)  $\nu/\text{cm}^{-1}$ : 3537b, 3042s, 2942s, 2850s, 1636w, 1610w, 1581m, 1482m, 1367m, 1195w, 1107m, 729w.

**Synthesis of Salpen( $\text{SO}_3\text{Na}$ )  $\text{GaNO}_3$ (23).** A rapidly stirred solution of salpen( $\text{SO}_3\text{Na}$ ) $\text{H}_2$  (0.505 g, 1.03 mmol) in methanol (30 mL) was combined with  $\text{Ga}(\text{NO}_3)_3 \cdot 9\text{H}_2\text{O}$  (0.477 g, 1.14 mmol). Clear reaction mass was stirred for 15 hours. Then it was concentrated under vacuum to about one third of its volume. The white precipitated was isolated by filtration, washed with cold methanol and dried under vacuum. Yield: 0.35 g (55.5%).  $^1\text{H}$  NMR ( $\text{D}_2\text{O}$ ):  $\delta$  2.2 (m, 2H,  $\text{CH}_2\text{CH}_2\text{CH}_2$ ), 3.6 (t,

4H, NCH<sub>2</sub>), 6.8 (d, 2H, Ph-H), 7.6 (dd, 2H, Ph-H), 7.9 (d, 2H, Ph-H), 8.5 (s, 2H, N=CH). IR (KBr)  $\nu$ /cm<sup>-1</sup>: 3530b, 3042s, 2942s, 2850s, 1636w, 1610w, 1581m, 1482m, 1367m, 1195w, 1107m, 729w.

**Synthesis of Salopen(SO<sub>3</sub>Na) GaNO<sub>3</sub> (24).** A rapidly stirred solution of salopen(SO<sub>3</sub>Na)H<sub>2</sub> (0.5 g, 0.96 mmol) in methanol (30 mL) was combined with Ga(NO<sub>3</sub>)<sub>3</sub>.9H<sub>2</sub>O (0.44 g, 1.05 mmol). Clear reaction mass was stirred for 15 hours. Then it was concentrated under vacuum to about one third of its volume. The white precipitate was isolated by filtration, washed with cold methanol and dried under vacuum. Yield: 0.35 g (56.4%). <sup>1</sup>H NMR (D<sub>2</sub>O):  $\delta$  6.98 (d, 2H, Ph-H), 7.3 (m, 4H, Ph-H), 7.8 (dd, 2H, Ph-H), 8.00 (d, 2H, Ph-H), 8.92 (s, 2H, N=CH). IR (KBR)  $\nu$ /cm<sup>-1</sup>: 3537b, 1636w, 1610w, 1581m, 1482m, 1367m, 1195w, 1107m, 729w.

## Chapter 4 Detection of Nerve Agents in Water

### 4.1. Introduction

Among the different types of Chemical Weapon Agents (CWAs) nerve agents (NAs) are the most significant with respect to their toxicity, past use, military capacity and mode of action. Exposure to G-type nerve agents such as GA (Tabun), GB (Sarin), GD (Soman) and V-type nerve agents, such as VX, can take place through inhalation, contact with the eyes or skin, and by ingestion. The G-type agents are not persistent and degrade, depending on conditions, within hours when warm to days when cold. However, VX is highly persistent and the hydrolysis product, ethylmethylphosphonic acid (EMPA), retains extreme toxicity and is highly water-soluble.

Efforts to prevent chemical weapon attacks or accidental releases prompted the Chemical Weapons Convention (CWC) to mandate that countries must destroy all CWAs stockpiles held in reserve.<sup>98</sup> However, the use of CWAs by terrorists or non-signatory countries is still a threat to civilian health and safety. The recent chemical weapon attack on civilians in Syria has confirmed this threat. LC/MS and GC/MS analyses confirmed the use of Sarin in Syria.

One of the most difficult problems in responding to a CWA release is the decontamination of any affected objects and detection of any residual CWA or degradation products in complex environmental matrices. Several detection techniques like GC/MS<sup>99</sup>, ion mobility spectrometry<sup>100</sup> or flame photometric detection<sup>101</sup> are commercially available. All these techniques have their own pros and cons, for example flame photometric detection is fast and sensitive but produces false positives. Ion mobility spectrometry operates at ambient temperature but has low resolving power and limited selectivity.

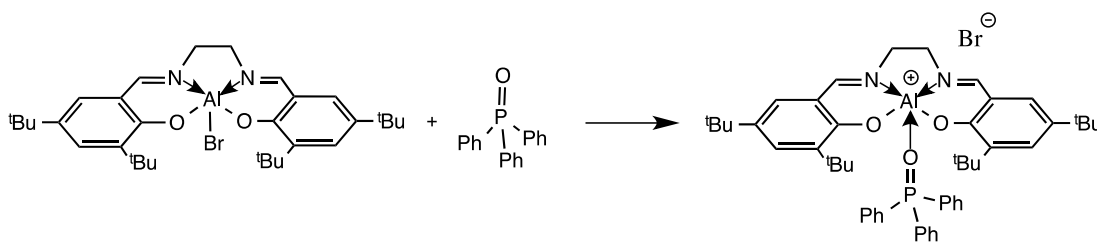
Mass spectrometric methods could provide identification of NAs. The most commonly used method to detect NAs is GC/MS but the NA degradation products like alkyl methylphosphonic acids must be derivatized before the analyses.<sup>102-104</sup> Derivatization adds time, difficulty, and increases the potential for exposure to the NAs. The most common derivatization methods include the formation of trimethylsilyl (TMS) ethers or tert-butyldimethylsilyl (t-BDMS) esters, methylation with diazomethane, and formation of an ion pair with trimethylphenyl ammonium hydroxide (TMPAH). Most of these derivatives are unstable and moisture sensitive. In particular, the use of diazomethane is problematic since it is explosive and carcinogenic. Liquid chromatography coupled with mass spectrometry (LCMS) employing various ionization techniques has also been used to detect NAs.<sup>105,106</sup> LC/MS/MS and LC/ICP/MS have been used to detect G-agents, V- agents and their degradation products. However, the low ionization efficiency of G-type NAs makes LC/MS analyses difficult.

Salen(<sup>t</sup>Bu)Al(Ac), prepared *in situ* from Salen(<sup>t</sup>Bu)AlBr and NaAc, forms Lewis acid-base adducts with G-type NAs, GB (Sarin) and GD (Soman), and the VX hydrolysis product EMPA in aqueous solution. The resulting compounds, [Salen(<sup>t</sup>Bu)Al(NA)]<sup>+</sup>[Ac]<sup>-</sup> are sufficiently stable to be identified by ESI-MS. This chapter presents results and discussion of the ESI-MS detection method for the NAs and their degradation product in water.

## 4.2. Research Background

Chapter 2 described how chelated salen aluminum bromide compounds effectively dealkylate organophosphate compounds to give aluminum phosphate, where dealkylated phosphate is covalently bound to the aluminum center (Scheme 2.2). We have discussed the proposed mechanism of this reaction in chapter 3. According to this mechanism, the dealkylation reaction proceeds via formation of a cation through coordination of

organophosphate molecule to aluminum (Figure 3.1). In an effort to confirm the formation of such a cation, we attempted the isolation of a cation formed by the combination of  $\text{salen}^{\text{tBu}}\text{AlBr}$  with triphenylphosphine oxide in an equimolar ratio. Absence of a P-O-C linkage in the phosphine oxide precluded the dealkylation. Hence, reaction should give a cation formed by coordination of Lewis basic phosphine oxide to aluminum (Scheme 4.1). Although single crystals suitable for X-ray analysis could not be isolated, a MALDI mass spectrum provides strong evidence for the formation of a salen aluminum cation. MALDI mass spectra shows a peak ( $m/z = 795$ ) corresponding to  $[\text{salen}^{\text{tBu}}\text{AlOP}(\text{O})\text{Ph}_3]^+$  (Figure 4.1). Thus,  $\text{Salen}^{\text{tBu}}\text{AlBr}$  forms a Lewis acid-base adduct with phosphine oxide that is sufficiently stable to identify by MS.



**Scheme 4.1. Coordination of phosphine oxide to aluminum**

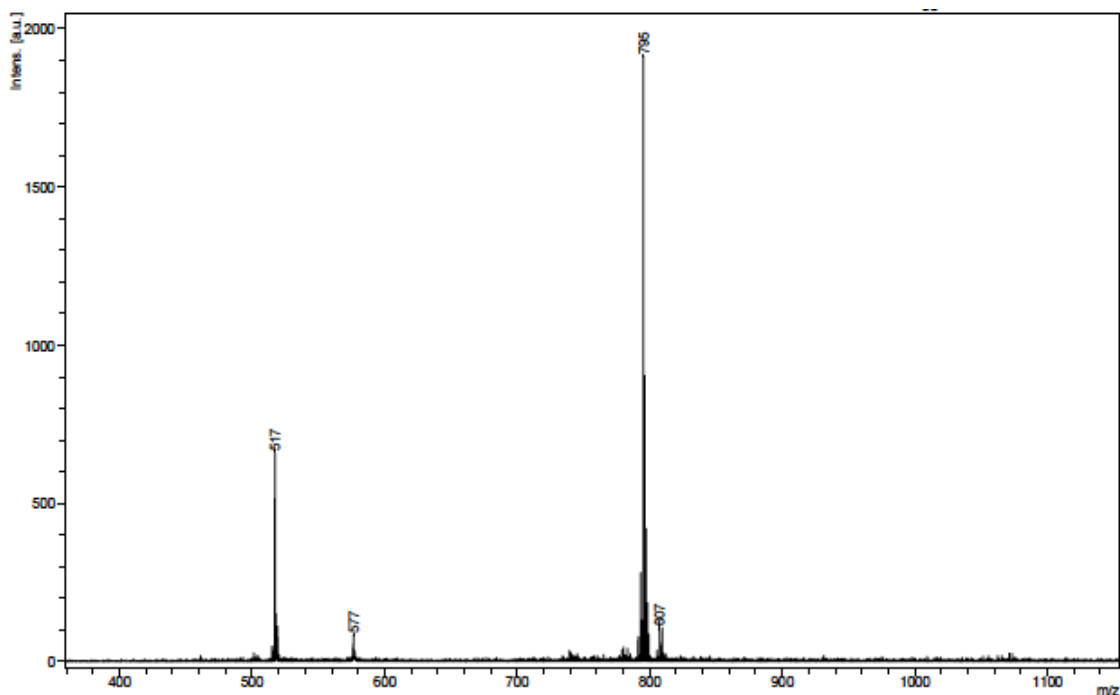


**Figure 4.1. MALDI MS (+) of Lewis acid-base adduct of phosphine oxide with salen(<sup>t</sup>Bu)AlBr**

Similarly, Lewis acid-base adduct formation can be expected when NAs are combined with Salen aluminum chelate. The detection of this adduct could provide a useful technique for identifying NAs. Salen(<sup>t</sup>Bu)Al(Ac) was prepared *in situ* by combination of Salen(<sup>t</sup>Bu)AlBr and sodium acetate. Unlike bromide anion, acetate anion is incapable of inducing dealkylation of organophosphate compounds. Hence, when Salen(<sup>t</sup>Bu)Al(Ac) was combined with G-type NAs, GB (Sarin) and GD (Soman), and the VX hydrolysis product EMPA in aqueous solution, no dealkylation was observed. These organophosphate compounds coordinate to aluminum to form [Salen(<sup>t</sup>Bu)Al(NA)]<sup>+</sup>[Ac]<sup>-</sup>, which was detected and identified by ESI-MS. Trained personnel using applicable safety precautions conducted the study with chemical warfare agents at the Edgewood Chemical and Biological Center at APG. Studies on NAs can only be conducted in government-approved laboratories.

### 4.3. ESI-MS Analysis

Electrospray ionization-mass spectrometry (ESI/MS) has become an important technique for characterization of biomolecules, inorganic species, and synthetic polymers. It is a simple technique that takes place at atmospheric pressure and at a moderate temperature, and is a “soft” ionization technique. The ionization is soft in the sense that a very little residual energy is retained by the analyte, and generally no fragmentation occurs upon ionization. Not only that but also very weak non-covalent interactions are preserved in the gas phase. Since fragmentation of molecular ions is generally limited, mass spectra are relatively simple. ESI-MS can be divided into three steps: Dispersal of a sample solution into electrically charged droplets, generation of multiply charged ions from droplets by solvent evaporation, and transportation of ions from ionization source to mass analyzer.

Schematic diagram of ESI is shown in Figure 4.2. Within ESI apparatus, a stainless steel capillary needle is maintained at high voltage relative to a wall of a chamber that surrounds the needle. When a sample solution is passed through the capillary, a mist of highly charged droplets generates at the tip of the capillary. The electrospray of fine droplets then enters into desolvating chamber, where solvent from droplets is evaporated with the help of elevated ESI temperature and/ or stream of nitrogen drying gas. The charged droplets are continuously reduced in size by evaporation of solvent, which results in an increase of surface charge density. This process continues until a point called the *Rayleigh limit*, where the surface tension can no longer support the charge. Here a so-called *Coulombic explosion* occurs and the droplet is torn apart into smaller droplets. These droplets repeat the process until all solvent is removed from the analyte, leaving a multiply charged analyte molecule. These ions are then accelerated into the mass analyzer for analysis of molecular mass and measurement of ion density. To obtain structural information, precursor ion of interest can be mass selected and further fragmented in

collision cell. The fragmented ions can then be mass analyzed in second mass analyzer of a tandem mass spectrometer system.

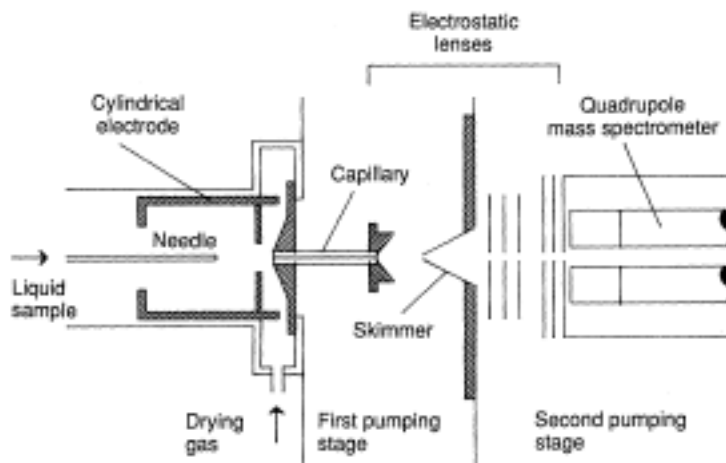


**Figure 4.2. Sketch of the apparatus for electrospray ionization**

(Reprinted from J.B. Fenn et al., *Science*, **1989**, *65*, 246. with permission from The American Association for the Advancement of Science) (License Number 3471480189669)

**The quadrupole mass analyzer:** When ions travel through a magnetic or electrical field their movements are affected by their  $m/z$  ratio and this is a main principle of separating ions in mass analyzer. A quadrupole mass analyzer is composed of the four parallel cylindrical rods kept at equal distance. (Figure 4.3) Opposite rods are connected electrically, one pair being attached to the positive side of a variable DC source and the other pair to the negative terminal. In addition, variable radio frequency ac voltage is applied to the diagonally placed pair of rods. Ions are accelerated into the space between the rods by a potential difference of 5 to 10V. Resulting field causes the ions to travel forward in the  $z$  direction with oscillatory motion in the  $x$ - $y$  plane. The ac and dc voltages on the rods are increased simultaneously while maintaining their ratio constant. These voltages can be set so that all the ions except with desirable  $m/z$  value strike the rods and are converted to neutral molecules. The only ions having limited range of  $m/z$  values

oscillate with stable amplitude and reach the transducer without hitting the quadrupole rod. Normally ions that differ in mass by one unit can be resolved.

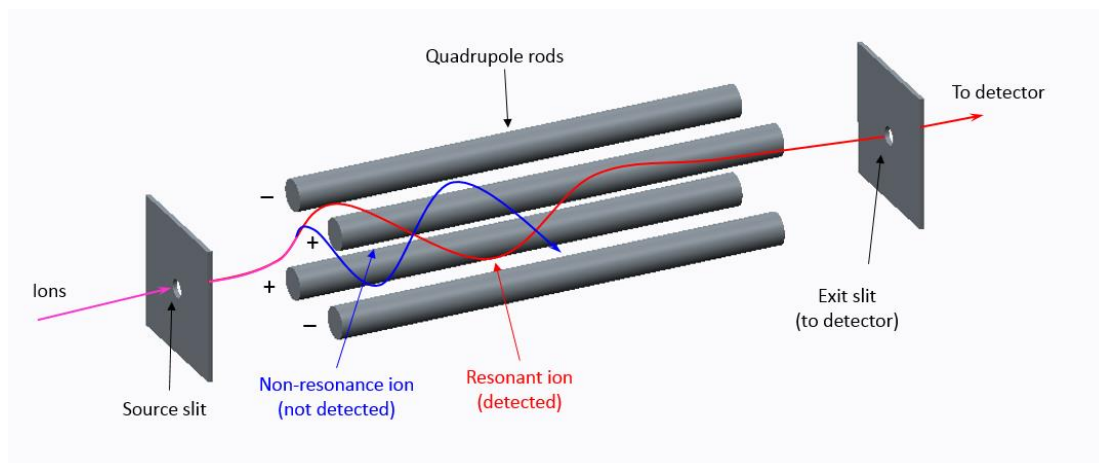


**Figure 4.3. Schematic diagram of a quadrupole mass spectrometer**

In a tandem quadrupole system, which is often called “Triple quadrupole”, there are three quadrupoles set up in a linear fashion. (Figure 4.4) Precursor ion, mass selected by first quadrupole (Q1), enters into second quadrupole (Q2). There it reacts with a collision gas, or interacts with an intense laser beam to produce fragments, called product ions. These ions are then mass analyzed by the second mass analyzer (Q3) and detected by the ion detector. This tandem system is commonly denoted as MS/MS in the literature.

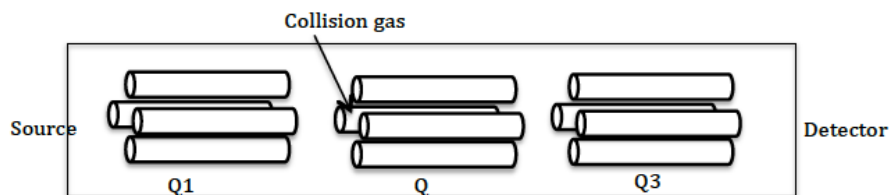


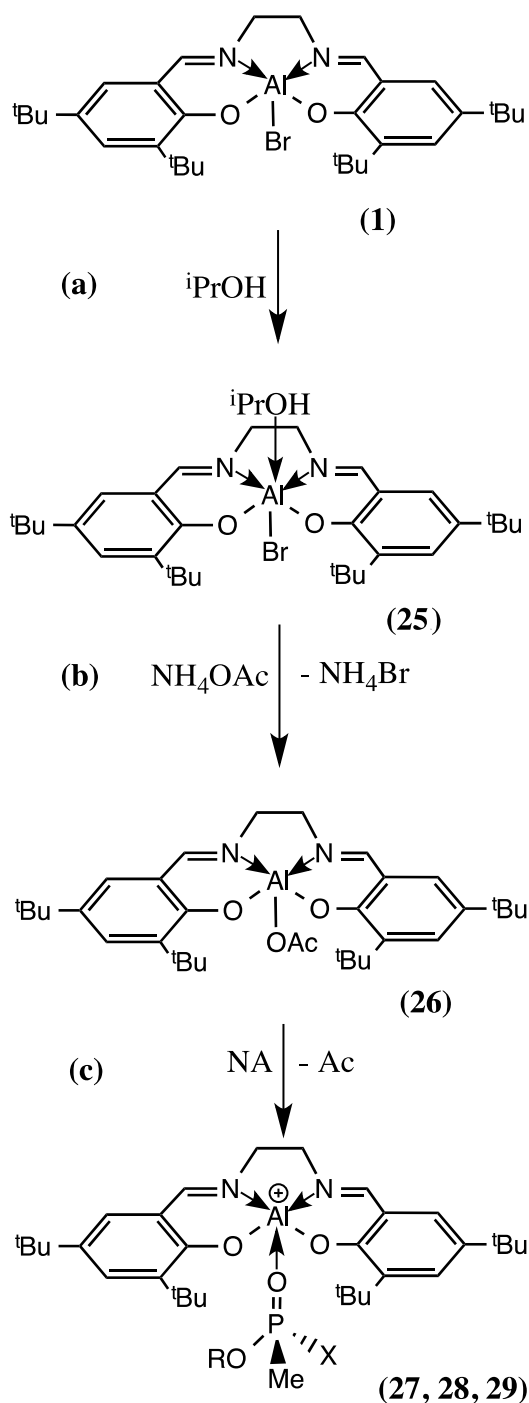
**Figure 4.4. Schematic diagram of a triple quadrupole system**

#### 4.4. Result and Discussion

Scheme 4.2 shows a sequence of reactions (a-c) leading to formation of Lewis acid-base compounds between Salen(<sup>t</sup>Bu)AlBr (**1**) and the nerve agents GB (Sarin) GD (Soman) and VX hydrosylate EMPA (ethylmethylphosphonate). Salen(<sup>t</sup>Bu)Ac is prepared *in situ* by a reaction of SalenAlBr with NaAc. It is then combined with nerve agents to form Lewis acid-base adducts. These resulting Lewis acid-base adducts, [Salen(<sup>t</sup>Bu)AlNA]<sup>+</sup>[Ac]<sup>-</sup>, were identified by electrospray ionization-mass spectroscopy (ESI-MS). Mass number for each compound in this sequence of the reactions is give in Table 4.1

**Table 4.1. Mass numbers for each compound formed in a sequence of reactions leading to formation of Lewis acid-base compounds between salen(<sup>t</sup>Bu)Al and the nerve agents**

#	Compound	MW (g/mol)
<b>1</b>	Salen( <sup>t</sup> Bu)AlBr	597.61
<b>26</b>	Salen( <sup>t</sup> Bu)Al(OAc)	576.75
<b>27</b>	[Salen( <sup>t</sup> Bu)Al(GB)] <sup>+</sup>	657.79
<b>28</b>	[Salen( <sup>t</sup> Bu)Al(GD)] <sup>+</sup>	699.87
<b>29</b>	[Salen( <sup>t</sup> Bu)Al(EMPA)] <sup>+</sup>	641.78



**Scheme 4.2.** Sequence of reactions (a – c) leading to formation of Lewis acid-base compounds between  $\text{salen}(\text{tBu})\text{AlBr}$  (1) (which forms the ion pair,  $[\text{salen}(\text{tBu})\text{Al}(\text{iPrOH})\text{Br}]$  (25) and the nerve agents GB (sarin,  $\text{R} = \text{CHMe}_2$ ,  $\text{X} = \text{F}$  (27)) GD (soman,  $\text{R} = \text{CH}(\text{Me})\text{CMe}_3$ ,  $\text{X} = \text{F}$  (28)) and VX hydrosylate EMPA (ethylmethylphosphonate,  $\text{R} = \text{Et}$ ,  $\text{X} = \text{OH}$  (29)).

The ESI-MS of **1** in isopropanol was obtained as a baseline for comparison to the NA derivatives. The positive ionization spectrum had  $m/z$  values attributed to  $[\text{Salen}(\text{tBu})\text{Al}]^+$  (517) from loss of bromide and  $[\text{Salen}(\text{tBu})\text{Al}(\text{PA})]^+$  (577) with coordinated solvent (Figure 4.5). These two peaks indicated that the compound readily loses bromide and that compounds with coordinated Lewis bases could be detected. The assignment for  $m/z$  1051 probably corresponds to  $[\{\text{Salen}(\text{tBu})\text{Al}\}_2\text{O}]^+$  with a bridging oxide, a known structural motif for SalenAl compounds. In the negative ionization mode the largest peak in the spectrum corresponded to  $[\{\text{Salen}(\text{tBu})\text{Al}(\text{PA})(\text{H}_2\text{O})\}\text{Br}]$  ( $m/z$  675) which indicated that the compound and coordinated solvent remained intact under the ESI-MS(+ and -) conditions (Figure 4.6).

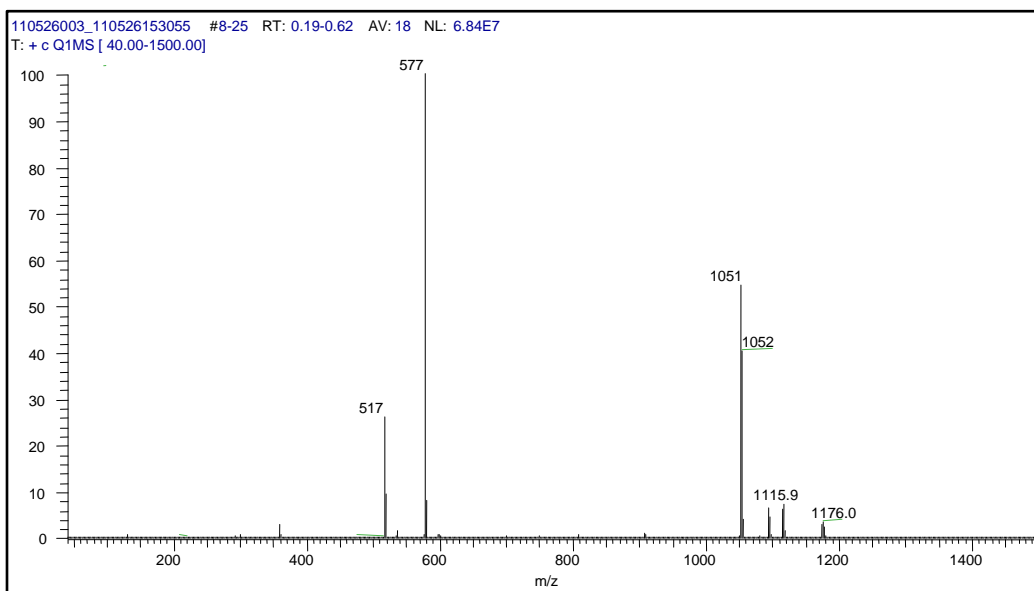


**Figure 4.5. ESI-MS (+) of **1** in isopropanol**

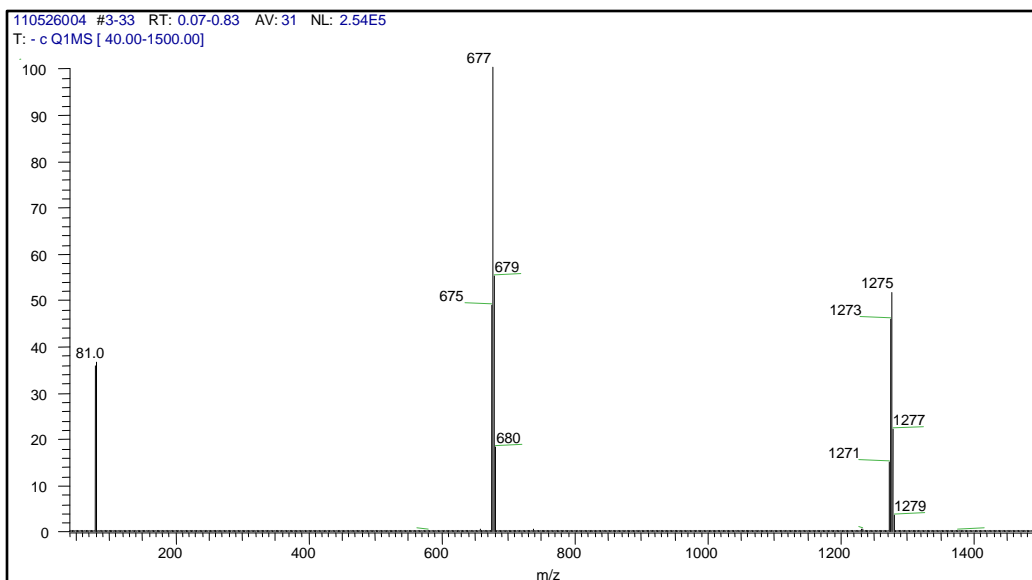


**Figure 4.6. ESI-MS (-) of 1 in isopropanol**

It has been established that Lewis basic solvents such as H<sub>2</sub>O, MeOH, and tetrahydrofuran displace the anion from SalenAl (X = Br<sup>-</sup> and OTs<sup>-</sup>, for example) to form solvated six-coordinate derivatives.<sup>107</sup> In the present study the bromide anion in **25** was exchanged for acetate through a salt elimination reaction. The ESI-MS(+) spectrum detected **26** (m/z 577) without water, in addition to an acetate-bridged compound, [{Salen(<sup>t</sup>Bu)Al}<sub>2</sub>Ac]<sup>+</sup> (m/z 1093) (Figure 4.7). In negative ionization mode the largest peak for **26** was [Salen(<sup>t</sup>Bu)Al(Ac)<sub>2</sub>]<sup>-</sup> (m/z 635) and fragments corresponding to compounds containing bromide: [Salen(<sup>t</sup>Bu)AlBr(Ac)]<sup>-</sup> m/z 657 and [{Salen(<sup>t</sup>Bu)Al}<sub>2</sub>Br(Ac)<sub>2</sub>]<sup>-</sup>, m/z 1233 (Figure 4.8). Such salen acetate compound is known in literature.<sup>108</sup> Salcen(<sup>t</sup>Bu)AlOC(O)Me, formed by combination of salcen(<sup>t</sup>Bu)AlMe with acetic acid have been structurally characterized (Figure A3).

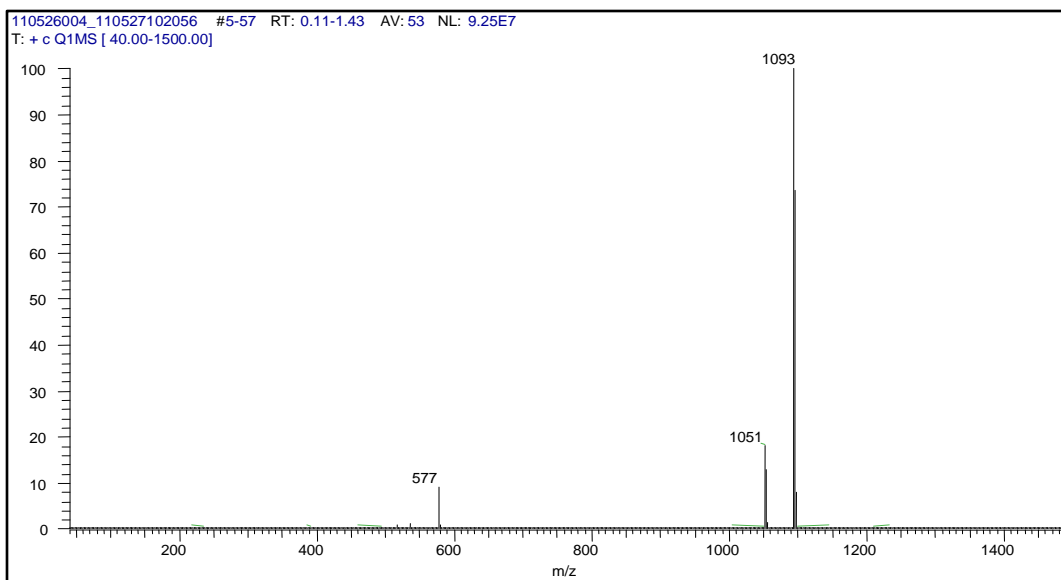


**Figure 4.7. ESI-MS (+) of 26**

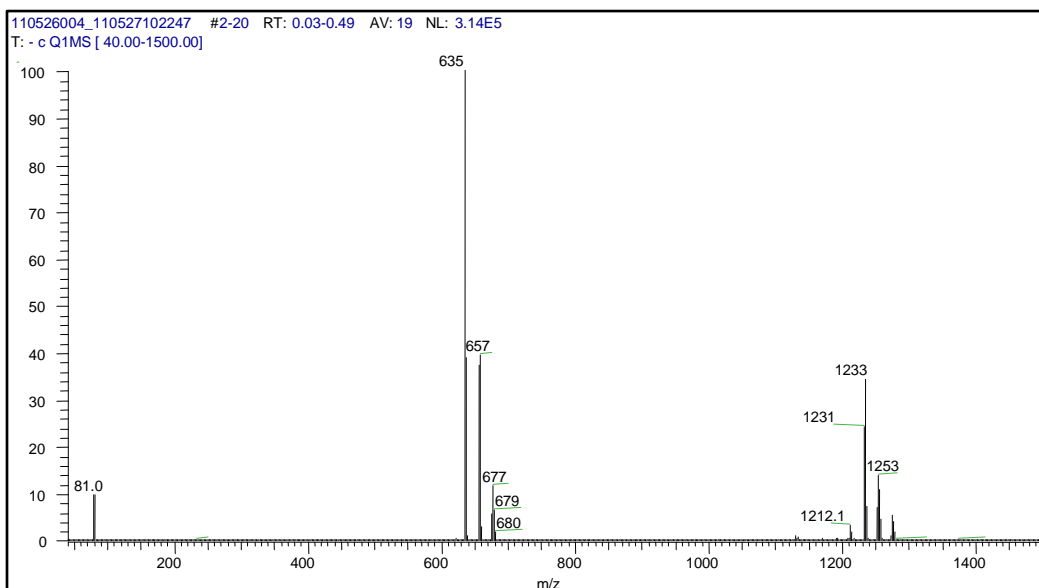


**Figure 4.8. ESI-MS (-) of 26**

In separate experiments, aqueous solutions of **26** were combined with micromolar quantities of GB (0.02 mM) and GD (0.02 mM) and EMPA (0.8 mM) to form the Lewis acid-base adducts,  $[\text{Salen}(\text{tBu})\text{Al}(\text{NA})]^+$  (Scheme 1c). In positive ionization mode, parent peaks were observed for the compounds containing GB ( $m/z$  657, **27**) and GD ( $m/z$  699, **28**) (Figure 4.9 and

4.10). The peaks are weaker than that for **26** ( $m/z$  577) due to the lower concentrations used, but easily identified. Moreover, the peak at  $m/z$  517 could correspond to loss of GD from **28** or loss of Ac from **26**. For **28**, the MS/MS spectrum of  $m/z$  699 has a peak at  $m/z$  615, which is likely due to loss of dimethyl butene (Figure 4.11). The positive ionization spectrum of **29** has a parent peak at  $m/z$  641 and another at  $m/z$  1157 corresponding to dimeric, EMPA-bridged  $[\{\text{Salen}(\text{tBu})\text{Al}\}_2(\text{EMPA})]^+$  (Figure 4.12). Such dimeric compounds are known for SalenAl combinations with phosphonic and phosphinic acids.<sup>81</sup>  $[\text{salpen}(\text{tBu})\text{AlO}_2\text{P}(\text{H})\text{Ph}]_2$ ,  $[\text{salben}(\text{tBu})\text{AlO}_2\text{P}(\text{H})\text{Ph}]_2$ ,  $[\text{salohen}(\text{tBu})\text{AlO}_2\text{P}(\text{H})\text{Ph}]_2$  are some of the compounds which have been structurally characterized. Acetate adducts are observed at  $m/z$  577 and  $m/z$  1093. In the negative ionization spectrum (Figure 4.13), EMPA adducts were observed at  $m/z$  699 for  $[\text{Salen}(\text{tBu})\text{Al}(\text{EMPA})(\text{Ac})]^-$  and  $m/z$  763 for  $[\text{Salen}(\text{tBu})\text{Al}(\text{EMPA})_2]^-$ .

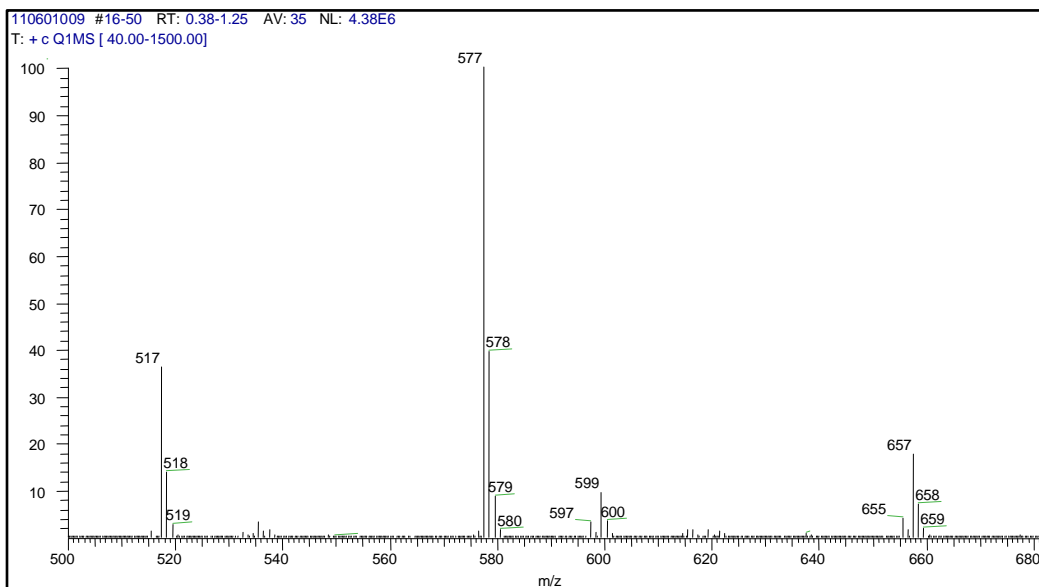


**Figure 4.9.** ESI-MS (+) of **27**

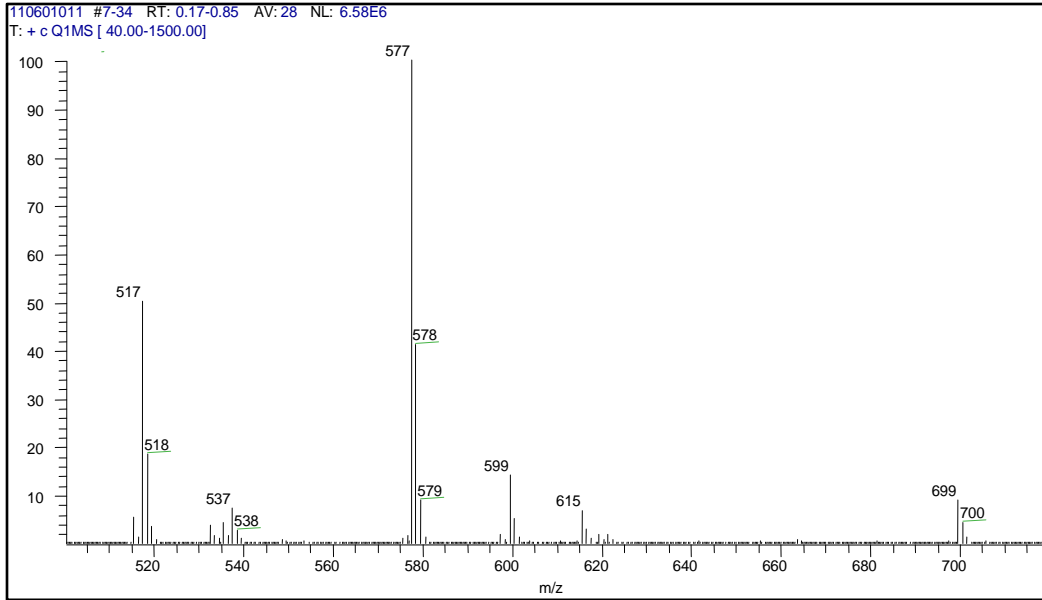


Figure 4.10. ESI-MS (+) of 28

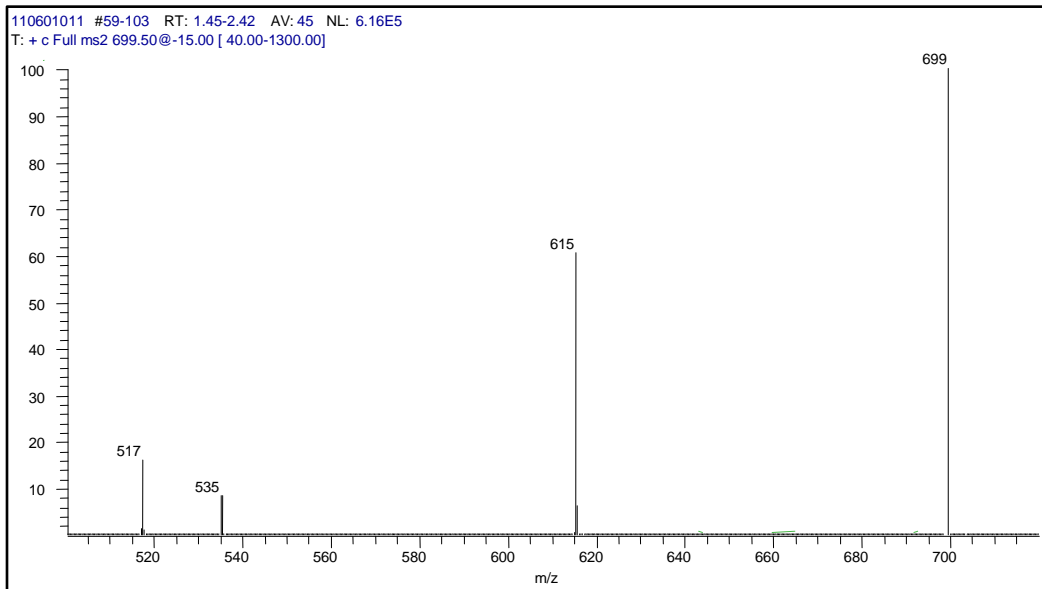


Figure 4.11. MS-MS of 28

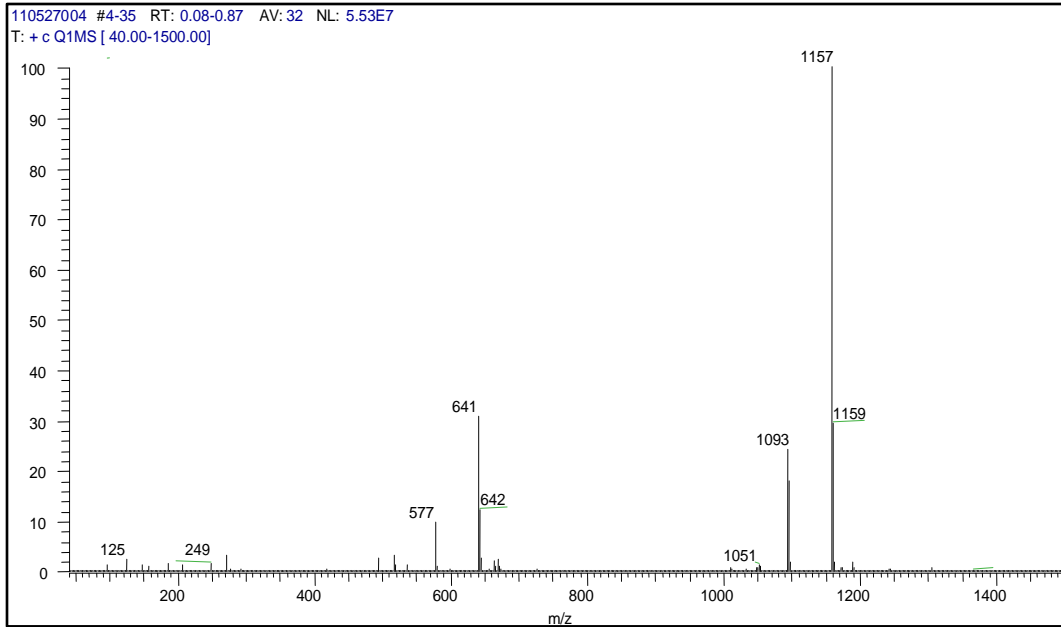


Figure 4.12. ESI-MS (+) of 29

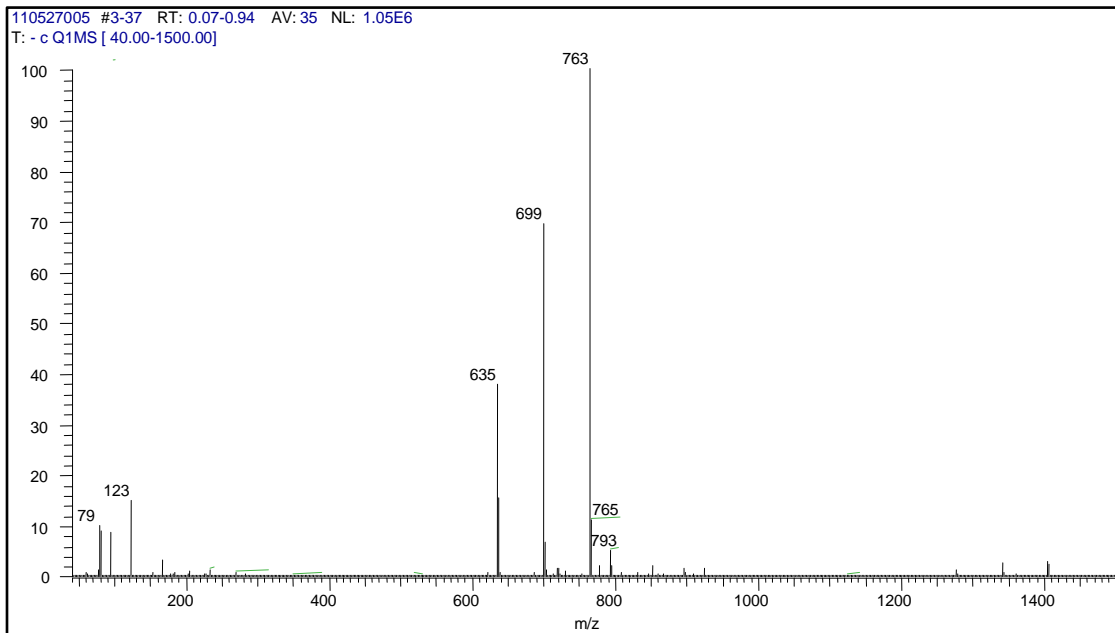


Figure 4.13. ESI-MS (-) of 29

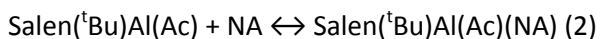
**Table 4.2. Computational determination of  $\Delta G$  values (kcal/mol) for the combination of SalenAl cations with Ac- (a), water (b) and (c), G-type nerve agents (d-g) and EMPA (h)**

	Compound		L = Salen	L = Salen(Me)
a	LAl(Ac)		-33	-31.5
b	[L(Al)(H <sub>2</sub> O)] <sup>+</sup>		-19.8	--
c	[L(Al)(H <sub>2</sub> O) <sub>2</sub> ] <sup>+</sup>		-26	--
	[LAlP(O)(Me)(R)(X)] <sup>+</sup>			
	R	X		
d	Me	F	-20.7	-19.6
e	CHMe <sub>2</sub>	F	--	-24.3
f	CH(Me)iPr	F	--	-19.9
g	CH(Me)tBu	F	--	-19.9
h	Et	OH	-24.3	--

**(The X and R groups correspond to substitutions in Figure 1. The compound, [SalenAl]<sup>+</sup> does not have <sup>t</sup>Bu groups while in [Salen(Me)Al]<sup>+</sup> the <sup>t</sup>Bu groups were replaced with Me to make the computations manageable.)**

Table 4.2. shows the computationally determined free energies for binding two types of Salen-aluminum cations with acetate (Eq. 1) and NAs (Eq. 2). The calculations incorporate the influence of hydration energy in the formation of **27**, **28**, and **29**. The  $\Delta G$  for Ac binding with **1** (-33 kcal/mol) is greater than the  $\Delta G$  values for the nerve agents, which implies that the equilibrium should favor coordination of acetate over the NAs. However, the NAs are, by design, hydrophobic so that they can readily penetrate human skin. In contrast, the acetate anion is hydrophilic, meaning that the NA will segregate out of the aqueous phase to coordinate to the more hydrophobic **26**. The displacement of Ac<sup>-</sup> from the complex (Eq. 3) would be facilitated by coordination of the NA to **26**, forming a six-coordinate intermediate. This compound has

precedent in the X-ray structure of Salen(<sup>t</sup>Bu)Al(OMe)(MeOH), where the Al is in a distorted octahedral geometry.<sup>109</sup>



#### 4.5. Conclusion

G-type nerve agents are difficult to analyze by LCMS due to low ionization efficiency. Analyzing for nerve agents after coordination to  $[\text{Salen}(\text{}^t\text{Bu})\text{Al}]^+$  has several advantages: 1) reduction of low mass noise by moving the ion to higher mass (e.g. GB, MW 140.1, shifted to  $m/z$  657 with SalenAl), 2) ability to detect nerve agents and degradation compounds without any additional water-sensitive derivatization, 3) additional sample preparation options based on extraction of the Lewis acid complex, and 4) presumed reduction in toxicity due to the moderate strength of the NA-Al coordinate covalent bond. Replacement of the <sup>t</sup>Bu groups on the Salen ligand with electron-withdrawing or more hydrophilic groups could be used to increase the binding strength to particular compounds of interest and adjust the hydrophobicity of the complex. Further work is still necessary to identify the Lewis Acid/Base adducts in solution phase to determine their thermodynamic properties.

#### 4.6. Experimental

**Synthesis and Characterization of Salen(<sup>t</sup>Bu)AlBr (1).** A rapidly stirred solution of Et<sub>2</sub>AlBr in toluene, prepared in situ by the redistribution of triethylaluminum (0.75 g, 6.57 mmol) and aluminum(III) bromide (0.89 g, 3.34 mmol), was combined with a solution of salen(<sup>t</sup>Bu)H<sub>2</sub> (5.0 g, 10.15 mmol) in toluene by cannula. The reaction mixture was refluxed for 8 h and filtered. The

volatiles were removed under vacuum from the clear yellow filtrate to give a yellow microcrystalline solid, which was purified by recrystallization from toluene. Yield: 4.8 g (79.20 %). mp: 330-332°C. <sup>1</sup>H NMR (CDCl<sub>3</sub>): δ 1.48 (s, 18H, C(CH<sub>3</sub>)<sub>3</sub>), 1.72 (s, 18H, C(CH<sub>3</sub>)<sub>3</sub>), 3.93 (m, 4H, NCH<sub>2</sub>), 7.35 (d, 2H, PhH), 7.43 (d, 2H, PhH), 8.56 (s, 2H, N=CH). IR (KBr; cm<sup>-1</sup>): 2962 (m), 2905 (w), 2866 (w), 1648 (s), 1628 (s), 1544 (m), 1475 (m), 1444 (m), 1421 (w), 1390 (w), 1361 (w), 1310 (w), 1257 (w), 1180 (w), 867 (w), 845 (m), 816 (w), 786 (w), 756 (w), 608 (m), 586 (w). MS (EI, positive): *m/z* 597 (M<sup>+</sup>, 8%), 517 (M<sup>+</sup> - Br, 100%).

### Electro-Spray Mass Spectroscopy

**Procedure and Instrumentation.** Compound **1** was prepared as described in Section A. It was transferred to a glass tube with a Teflon cap under nitrogen in an inert-atmosphere glovebox. The glass tube was sealed in a fire-proof air-sealed aluminum container and shipped to ECBC, MD.

At ECBC, compound **1** was used as received. It was dissolved in isopropanol at a stock concentration of 4 mg/mL, and diluted further to make standards. The samples were prepared by mixing (by volume) 10 μl of the stock solution with 100 μl of isopropanol, 10 μl of 0.5 M ammonium acetate solution in water, and 1-10 μl of acid or G agent standards. The final concentration of compound **1** was 0.55 mM. This concentration was not optimized, and a lower concentration could decrease the amount of dimer formation.

The solution of 0.5 M ammonium acetate buffer was used to exchange Br<sup>-</sup> for acetate anions, and to provide a buffer for electrospray mass spectroscopy. Solutions of analyte acid or G agents were used at various concentrations.

Samples were analyzed on a ThermoFinnigan TSQ Quantum triple quadrupole mass spectrometer by flow injection at 5-50  $\mu\text{l}/\text{min}$  with an electrospray ion source with default conditions and tuning, and using nitrogen drying gas. The spectrometer was calibrated to unit mass. Samples were analyzed in less than one hour after preparation.

**Computational Study.** The program package G09 was used for optimizations, frequency calculations, and solvation calculation. Complexes were optimized and frequencies calculated at the M05-2X/6-31+G(d) level while implicit solvation in water was modeled with SMD/B3LYP/6-31+G(2d,p). Estimated free energies of reaction were computed directly from SMD total energies. When free energies were computed with zero-point energies, integrated heat capacities and entropies using the equation  $DG(\text{aq},298\text{K}) = DG(\text{g},298\text{K},\text{M05-2X}/\text{M05-2X}/6-31+\text{G}(\text{d})) + DG(\text{sol},\text{SMD}/\text{B3LYP}/6-31+\text{G}(2\text{d},\text{p}))$ , the resulting free energies of reaction agreed to within one kcal/mol.

## Chapter 5 Conclusion and Future Work

This research is based on the previous finding where mononuclear aluminum bromide compounds based on the salen ligand effectively dealkylate a wide range of organophosphate compounds including nerve agents and pesticides. Dealkylation of phosphate esters can be used for deactivation and decontamination of these compounds. For effective use of this chemistry, it is necessary to gain a full understanding of the reaction. It would be interesting to elucidate the structures of the dealkylated products resulting from the dealkylation of different phosphates with different SAB-X. The extreme toxicity makes it impossible to study nerve agents in an academic research lab. Thus, dealkylation reactions were carried out using less trialkylphosphate, which could be model compounds for toxic nerve agents. In these reactions, the resulting product is a compound where the dealkylated phosphate ester is covalently bound to the aluminum through an Al-O-P linkage. Unique organic-soluble aluminum phosphate compounds containing a six-coordinate aluminum were isolated and structurally characterized. The resulting compounds are either polymeric or dimeric depending on the number of methylene units in the salen backbone. For example, the combination of salen(<sup>t</sup>Bu)AlBr (two methylene units) with alkyl phosphate in a 1:1 stoichiometry produces the polymer, and the combination of salpen(<sup>t</sup>Bu)AlBr (three methylene units) produces the dimer. While these compounds show structural variations, there are some common features among these compounds such as: non-volatility, high melting point (200 – 300 °C), and the presence of a stable, covalent Al – O – P linkage. Thus, the nerve agents can be both deactivated and locked into salen units at the same time. Also, these compounds do not decompose in neutral water, which is an additional advantage in the use of SalenAlBr compounds in the deactivation of nerve agents. Most of the molecular aluminum phosphates reported in the literature exhibit four or five coordinated aluminum. The resulting products of the dealkylation reactions contain a six-

coordinated aluminum, which is rare for molecular aluminophosphate materials. Also, the reaction conditions for all these compounds are very mild. Hence, this method could be developed to prepare aluminophosphate ring, cage, or chain structures for soluble models of aluminophosphate materials. This will be an additional application of dealkylation reaction beside the potential application in deactivation of nerve agents and pesticides. Although the attempts to isolate a single crystal of fully dealkylated products,  $[\{\text{Salen}(\text{}^t\text{Bu})\text{AlO}\}_3\text{P}(\text{O})]$ , were not successful, these compounds were characterized by spectroscopic and spectrometric analysis. The isotope patterns from the MALDI mass spectra of these compounds show a very good match with the isotope patterns obtained from the simulation experiment. This could be considered as evidence for formation of such compounds.

The salen aluminum bromide compounds used in this research dealkylate organophosphates effectively in non-nucleophilic solvents. However, for the possible applications, destruction of nerve agents and pesticides, dealkylation should be carried out in water. As a first step towards a water-stable dealkylation system, attempts have been made to examine the effect of strong donor solvents like methanol or water in dealkylation reaction. It appears that the solvent molecule, which is a stronger nucleophile, compared to the phosphate, block the coordinating site of aluminum. Percent dealkylation in donor solvents is lower compared to non-nucleophilic solvent. However, longer reaction time and excess of salen aluminum reagent might result in increase in dealkylation. Next step was to synthesize water-soluble group 13 chelates. This was achieved by introducing a sulfonate group on a salen ligand. Although  $\text{salen}(\text{SO}_3\text{Na})\text{MNO}_3$  ( $\text{M} = \text{Al}, \text{Ga}$ ), water soluble group 13 chelates, do not show any activity in dealkylation of organophosphate, this work will be useful in the creation of a water-stable dealkylating system in the future.

In collaboration with Edgewood Chemical Biological Center, we have developed a detection method for nerve agents based on the ESI-MS technique. Salen(<sup>t</sup>Bu) Al acetate, obtained by combination of SAB and sodium acetate, forms Lewis acid base adducts with nerve agents and other organophosphate compounds. These adducts are sufficiently stable to allow detection of nerve agents by ESI/MS. These adducts give distinctive mass spectrometry signatures. Molecular ion peaks were detected for adducts with GB, GD, and EMPA (VX hydrolysis product). Nerve agents are difficult to analyze by LC/MS due to low ionization efficiency and identification by GC-MS required prior derivatization. The adduct formation with Salen aluminum compounds may be viewed as a promising way for detection of nerve agents in aqueous solution with greater sensitivity.

The studies described in this dissertation could be useful to carry out more expanded studies in the future. Toxic nerve agents can be deactivated by salenAlBr but it would be necessary to determine the toxicity of resulting salen aluminum phosphate compound. The detection study could be expanded to develop detection method for pesticides and other toxic OPs. Also detailed quantification study should be undertaken to confirm applicability.

## Appendix

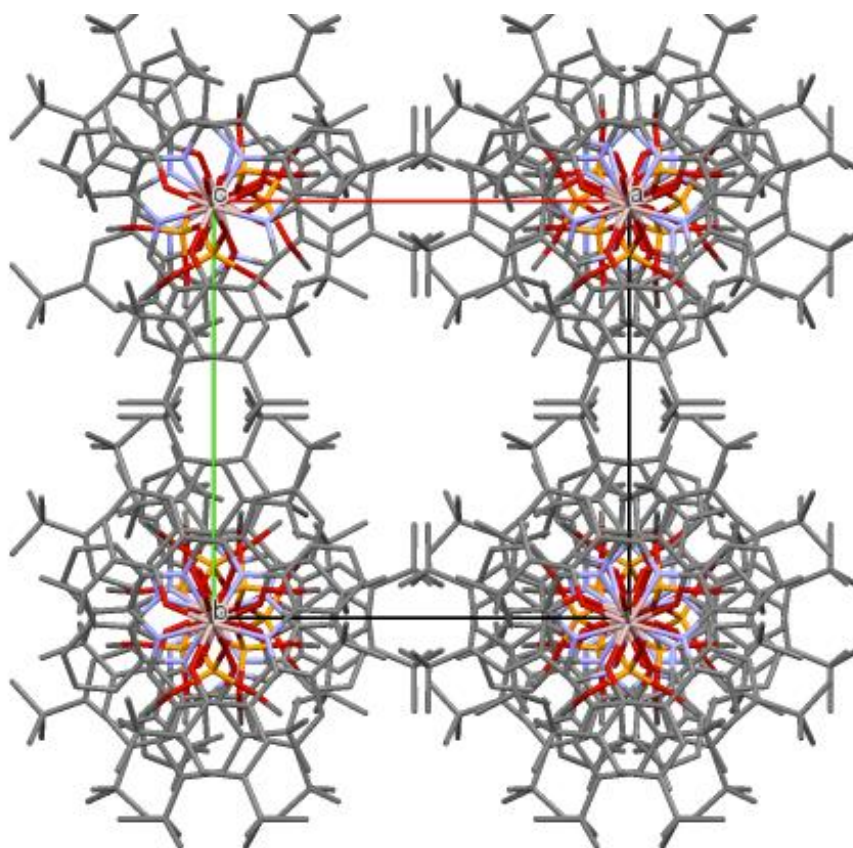


Figure A1. Crystal Structure of 7 viewed down the *c*-axis showing staggered confirmation of tBu groups

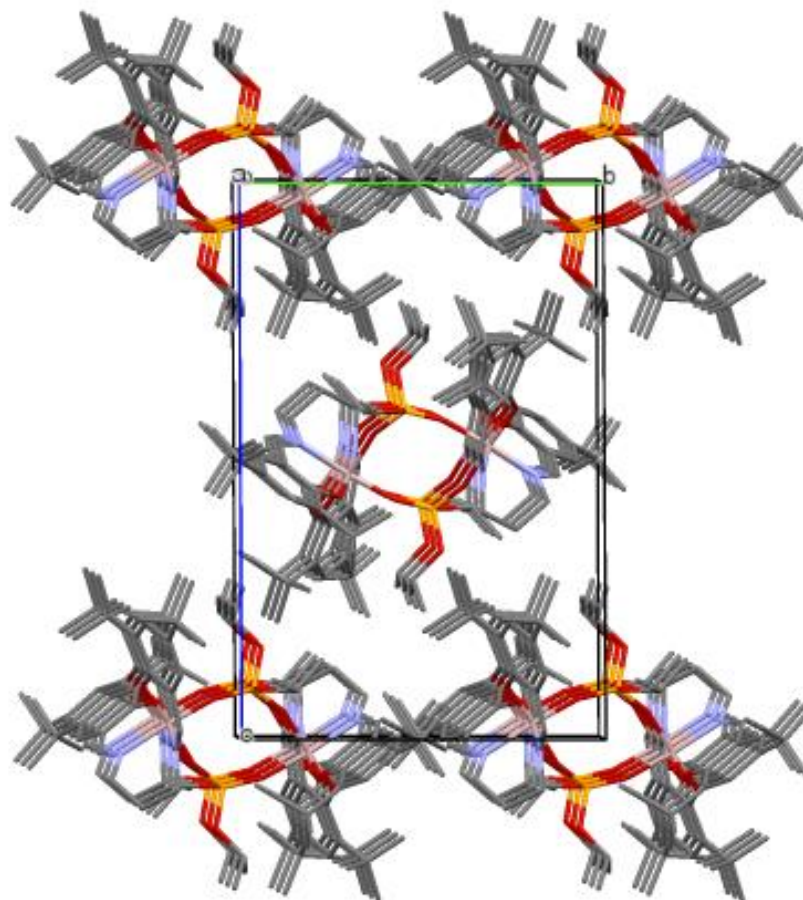


Figure A2. Crystal packing of 8 viewed down the a-axis showing stacking of aluminophosphate rings

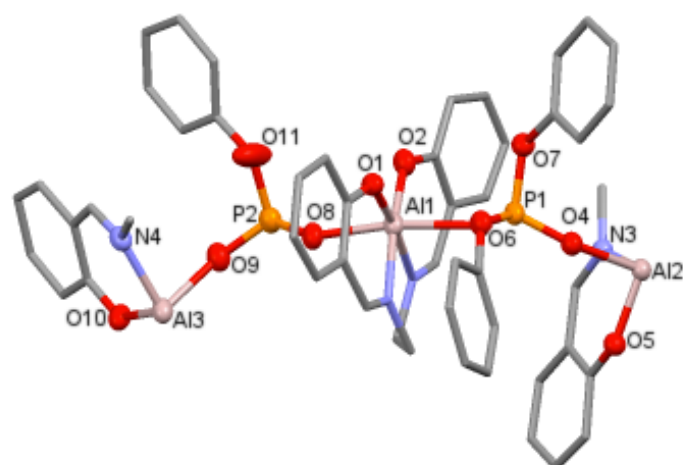


Figure A1. Asymmetric unit of **6** (<sup>t</sup>Bu groups not shown for clarity)

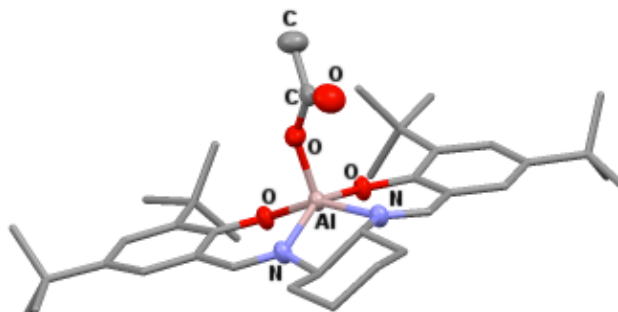


Figure A4. Crystal Structure of Salcen(<sup>t</sup>Bu)AlOC(O)Me

Table A1. Crystallographic data and refinement details for compound 5-8

	5	6	7	8
<b>Empirical Formula</b>	$C_{73.42}H_{114.84}N_4O_{12}$	$C_{177}H_{226}Al_4Cl_2N_8O_{24}$	$C_{38}H_{52}AlN_2O_6P$	$C_{39}H_{62}AlN_2O_6$
<b>Formula Weight</b>	1461.94	3152.26	690.77	712.86
<b>Crystal Size (mm)</b>	0.20 × 0.04 × 0.03	0.18 × 0.10 × 0.08	0.12 × 0.12 × 0.08	0.18 × 0.14 × 0.04
<b>λ (Å)</b>	1.54178	1.54178	1.54178	1.54178
<b>Crystal system</b>	Orthorhombic	Orthorhombic	Tetragonal	Monoclinic
<b>Space group</b>	$P 2_1 2_1 2_1$	$F d d d$	$P 4_1 2 2$	$P 2_1/c$
<b>a/ Å</b>	17.0858(4)	31.4350(6)	13.9887(2)	16.3345(3)
<b>b/ Å</b>	19.2770(4)	43.7636(8)	13.9887(2)	13.0287(2)
<b>c/ Å</b>	24.6768(6)	50.3936(9)	13.9887(2)	21.0652(3)
<b>α/ °</b>	90.00	90.00	90.00	90.00
<b>β/ °</b>	90.00	90.00	90.00	90.00
<b>γ/ °</b>	90.00	90.00	90.00	90.00
<b>V/ (Å<sup>3</sup>)</b>	8127.6(3)	69327(2)	8948.8(3)	4226.26(12)
<b>Z</b>	4	16	8	4
<b>ρ<sub>calc</sub>/mg m<sup>-3</sup></b>	1.195	1.208	1.025	1.120
<b>μ/ mm<sup>-1</sup></b>	2.013	1.422	1.048	1.118
<b>F(000)</b>	3134	26912	2960	1544
<b>θ range / °</b>	2.91-68.68	1.94-68.63	3.30 -68.51 <sup>o</sup>	4.06-67.96
<b>hkl range</b>	-20 ≤ h ≤ 20 -23 ≤ k ≤ 18 -29 ≤ l ≤ 29	0 ≤ h ≤ 37 0 ≤ k ≤ 52 0 ≤ l ≤ 60	-16 ≤ h ≤ 16 -16 ≤ k ≤ 16 -55 ≤ l ≤ 48	-19 ≤ h ≤ 19 -15 ≤ k ≤ 15 -25 ≤ l ≤ 25
<b>Reflections collected</b>	111047	15968	127767	59536
<b>Reflection unique, R(int)</b>	14729, 0.0745	15968, 0.0873	8235, 0.0613	7673, 0.0400
<b>Refinement</b>	Full-matrix least-	Full-matrix least-	Full-matrix	Full-matrix

<b>method</b>	squares on $F^2$	squares on $F^2$	least-squares on $F^2$	least-squares on $F^2$
<b>Restrains/ parameters</b>	10 / 923	126 / 1132	169 / 455	6 / 471
<b>Final R indices</b>	$R_1 = 0.0434$ , $wR_2 = 0.0999$	$R_1 = 0.0534$ , $wR_2 = 0.1675$	$R_1 = 0.0388$ , $wR_2 = 0.1012$	$R_1 = 0.0390$ , $wR_2 = 0.1003$
<b>R indices (all data)</b>	$R_1 = 0.0579$ , $wR_2 = 0.1088$	$R_1 = 0.0712$ , $wR_2 = 0.1851$	$R_1 = 0.0410$ , $wR_2 = 0.1026$	$R_1 = 0.0410$ , $wR_2 = 0.1002$
<b>Goodness-of- fit on <math>F^2</math></b>	1.046	1.139	1.088	0.975
<b>Largest diff. peak and hole (<math>e \cdot \text{\AA}^{-3}</math>)</b>	0.412 and -0.372	0.524 and -0.484	0.184 and - 0.308	0.385 and - 0.341

Table A2. Crystallographic data and refinement details for compound 5-8

	15
<b>Empirical Formula</b>	C <sub>7</sub> H <sub>9</sub> NaO <sub>7</sub> S
<b>Formula Weight</b>	260.19
<b>Crystal Size (mm)</b>	0.35 × 0.20 × 0.18
<b>Wavelength (Å)</b>	0.71073
<b>Crystal system</b>	Monoclinic
<b>Space group</b>	P2 <sub>1</sub> /c
<b>a/ Å</b>	11.9935(2)
<b>b/ Å</b>	11.9750(3)
<b>c/ Å</b>	7.0803(3)
<b>α/ °</b>	90.00°
<b>β/ °</b>	103.58°
<b>γ/ °</b>	90.00°
<b>Volume (Å<sup>3</sup>)</b>	988.43(5)
<b>Z</b>	4
<b>Calculated Density (Mg/m<sup>3</sup>)</b>	1.748
<b>Absorption coefficient (mm<sup>-1</sup>)</b>	0.389
<b>F(000)</b>	536

<b>θ range / °</b>	1.75-27.48
<b>hkl range</b>	-15 ≤ h ≤ 15 -14 ≤ k ≤ 15 -9 ≤ l ≤ 9
<b>Reflections collected</b>	14329
<b>Reflection unique, R(int)</b>	2259, 0.0600
<b>Refinement method</b>	Full-matrix least-squares on F <sup>2</sup>
<b>Restraints/ parameters</b>	6/ 159
<b>Final R indices</b>	R <sub>1</sub> = 0.0453, wR <sub>2</sub> = 0.1141
<b>R indices (all data)</b>	R <sub>1</sub> = 0.0565, wR <sub>2</sub> = 0.1206
<b>Goodness-of-fit on F<sup>2</sup></b>	1.125
<b>Largest diff. peak and hole (e.Å<sup>-3</sup>)</b>	0.583 and - 0.549

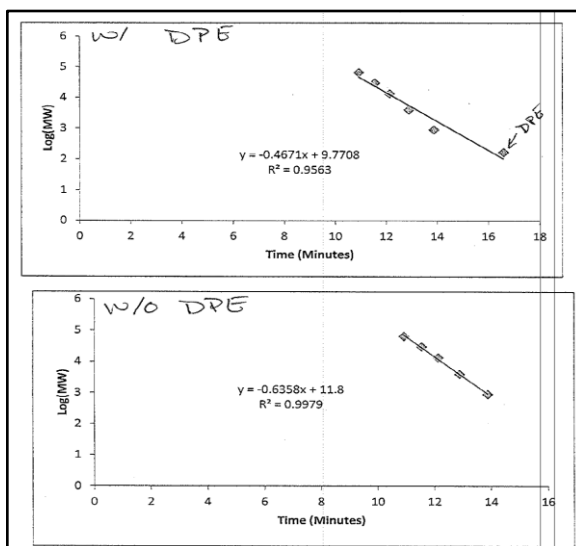


Figure A5. A. Calibration curve using polystyrene standards and with diphenyl ether ; B. GPC elution curve of diphenyl ether

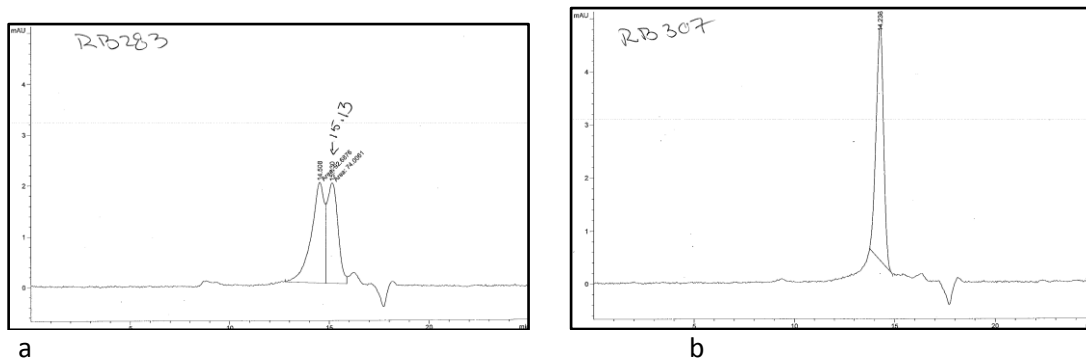


Figure A6. A. GPC elution curve of 7; B. GPC elution curve of 8.

## References

- (1) Corbridge, D. E. C. *Phosphorus: An Outline of its Chemistry, Biochemistry and Technology*; 5th ed.; Elsevier: Amsterdam, Netherlands, 1995, p 501.
- (2) Gilheany, D. G. *Chem. Rev.* **1994**, *94*, 1339.
- (3) Gilheany, D. G. In *The Chemistry of Organophosphorus Compounds*; Hartley, F. R., Ed.; John Wiley and Sons Ltd: New York, 1992; Vol. 2, p 9.
- (4) Emsley, J.; Hall, D. In *The Chemistry of Phosphorus*; John Wiley & Sons: New York, 1976, p 33.
- (5) Chesnut, D. B. *J. Am. Chem. Soc.* **1998**, *120*, 10504.
- (6) Chesnut, D. B. *J. Phys. Chem. A* **2003**, *107*, 4307.
- (7) Huheey, J. E.; Keiter, E. A.; Keiter, R. L. *Inorganic Chemistry: Principles of Structure and Reactivity*; 4th ed.; Harper Collins: New York, 1993, p 869-870.
- (8) Purcell, K. F.; Kotz, J. C. *Inorganic Chemistry*; W. B. Saunders Co.: Philadelphia, PA,, 1977, p 332.
- (9) Gamoke, B.; Neff, D.; Simons, J. *J. Phys. Chem. A* **2009**, *113*, 5677.
- (10) Mitchell, K. A. R. *Chem. Rev.* **1969**, *69*, 157.
- (11) Magnusson, E. *J. Am. Chem. Soc.* **1990**, *112*, 7940.
- (12) Yamada, K.; Koga, N. *J. Comput. Chem.* **2013**, *34*, 149.
- (13) Emsley, J.; Hall, D. In *The Chemistry of Phosphorus*; John Wiley & Sons: New York, 1976, p 471.
- (14) Blumenthal, E.; Herbert, J. B. M. *Trans. Faraday Soc.* **1945**, *41*, 611.
- (15) Westheimer, F. H. *Acc. Chem. Res.* **1968**, *1*, 70.
- (16) Barnard, P. W. C.; Bunton, C. A.; Llewellyn, D. R.; Vernon, C. A.; Welch, V. A. *J. Chem. Soc.* **1961**, 2670.
- (17) Teichmann, H.; Hilgetag, G. *Angew. Chem. Int. Ed.* **1967**, *6*, 1013.
- (18) Fest.C; Schmidt.K.-J. *The Chemistry of Organophosphorus Pesticides*; 2 ed.; Springer-Verlag Berlin Heidelberg: New York, 1982.
- (19) Rueggeberg, W. H. C.; Chernack, J. J. *J. Am. Chem. Soc.* **1948**, *70*, 1802.
- (20) Klement, R.; Wild, A. *Chem. Ber.* **1963**, *96*, 1916.
- (21) Miller, B. *Proc. Chem. Soc.* **1962**, 303.
- (22) Lecocq, J.; Todd, A. R. *J. Chem. Soc.* **1954**, 2381.
- (23) Di Sabato, G.; Jencks, W. P. *J. Am. Chem. Soc.* **1961**, *83*, 4393.
- (24) Bunton, C. A.; Robinson, L. B. *J. Org. Chem.* **1969**, *34*, 773.
- (25) *Flame Retardants: Frequently Asked Questions*, The European Flame Retardants Association, 2007.
- (26) van der Veen, I.; de Boer, J. *Chemosphere* **2012**, *88*, 1119.
- (27) Aaronson, A. M. In *Phosphorus Chemistry*; Walsh, E. N., Graffith, E. J., Parry, R. W., Quin, L. D., Eds.; American Chemical Society: 1992; Vol. 486, p 218.
- (28) Fisher, E. B.; Van Wazer, J. R. In *Phosphorus and Its Compounds: Technology, Biological Functions, and Applications*; Van Wazer, J. R., Ed.; Interscience: New York, 1961; Vol. 2, p 1889.
- (29) LaDou, J. *Current Occupational & Environmental Medicine*; McGraw-Hill: United State of America, 2004.
- (30) Costa, L. G. In *Casarett and Doull'S Toxicology: The Basic Science of Poisons*; 7th ed.; Klaassen, C. D., Ed.; Mc-Graw Hill New York, p 883.

- (31) U.S. Environmental Protection Agency, [http://www.epa.gov/pesticides/reregistration/status\\_op.html](http://www.epa.gov/pesticides/reregistration/status_op.html) (accessed March 07, 2014).
- (32) Eskenazi, B.; Bradman, A.; Castorina, R. *Environ. Health Perspect.* **1999**, *107* (suppl 3), 409.
- (33) Ordentlich, A.; Barak, D.; Kronman, C.; Ariel, N.; Segall, Y.; Velan, B.; Shafferman, A. *J. Biol. Chem.* **1996**, *271*, 11953.
- (34) Joshi, K. A.; Prouza, M.; Kum, M.; Wang, J.; Tang, J.; Haddon, R.; Chen, W.; Mulchandani, A. *Anal. Chem.* **2005**, *78*, 331.
- (35) Pumera, M. *J. Chromatogr. A* **2006**, *1113*, 5.
- (36) Wilson, E. K. In *Chem. Eng. News*; ACS: 2013; Vol. 91, p 20.
- (37) Organization for the Prohibition of Chemical Weapons, <http://www.opcw.org/about-chemical-weapons/types-of-chemical-agent/nerve-agents/> (accessed November 06, 2014).
- (38) *Special Report on Use of Chemical Weapons in Damascus Suburbs*, Center for Documentation of Violations in Syria., 2013.
- (39) Friboulet, A.; Rieger, F.; Goudou, D.; Amitai, G.; Taylor, P. *Biochemistry* **1990**, *29*, 914.
- (40) Shih, T.-M.; Kan, R. K.; McDonough, J. H. *Chem. Biol. Interact.* **2005**, *157–158*, 293.
- (41) Maxwell, D.; Brecht, K.; Koplovitz, I.; Sweeney, R. *Arch. Toxicol.* **2006**, *80*, 756.
- (42) Delfino, R. T.; Ribeiro, T. S.; Figueroa-Villar, J. D. *J. Braz. Chem. Soc.* **2009**, *20*, 407.
- (43) Quinn, D. M. *Chem. Rev.* **1987**, *87*, 955.
- (44) Mercey, G.; Verdelet, T.; Renou, J.; Kliachyna, M.; Baati, R.; Nachon, F.; Jean, L.; Renard, P.-Y. *Acc. Chem. Res.* **2012**, *45*, 756.
- (45) Millard, C. B.; Koellner, G.; Ordentlich, A.; Shafferman, A.; Silman, I.; Sussman, J. L. *J. Am. Chem. Soc.* **1999**, *121*, 9883.
- (46) Carletti, E. n.; Colletier, J.-P.; Dupeux, F.; Trovaslet, M.; Masson, P.; Nachon, F. *J. Med. Chem.* **2010**, *53*, 4002.
- (47) Trovaslet-Leroy, M.; Musilova, L.; Renault, F.; Brazzolotto, X.; Misik, J.; Novotny, L.; Froment, M.-T.; Gillon, E.; Loiodice, M.; Verdier, L.; Masson, P.; Rochu, D.; Jun, D.; Nachon, F. *Toxicol. Lett.* **2011**, *206*, 14.
- (48) Farquharson, S.; Inscore, F. E.; Christesen, S. *Top. Appl. Phys.* **2006**, *103*, 447.
- (49) Gustafson, R. L.; Martell, A. E. *J. Am. Chem. Soc.* **1962**, *84*, 2309.
- (50) Ward, J. R.; Yang, Y.-C.; Wilson Jr, R. B.; Burrows, W. D.; Ackerman, L. L. *Bioorg. Chem.* **1988**, *16*, 12.
- (51) Larsson, L. *Acta Chem. Scand.* **1958**, *12*, 783.
- (52) Yang, Y. C.; Baker, J. A.; Ward, J. R. *Chem. Rev.* **1992**, *92*, 1729.
- (53) Epstein, J.; Demek, M. M.; Rosenblatt, D. H. *J. Org. Chem.* **1956**, *21*, 796.
- (54) Larsson, L. *Acta Chem. Scand.* **1958**, *12*, 723.
- (55) Wagner, G. W.; Yang, Y.-C. *Ind. Eng. Chem. Res.* **2002**, *41*, 1925.
- (56) Khan, M. A. S.; Kesharwani, M. K.; Bandyopadhyay, T.; Ganguly, B. *J. Mol. Struct. Theochem* **2010**, *944*, 132.
- (57) Kesharwani, M.; Khan, M. A.; Bandyopadhyay, T.; Ganguly, B. *Theor. Chem. Acc.* **2010**, *127*, 39.
- (58) Patterson, E. V.; Cramer, C. J. *J. Phys. Org. Chem.* **1998**, *11*, 232.
- (59) Yang, Y.-C. *Acc. Chem. Res.* **1999**, *32*, 109.
- (60) Yang, Y.-C.; J. Berg, F.; L. Szafraniec, L.; T. Beaudry, W.; A. Bunton, C.; Kumar, A. *J. Chem. Soc., Perkin Trans. 2* **1997**, 607.

- (61) Courtney, R. C.; Gustafson, R. L.; Westerback, S. J.; Hyytiainen, H.; Chaberek, S. C.; Martell, A. E. *J. Am. Chem. Soc.* **1957**, *79*, 3030.
- (62) Epstein, J.; Rosenblatt, D. H. *J. Am. Chem. Soc.* **1958**, *80*, 3596.
- (63) Epstein, J.; Bauer, V. E.; Saxe, M.; Demek, M. M. *J. Am. Chem. Soc.* **1956**, *78*, 4068.
- (64) Yang, Y.-C.; Szafraniec, L. L.; Beaudry, W. T.; Rohrbaugh, D. K.; Procell, L. R.; Samuel, J. B. *J. Org. Chem.* **1996**, *61*, 8407.
- (65) Pearson, G. S.; Magee, R. S. *Pure Appl. Chem.* **2002**, *74*, 187.
- (66) *Alternative Technologies for the Destruction of Chemical Agents and Munitions*; National Academies Press: Washington, DC, 1993.
- (67) *Review and Evaluation of Alternative Chemical Disposal Technologies*; National Academies Press: Washington, DC, 1996.
- (68) U.S. Army's Chemical Materials Agency: Richmond, KY, (<http://www.cma.army.mil/bluegrass.aspx>). (accessed March 04, 2014).
- (69) Mitra, A.; Atwood, D. A.; Struss, J.; Williams, D. J.; McKinney, B. J.; Creasy, W. R.; McGarvey, D. J.; Durst, H. D.; Fry, R. *New J. Chem.* **2008**, *32*, 783.
- (70) Florjańczyk, Z.; Wolak, A.; Dębowski, M.; Plichta, A.; Ryszkowska, J.; Zachara, J.; Ostrowski, A.; Zawadzak, E.; Jurczyk-Kowalska, M. *Chem. Mater.* **2007**, *19*, 5584.
- (71) Oliver, S.; Kuperman, A.; Ozin, G. A. *Angew. Chem. Int. Ed.* **1998**, *37*, 46.
- (72) Song, Y.; Li, J.; Yu, J.; Wang, K.; Xu, R. *Top. Catal.* **2005**, *35*, 3.
- (73) Kimura, T. *Chem. Mater.* **2003**, *15*, 3742.
- (74) Kimura, T. *Chem. Mater.* **2005**, *17*, 5521.
- (75) Maeda, K.; Akimoto, J.; Kiyozumi, Y.; Mizukami, F. *J. Chem. Soc., Chem. Commun.* **1995**, 1033.
- (76) Florjańczyk, Z.; Lasota, A.; Wolak, A.; Zachara, J. *Chem. Mater.* **2006**, *18*, 1995.
- (77) Pinkas, J.; Chakraborty, D.; Yang, Y.; Murugavel, R.; Noltemeyer, M.; Roesky, H. W. *Organometallics* **1999**, *18*, 523.
- (78) Lugmair, C. G.; Tilley, T. D.; Rheingold, A. L. *Chem. Mater.* **1999**, *11*, 1615.
- (79) Mitra, A.; DePue, L. J.; Parkin, S.; Atwood, D. A. *J. Am. Chem. Soc.* **2006**, *128*, 1147.
- (80) Wang, Y.; Parkin, S.; Atwood, D. *Chem. Commun.* **2000**, 1799.
- (81) Wang, Y.; Parkin, S.; Atwood, D. *Inorg. Chem.* **2002**, *41*, 558.
- (82) Richeter, S.; Thion, J.; van der Lee, A.; Leclercq, D. *Inorg. Chem.* **2006**, *45*, 10049.
- (83) Ghanem, E.; Li, Y.; Xu, C.; Raushel, F. M. *Biochemistry* **2007**, *46*, 9032.
- (84) Mukherjee, A. K. *Anal. Chim. Acta* **1955**, *13*, 268.
- (85) Mukherjee, A. K.; Ray, P. *J. Indian Chem. Soc.* **1955**, *32*, 633.
- (86) Langenbeck, W.; Oehler, K. *Chem. Ber.* **1956**, *89*, 2455.
- (87) Botsivali, M.; Evans, D. F.; Missen, P. H.; Upton, M. W. *J. Chem. Soc., Dalton Trans.* **1985**, 1147.
- (88) Evans, D. F.; Missen, P. H. *J. Chem. Soc., Dalton Trans.* **1985**, 1451.
- (89) Evans, D. F.; Missen, P. H. *J. Chem. Soc., Dalton Trans.* **1987**, 1279.
- (90) Berry, K. J.; Moya, F.; Murray, K. S.; van den Bergen, A. M. B.; West, B. O. *J. Chem. Soc., Dalton Trans.* **1982**, 109.
- (91) Delahaye, É.; Diop, M.; Welter, R.; Boero, M.; Massobrio, C.; Rabu, P.; Rogez, G. *Eur. J. Inorg. Chem.* **2010**, *2010*, 4450.
- (92) Tanaka, T.; Tsurutani, K.; Komatsu, A.; Ito, T.; Iida, K.; Fujii, Y.; Nakano, Y.; Usui, Y.; Fukuda, Y.; Chikira, M. *Bull. Chem. Soc. Jpn.* **1997**, *70*, 615.
- (93) Routier, S.; Bernier, J.-L.; Waring, M. J.; Colson, P.; Houssier, C.; Bailly, C. *J. Org. Chem.* **1996**, *61*, 2326.
- (94) Gravert, D. J.; Griffin, J. H. *Inorg. Chem.* **1996**, *35*, 4837.

- (95) Bahramian, B.; Mirkhani, V.; Moghadam, M.; Amin, A. H. *Appl. Catal., A* **2006**, *315*, 52.
- (96) Jegier, J. A.; Munoz-Hernandez, M.-A.; Atwood, D. A. *J. Chem. Soc., Dalton Trans.* **1999**, 2583.
- (97) Choudary, B. M.; Ramani, T.; Maheswaran, H.; Prashant, L.; Ranganath, K. V. S.; Kumar, K. V. *Adv. Synth. Catal.* **2006**, *348*, 493.
- (98) Mesilaakso, M. In *Chemical Weapons Convention Chemicals Analysis*; John Wiley & Sons, Ltd: 2006, p 1.
- (99) Steiner, W. E.; Klopsch, S. J.; English, W. A.; Clowers, B. H.; Hill, H. H. *Anal. Chem.* **2005**, *77*, 4792.
- (100) Mäkinen, M. A.; Anttalainen, O. A.; Sillanpää, M. E. T. *Anal. Chem.* **2010**, *82*, 9594.
- (101) Kendler, S.; Zaltsman, A.; Frishman, G. *Instrum Sci. Technol.* **2003**, *31*, 317.
- (102) D'Agostino, P. A.; Provost, L. R.; Brooks, P. W. *J. Chromatogr. A* **1991**, *541*, 121.
- (103) Wang, Q.; Xie, J.; Gu, M.; Feng, J.; Ruan, J. *Chromatographia* **2005**, *62*, 167.
- (104) Tørnes, J. A.; Johnsen, B. A. *J. Chromatogr. A* **1989**, *467*, 129.
- (105) Ciner, F. L.; McCord, C. E.; Plunkett Jr, R. W.; Martin, M. F.; Croley, T. R. *J. Chromatogr. B* **2007**, *846*, 42.
- (106) Richardson, D. D.; Sadi, B. B. M.; Caruso, J. A. *J. Anal. At. Spectrom.* **2006**, *21*, 396.
- (107) A. Jegier, J.; Munoz-Hernandez, M.-A.; A. Atwood, D. *J. Chem. Soc., Dalton Trans.* **1999**, 2583.
- (108) Chen, P.; Chisholm, M. H.; Gallucci, J. C.; Zhang, X.; Zhou, Z. *Inorg. Chem.* **2005**, *44*, 2588.
- (109) Muñoz-Hernandez, M.-A.; Keizer, T.; Parkin, S.; Zhang, Y.; Atwood, D. *J. Chem. Crystallogr.* **2000**, *30*, 219.

## Vita

- Education           **Master of Science**  
(2003-2005), Organic chemistry, Mumbai University, Maharashtra, India
- Bachelor of Science**  
(2000-2003), Chemistry, Mumbai University, Maharashtra, India
- Work Experience   **Gharda Chemical Limited, Chiplun, India**  
(2005-2006), Jr. Research Assistant, Pigment division
- IPCA Laboratories Limited, Mumbai, India**  
(2006-2009), Research Officer, API research division
- Awards               **J. R. D. Tata Trust Award for quality academic achievement by Master's student**  
Awarded by J.R.D. Tata Trust. 2003 and 2004
- Departmental Merit Scholarship**  
Awarded by Department of Chemistry, Mumbai University, India. 2004-05
- Publications       Raman, B.; Sharma, B. A.; Butala, R.; Ghugare, P. D.; Kumar, A., Structural elucidation of a process-related impurity in ezetimibe by LC/MS/MS and NMR. *J. Pharm. Biomed. Anal.* 2010, 52, 73-78.
- Butala, R. R.; Cooper, J. K.; Mitra, A.; Webster, M. K.; Atwood, D. A., Dealkylation of chemical weapon agents and pesticides with group 13 salen compounds. *Main Group Chem.* 2010, 9 (3), 315-335.
- Butala, R.R.; Atwood, D. A., Aluminum: Organometallics. In *Comprehensive Organometallic Chemistry III*; Robert, H. C.; Mingos, D. M. P., Ed.; Elsevier: Oxford University Press, 2013; pp 265-285. (Updated of original article by Mitra, A.; Atwood, D. A. 2007)
- Butala, R. R.; Creasy, W, R.; Frye, R. A.; Atwood, D. A., Lewis Acid Assisted Detection of Nerve Agents in Water. *Chem. Commun.* (To be submitted).
- Butala, R. R.; Parkin, S.; Atwood, D. A., Salen Aluminum Phosphates. To be submitted, *Inorg. Chem.* (To be submitted).